DESIGN OF OPTIMIZED PES-ALUMINA POLYMER MATRIX NANOCOMPOSITE MEMBRANES FOR HEAVY METAL IONS REMOVAL FROM WATER

by

Behnam Gohari

A Dissertation Submitted in

Partial Fulfillment of the

Requirements for the Degree of

Doctor of Philosophy

in Engineering

at

The University of Wisconsin-Milwaukee

May 2019

ABSTRACT

DESSIGN OF OPTIMIZED PES-ALUMINA POLYMER MATRIX NANOCOMPOSITE MEMBRANES FOR HEAVY METAL IONS REMOVAL FROM WATER

by

Behnam Gohari

The University of Wisconsin-Milwaukee, 2019

Under the Supervision of Professor Nidal Abu-Zahra

Membrane filtration has become the focus of separation processes in different industries including water and waste water treatment. Synthetic asymmetric polymeric membranes are the most widely used membrane type for filtration technologies such as ultrafiltration, nanofiltration, and reverse osmosis due to better control of the pore forming mechanism, higher flexibility, lower cost, and ease of operation compered to inorganic membranes. Among the available polymers, polyethersulfones polymers (PES) demonstrate strong chemical and thermal stability, making them popular as basic materials for filtration and support materials for composite membranes. They are hydrophobic intrinsically and the application of such membranes is still limited by some challenges such as permeability and selectivity trade-off, and low resistance to fouling. Unique properties of nanomaterials including high reactivity, strong sorption, fast dissolution, and specific interaction with contaminants in water make them a great option for water/wastewater treatment. It is well known that the nanoparticles especially metal

oxide nanoparticles have high adsorption capacities for heavy metal ions. Their extremely small size, however, brings forth some issues in utilizing nanomaterials. These issues include mass transport and pressure drop when applied in fixed bed or any other flow-through systems, difficulties in separation and reuse, and even possible risk to ecosystems and human health caused by a potential release into the environment.

Incorporation of nanoparticles such as (TiO_2), alumina (Al_2O_3), silica (SiO_2), silver and many others into PES membranes has been a recent trend in membrane research. This can influence structural and physicochemical properties of membranes (e.g. porosity, charge density, and mechanical stability) and introduce new functionalities, including heavy metal ions removal. Recently, modification of nanoparticles before incorporating into polymeric materials has attracted great interests. A common method to modify the nanoparticles is treating them with silane coupling agents; such as methacryloyloxy methylenemethyl diethoxysilane (MMDES), and 3-aminopropyltriethoxysilane (APTES). Silane coupling agents are used extensively in inorganic polymer composites such as mineral filled polymer composites. Choosing the appropriate silane group can alter the surface of an inorganic material from hydrophilic to hydrophobic and increase its affinity to functional groups of the polymer matrix and decrease the agglomeration of nanoparticles.

In this project, asymmetric ultrafiltration membranes were synthesized by phase inversion immersion precipitation method. The effect of main synthesizing parameters

(casting temperature and polymer concentration in the casting solution) on the morphology and performance of the membranes were investigated in order to optimize the performance of the prepared membranes. Afterward, PES/Alumina nanocomposite membranes with optimized pore structure, mechanical and thermal stability, and permeability were synthesized. The performance of the nanocomposite membranes in removal of copper ions from water were also investigated. The prepared membranes were characterized using FTIR, XRD, FESEM, AFM, contact angle, viscosity measurement, BET, and BJH techniques. The performance of the membranes including solute rejection and water flux was also investigated.

Alumina nanoparticles were also modified by 3-aminopropyltriethoxysilane (APTES) and were used to fabricate novel nanocomposite PES membranes. The morphology and physio-chemical properties of the modified nanoparticles and membranes were investigated. The performance of the membranes was also examined in terms of Cu (II) ion removal from water as well as pure water flux measurements. Finally, the Spiegler-Katchalsky-Kedem model was used to develop a novel model to analyze the separation mechanism and predict the rejection performance of the synthesized membranes. The model parameters were obtained from the Steric Hindrance model. The developed model was able to predict the copper ion rejection of the membranes by about 20% accuracy.

TABLE OF CONTENTS

LIST OF FIGURES

LIST OF TABLES

Chapter 1) Introduction

Introduction:

All known life forms need liquid water to function properly and water is a vital element of life. However, due to the rapid growth of world population, abuse of water resources, and water pollution, water shortage problem has become more and more serious. Worldwide, around 780 million people still lack access to improved drinking water sources (WHO, 2012). Hence, cost-effective technologies must be developed to extend water resources and solve water pollution problems. Membrane technology is one of the most promising technologies that may provide a solution to challenging water problem. It has already been widely used in many areas including drinking water treatment, brackish and seawater desalination, and wastewater treatment and reuse, largely because it is simple in concept and operation, does not involve phase changes or chemical additives, can be made modular for easy scale up.

Membrane, as one of the widely used and principal techniques in water treatment, can be defined as a thin and selective barrier which enables the transport or the retention of compounds between two media. Basically membrane allows some compounds and molecules to pass through but stop others. Membrane can be prepared by inorganic materials (such as ceramics) or organic materials (such as polymers). Inorganic materials including ceramics and metallic materials usually have better chemical/solvent resistance and could tolerate a wide range of temperature, pH, and pressure. However, they are also restricted by several disadvantages such as limited pore size availability and high operating and capital

costs [3]. Current research on membranes primarily focuses on polymeric membranes because of the better control of pore forming mechanism, higher flexibility, smaller footprints required for installation, and lower costs compared to inorganic membranes [3, 4].

Different types of polymeric materials have been used to prepare polymeric membranes, such as polysulfone (PSU), polyethersulfone (PES), cellulose acetate (CA), polyethylene (PE), polypropylene (PP), poly(vinylidene fluoride) (PVDF), , polycarbonates (PC) and polyacrylonitrile (PAN). Among them, PSU, PVDF and PES are the most commonly used materials because of their relatively low cost, decent thermal and chemical stabilities [3, 5]. One of the common polymer materials utilized to fabricate membranes is polyethersulfone (PES). This polymer is highly favorable because of wide application temperature limit, high chemical resistance, and easiness of manufacturing in a wide range of pore size from microfiltration to nanofiltration [6].

The degree of selectivity of a membrane depends on the membrane pore size. Depending on the pore size. Based on thee pore size membranes can be classified as microfiltration (MF), Ultrafiltration (UF), nanofiltration (NF) and reverse osmosis (RO) membranes. Basic properties and membrane classes are listed in table 1.1.

Table 1. 1 Membrane types and operating pressure [3]

Membrane Class	Pore size	Typical targets removed	Operating Pressure
MF	0.1-10 μm	Suspended solids, bacteria, protozoa	0.1-2 bar
UF	3-100 nm (1-100 kDa)	Colloidal or molecular particles, proteins, most bacteria, partially viruses	2-5 bar
NF	1-3 nm (250-400 Da)	Viruses, natural organic matter (NOM), divalent or multivalent ions	5-20 bar
RO	< 100 Da	Almost all impurities, including monovalent ions	10-100 bar

In spite of all the advantages that polymeric membranes possess, the have also some drawbacks and challenges. The most common disadvantages include fouling and high hydrophobic property, and trade-off between selectivity and rejection. Membrane fouling results in flux decline during the operation. There are several kinds of fouling which may occur in membrane systems, such as crystalline fouling, organic fouling, particulate and colloidal fouling, and microbial fouling. Membrane fouling causes a number of problems including the increase in the operational pressure and the decline in the permeate quantity and quality of the membrane systems. [7]. The other challenge in polymeric membranes is the trade-off between permeability and selectivity in which, membranes

with higher water permeability usually possess relatively lower solute rejection. Low thermal and mechanical stability of the polymeric membranes are another challenges which need to be improved.

Utilizing nanomaterials in the fabrication process of polymeric membranes has received a lot of attention during recent years. Nanoparticles have the potential to enhance permeability and fouling resistance of the membranes along with adding antimicrobial properties and heavy metal ion removal ability [8-10]. Furthermore, it has been reported that surface charge density of the membranes also changes with the addition of nanoparticles due to the their surface functional groups [8, 11]. Studies have shown that adding metal oxide nanoparticles also improves the mechanical and thermal stability of the membranes [8, 12]. Incorporating nanoparticles into the membranes primarily enhances a multitude of characteristics such as permeability, selectivity, mechanical stability, and fouling resistance. Additionally, new functionalities including antibacterial properties, antiviral properties, and heavy metal ion removal capability were induced to the polymeric membranes.

Recently, the incorporation of modified nanoparticles into polymeric materials has attracted great interests. One common method to modify the nanoparticles is treating them by silane coupling agents; such as methacryloyloxy methylenemethyl diethoxysilane (MMDES), and 3-aminopropyltriethoxysilane (APTES) [13, 14]. Silane

coupling agents are extensively used in inorganic polymer composites such as mineral filled polymer composites [15, 16]. Choosing the appropriate silane group can modify the surface of an inorganic material from hydrophilic to hydrophobic and increase its affinity to the functional groups of the polymer matrix [1, 2], and decrease the agglomeration of nanoparticles.

In this work, alumina nanoparticles treated by APTES, were used to fabricate novel PES membranes to remove Cu(II) ions from water. The morphology and physio-chemical properties of the modified nanoparticles and membranes were characterized by FTIR, XRD, FESEM, DMA, porosity, and water contact angle. The performance of the membranes was tested in terms of Cu(II) ion removal from water as well as pure water flux measurements. Moreover, a novel mechanism- based model was developed to analyze and predict the performance of the nanocomposite membranes. The proposed system of PES nanocomposite membrane offers a potential for the removal of heavy metal ions at lower operating pressure and higher flux than current available membrane systems.

Research Goal

The goal of this research is to design, synthesize, and optimize nanocomposite PES membranes with the ability to remove heavy metal ions from water. These membranes possess a high flux of ultrafiltration membranes, while are able to remove heavy metal ions from water.

Research Objectives, Tasks, and Outline

The objective is to design and optimize nanocomposite membranes by incorporating alumina nanoparticles into PES membranes in order to improve their permeability, mechanical properties, and the removal of copper ions capability form water. This project investigates the structural and morphological properties, heavy metal adsorption capability, flux permeability and heavy metal ions rejection of PES asymmetric nanocomposite membranes synthesized by immersion precipitation phase inversion method. Surface treatment of nanoparticles is also utilized to improve the performance of the nanocomposite membranes. It is expected that the prepared nanocomposite membranes will result in lower energy consumption in the membrane filtration systems.

This project is been divided into six main tasks:

- Synthesizing PES asymmetric ultrafiltration membranes by phase inversion immersion precipitation method, and optimizing the process by investigating the main processing parameters (polymer concentration and casting temperature)
- Preparing PES nanocomposite membranes by incorporating different amounts of alumina nanoparticles (in the range of 0-5 wt. %) into the membrane structure
- Investigating the effect of incorporating nanoparticles into the membrane matrix on the morphology, thermal properties, water flux, adsorption, and Cu^{2+} removal capability of the nanocomposite membranes
- Improving the performance of alumina incorporated nanocomposite membranes; including permeability, and heavy metal ions removal ability, using chemical treatment of alumina nanoparticles (silane coupling method)
- Utilizing adsorption isotherms and composite theory to study the adsorption of the heavy metals ions by the membranes
- Developing a mechanism based model to analyze and predict the rejection performance of the nanocomposite membranes

The project has been divided to four phases as below:

Phase I: Synthesize and optimize the fabrication of polymeric asymmetric flat sheet membranes by immersion precipitation phase inversion method.

Phase II: Synthesize PES nanocomposite membranes with different nanoparticle concentration. The structure, physicochemical properties and performance of the membranes were also studied.

Phase III: Modify alumina nanoparticles with APTES ((3-Aminopropyl)triethoxysilane) silane agent, and investigate the effect of nanoparticles surface treatment on the performance of the membranes.

Phase IV: Model and study the mechanism of the heavy metal ions rejection of the nanocomposite membranes

Significance and Novelty

Nowadays, membrane filtration has been proven to be an efficient tool in water and wastewater treatment. Polyethersulfone (PES) is one of the most common polymers used in the preparation of commercial and laboratory membranes because of their commercial availability, ease of processing, and favorable selectivity-permeability characteristics. PES is also one of the most common polymers in the preparation of commercial and laboratory ultrafiltration membranes. Ultrafiltration membranes typically are unable to remove heavy metal ions since their pores sizes are larger than the size of the heavy metal ions. In this study, the ability of heavy metal ions removal was introduced to PES polymeric ultrafiltration membranes through incorporation of nanoparticles into the polymer matrix. These membranes possess high permeability of ultrafiltration membranes, while, incorporating nanoparticles into the membranes structure leads to heavy metal ions removal ability. The main drawback of incorporating of nanoparticles into polymeric membranes is the poor dispersibility of the nanoparticles in the polymer matrices and aggregation of the nanoparticles in the polymeric solution due to surface interactions. To address this issue, surface modification of the nanoparticles was also utilized to improve the dispersion of the nanoparticles in the polymer matrix and improve the performance of nanocomposite membranes. Also, a novel mechanism based model was developed to analyze and predict rejection of heavy metal ions by the nanocomposite membranes.

Although there is an extensive list of published work on the use of inorganic additives in PES membranes, there are few published papers on the use of these nanoparticles (as a very effective heavy metal ions adsorbent) to remove heavy metal ions from water. The significance of this work is to design and synthesize ultrafiltration membranes with the heavy metal ions removal ability. The main advantages of synthesized nanocomposite membranes over the current membranes used for heavy metal ions removal (nanofiltration and reverse osmosis) are higher flux, easier processing, and lower transmembrane pressures. The anticipated outcomes of this project will offer researchers, manufacturers of industrial membranes, and decision makers with scientific data and engineering guidelines on the use of inorganic nanoparticles to increase the performance of polymeric ultrafiltration membranes and introduction of the ability to remove heavy metal ions from water.

Chapter 2) Literature Review

2.1. Introduction

Increasing population and growth of industries and industry wastes have led to sever water pollution. Beside other water treatment techniques, membrane filtration has been proven to an efficient method in water treatment [3, 17]. Nowadays, membrane filtration has been proven to be an efficient tool in water and wastewater treatment [18-20]. Membrane filtration technologies such as ultrafiltration, nanofiltration, and reverse osmosis offer reliability, ease of operation, and cost and energy effective methods for water treatment [18, 20, 21]. Many kinds of synthetic materials can be used for the fabrication of membranes such as metals, ceramics, glasses, and polymers [22]. Due to their simplistic pore forming mechanism, good mechanical properties, and lower cost than inorganic membranes, polymeric membranes are the most widely used commercial membranes for water treatment technologies [8, 22, 23]. Polysulfone (PSf) and Polyethersulfone (PES) are two of the most common engineered polymers used in the preparation of commercial and laboratory membranes [22, 24-29]. These polymers consist of aromatic units bridged with sulfone and/or ether moieties [27]. These polymers are intrinsically hydrophobic and their application is still limited by some challenges such as the trade-off between permeability and selectivity, and low resistance to fouling [8, 30, 31]. The chemical structure of the two most used commercial sulfone polymers are presented in figure 2.1.

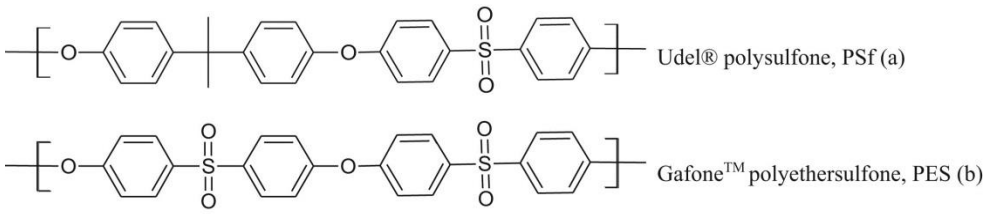

Figure 2. 1 Chemical structure of commercial a) PSf and b) PES polymers [27]

Several methods are used to fabricate polymeric membranes in which phase inversion (PI) techniques are the most important and commonly used methods [8, 22]. Dry or wet phase inversion processes such as solvent evaporation, precipitation from vapor phase, precipitation by controlled evaporation, thermal precipitation, and immersion precipitation can be used to prepare an asymmetric membrane with a very thin, dense skin layer [22]. Among these techniques, immersion precipitation is one of the most popular commercially explored membrane formation method [22]. To synthesize membranes using this method, a polymer solution is cast onto a suitable support using a film applicator. Afterwards, it is immersed into a nonsolvent (coagulation) bath, which consists of a poor solvent and may contain some additives [27, 32]. Subsequently, phase separation takes place by the exchange of solvent and nonsolvent, leading to solidification of the polymer film and forms an asymmetric membrane with a denser top layer [8, 22, 27, 32]. The morphology and separation performance of the synthesized membranes can be controlled by multiple parameters. The choice of the solvent-nonsolvent system, the composition of the polymer solution, additives in the polymer solution, the composition of the coagulation bath, and film casting conditions are among

the key factors that significantly influence the membrane morphology and performance [22, 32]. Figure 2.2 shows the schematic of the immersion precipitation phase inversion method.

Unique properties of nanomaterials including high reactivity, strong sorption, fast dissolution, and specific interaction with contaminants in water make them a great candidate for water/wastewater treatment [23, 33-36]. However, the extremely small size brings forth some issues in utilizing nanomaterials. These issues include mass transport and excessive pressure that drops when applied in fixed bed or any other flow-through systems, difficulties in separation and reuse, and even possible risk to ecosystems and

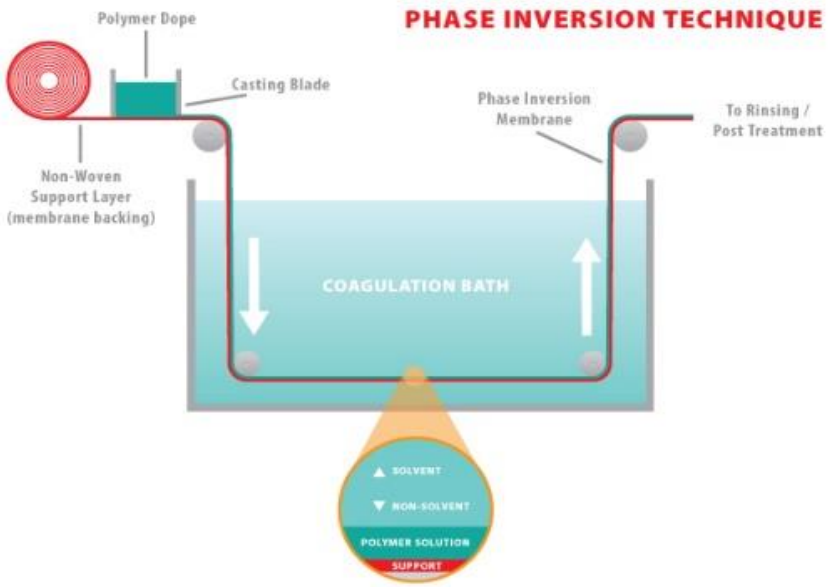

Figure 2. 2 Schematic of phase inversion technique

human health caused by a potential release into the environment [35]. Various inorganic and hybrid nanomaterials such as carbon nanotube, ZnO, Fe_3O_4, Al_2O_3, graphene oxide, Ag, and TiO_2 have been incorporated in polymeric membranes in order to improve their performance. [8, 20, 28, 37, 38]. To synthesize nanocomposite membranes by immersion precipitation phase inversion method, modified or unmodified nanoparticles are dispersed in the polymer solution prior to casting. The main challenge of incorporating such nanoparticles into polymeric membranes is obtaining a uniform dispersion throughout the polymeric matrix [39]. In this section a comprehensive review on the membrane process and formation especially polymeric membranes is provided. The recent scientific and technological advances of polymeric enhanced membranes using metal and metal oxides nanoparticles fabricated by the immersion precipitation phase inversion method for water treatment are also investigated.

2.2. Recent History of membrane science

The modern membrane science started after the Second World War. Before that practical applications of membranes were very limited. After 1950 the practical applications of the membrane became the main focus of research, and membrane industry grew very fast. Different types of synthetic polymers have been emerged as a result of progress in the organic chemistry. These new polymers had outstanding chemical and mechanical properties which made them able to be used for developing

membranes with good transport and physicochemical properties. Developing thermodynamics and mass transport of membrane processes was another important factor in growing the membrane technology. The membrane process theories developed by several researchers including Staverman (1951), Kedem and Katchalsky (1961), Schlogl and Spiegler [3].

In addition to theoretical development of membrane phenomena, increasing the need for the production of drinking water from sea water and brackish water triggered the large scale development of membranes with certain properties and led to the growth of various membrane based industries. Cellulose acetate was form the pioneer polymeric materials revealed good retention for salts in the reverse osmosis process. However, the permeation rate of the membrane was still very low. Loeb and Sourirajan (1962) overcame this low permeation rate issue with the discovery of anisotropic cellulose acetate. These anisotropic membranes later called asymmetric skin typed membranes. Kesting (1971) shown that the process for of making anisotropic membranes is a phase inversion process in which, a homogenous polymer solution is converted into two phases (a solid polymer rich phase providing the body of the membranes and a polymer poor phase forming the porosity) [3, 22]. It was also discovered that the phase inversion process could be applied to any polymer which is soluble in a solvent. After that different types of polymers such as polyamides, polyacrylonitrile, polysulfone, polyethylene, etc. were used for the preparation of phase inversion membranes. These polymers possess very better

mechanical strength, thermal and chemical stability than the cellulose esters. The next generation of the membranes which significantly changed the reverse osmosis membrane processes were thin film composite membranes (TFC). Development of interracially polymerized composite membranes by Riley and Cadotte (1980) provided higher flux and rejection compared to cellulose acetate membranes. Nowadays, large number of polymeric materials as well as compositing processes are used to develop new high performances membranes which some of them become commercially successful [3, 34].

2.3. Membrane processes

Membrane filtration is a primarily pressure driven separation process which uses semi-permeable membranes. Reverse osmosis and nanofiltration possess smallest pore size and utilize highest pressures, while microfiltration utilize the lowest pressure and has largest pore sizes [40]. Today synthetic membranes are widely used in many different applications including sea water and waste water treatment, dairy and food industry, separation of gasses and vapors, and pharmaceutical industries. It was the beginning of the 20th century when the first man made membranes with controlled pore size and morphology became commercially available and in the middle of this century, it became the main technique in water treatment and desalination.

Two different models have been proposed for describing the transport of water and salutes into permeate. Pore flow and solution diffusion are the two models which the

most significant difference between the two models is the size of the membrane pores. In the pore flow model, pressure flows the solution through the membranes pore which solutes that are larger to pass the pores remain behind the membrane resulting in the separation of solution components. Figure 2.3 (a) presents the pore flow model. In the solution diffusion model, the differences in the solubility of the solution components and the diffusion rate of the components across the membrane are the main reasons lead to separation process. Mobility of the components, concentration, and pressure gradients are the main factors that determine the separation process. Figure 2.3 (b) shows the solution diffusion model. Solution diffusion models normally applies on very dense membranes with the pore size of less than 10 angstrom, and larger pore size. It should be noted that measuring the pore size of the membranes could be very difficult and different indirect methods such as the size of the molecules that will permeate the membranes are used to quantify the membrane pore size [40].

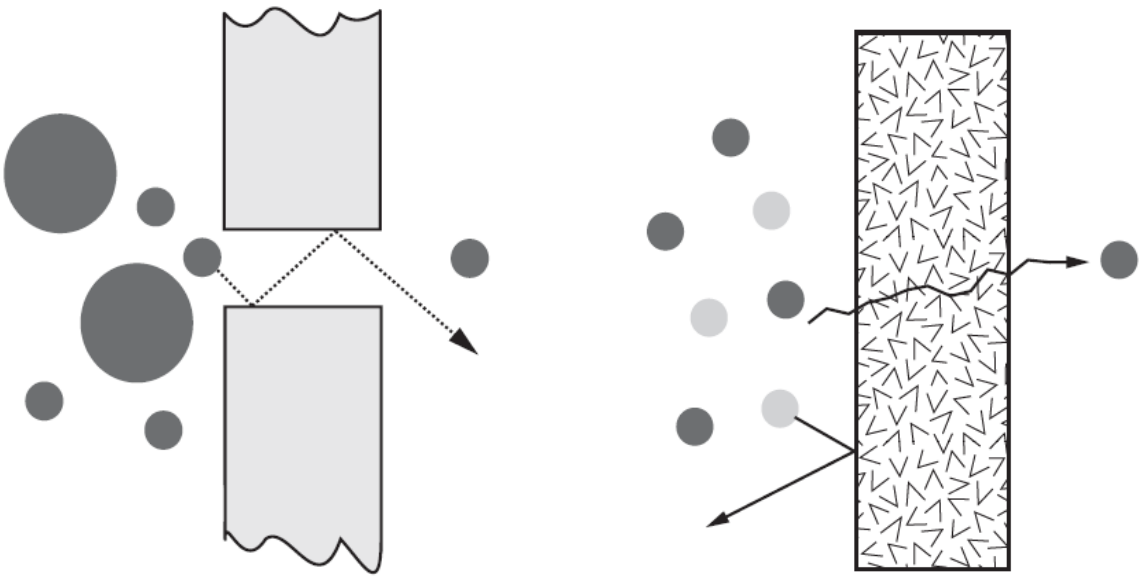

Figure 2. 3 Membrane transport models a) pore flow b) solution diffusion model [40]

Some properties and characteristics of the membranes are in particular important since they are affecting the application and economy of the membrane separation process. Pore size and rejection can be considered as an indication of the capability of the membrane to separate certain molecule sizes, while flux and fouling (membrane life) are influencing the economics of the process. Rejection (R) can be defined by the following equation:

$$R = \left(1 - \frac{C_p}{C_F}\right) \times 100 \qquad \text{Equation 2. 1}$$

where C_p and C_F are solute concentration (mg/l) in the permeate and feed, respectively.

If a solute completely pass the membranes then R will be zero, and in contrast if it rejected completely then R is 1. There are different factors affecting the rejection characteristics of a membrane; such as pore diameter, chemical composition, interaction

between the membrane material, and feed solution. Pore size is an indicator of a membrane separation ability. However, manufacturer often use molecular weight cut-off to present the separation performance of the membranes. Molecular weight cut-off (MWCO) is defined the minimum molecular weight that more than 90 percent of solute will be rejected by the membrane [40].

Compared to the conventional methods in water and waste water treatment, membrane processes are very energy efficient, simple to utilize and produce high quality product. For example, is sea water desalination, reverse osmosis is the only known process and competes directly with distillation. For very large capacity, distillation is generally considered more economic whereas in small and medium applications reverse osmosis is preferred. There are several drawbacks for membrane processes in water treatment. First, the long-term reliability of the membranes are still not very good. In addition, membranes are not mechanically enough robust and can easily damage by the not correct operation such as excessive pressure. However significant progresses have been made recently which resulted to better overall performance of the membranes. Membrane industry is growing very rapidly and developing new membranes with higher chemical, thermal, and mechanical properties extend the membrane industry far beyond its current level.

2.4. Polymeric membranes

Polymers are the most important class of membrane materials. Different polymers can be used to prepare membranes. Chemical and physical properties of the polymers are the important factors that make them suitable for membrane fabrication. A few class of polymers satisfy required properties and can be used to fabricate commercial membranes [3, 41]. In this section the major classes of polymers for membrane fabrication are discussed.

1.4.1. Cellulose acetate

Cellulose acetate is among the first explored polymeric materials to prepare membranes and it is the most investigated type of membrane polymers [41]. Figure 2.4 shows the schematic of cellulose acetate structure. These polymers are hydrophilic and made of cellulose units that have different degrees of acetylation. The optimum chain length of this polymer for membrane application has been reported to be around 100- 300 units with a molecular weight of 25,000-800,000 [41]. The main advantages of cellulose acetates are high flux, good rejection performance, and good mechanical stability. This material is also relatively inexpensive. The main disadvantages of this class of polymers are low thermal and chemical stability. Cellulose acetate membranes are normally can be used at pH ranges of 4-7 and in higher or lower pH numbers the membrane life is very

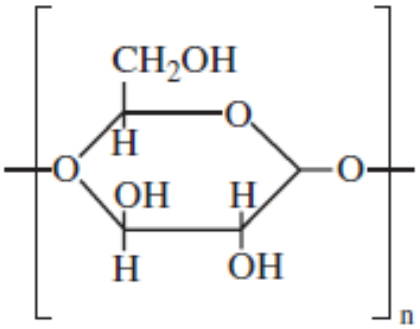

Figure 2. 4 Cellulose acetate polymer

limited. They also have a maximum temperature limit of 40° C. These polymers have low glass transition temperature, which is responsible for their low thermal stability [3, 41]. This restrictions limit the application of the cellulose acetate membranes for separation processes. Despite the disadvantages of this polymer, high permeability and good salt rejection make it a very good candidate for reverse osmosis application.

1.4.2. Polyamide

Figure 2.5 shows the structure of polyamide polymers. These polymers made of macromolecules that have an amide bond in their structure.

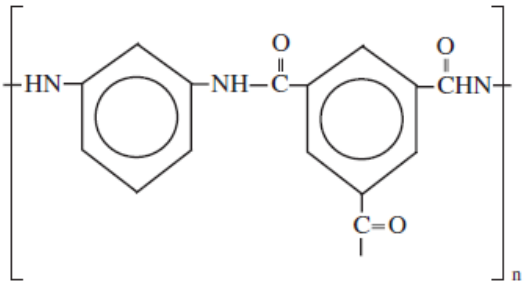

Figure 2. 5 Polyamide polymers

Major groups of polyamide polymers for membrane fabrication include polybenzamide, polyurethane, nylon, and polybenzimidazole. In water treatment applications, these polymers have lower resistance to chloride than cellulose acetates. In contract, polyamide polymers can withstand higher temperature (around 50° C). They also possesses higher mechanical strength and oxidant resistance compared to cellulose acetate. Polyamide membranes are used for reverse osmosis and nanofiltration application [41].

1.4.3. Polyvinylidene fluoride

Polyvinylidene fluoride (PVDF) is one of the polymers in the fluoropolymer group. This polymer has very good resistance to hydrocarbons and oxidizing compounds such as chlorine. PVDF polymers also have good chemical resistance and can withstand the pH in the range of 3-10. The maximum working temperature of PVDF membranes are same as the polyamide polymers (50° C). The disadvantage of this group of membranes that they are harder to process compare to cellulose acetate and polyamide polymers [17, 41]. Figure 2.6 shows the schematic of PVDF polymers.

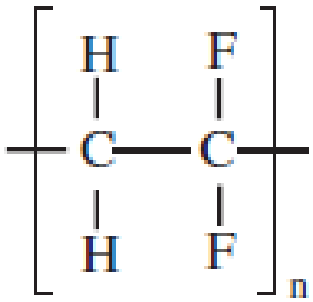

Figure 2. 6 Polyvinylidene fluoride polymer

1.4.4. Polysulfone/polyethersulfone

Polysulfones (PSf) and polyethersulfones (PES) are very important classes of polymers. These polymers are made of diphenylene sulfone units $[(C_6H_5)_2SO_2]_n$. The polysulfone polymers possess very good mechanical, chemical and thermal properties and high T_g values of 190°C for PSf and 230°C for PES. These polymers are widely used as a base materials for ultrafiltration membranes as well as a support material for composite membranes [3]. Figure 2.7 shows the structure of polysulfone and polyethersulfone polymers.

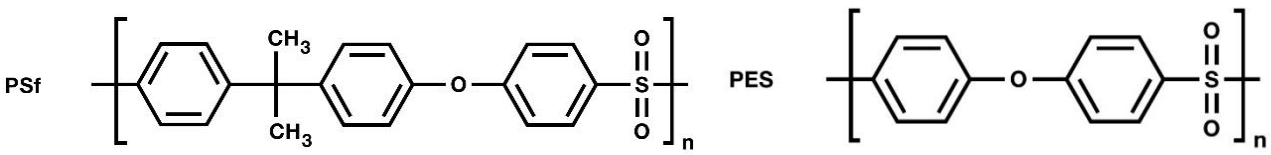

Figure 2. 7 Polysulfone (PSf) and Polyethersulfone (PES) polymers

These polymers has several advantages including a wider pH resistance, higher temperature resistance, and higher resistance to chlorine compared to other polymeric materials. They are also easy to manufacture which make them a suitable candidate to produce membranes with different thicknesses and pore sizes. PES and PSf membranes can tolerate temperatures around 120°C and pH in the range of 1 to 14. The other considerable difference of polysulfones and cellulose acetates are in their morphology. Cellulose acetated are spongy in the layer beneath the skin layer while PES and PSf membrane contain finger like pore structure. This cause to a higher flux of polysulfone membranes compared to the other class of polymeric membranes [3, 41].

2.5. Preparation of polymeric membranes

The aim of membrane fabrication is to modify the material by appropriate techniques to obtain a structure which is suitable for a specific separation. The type of material determines the fabrication method, membrane morphology, and the obtained applications. Several methods can be used to prepare polymeric membranes. The most important techniques are stretching, track etching, sintering, phase inversion, sol gel, and vapor deposition [3].

Among these methods phase inversion is the most widely used technique to prepare polymeric membranes. This method is very versatile allowing different types and morphologies to be achieved. This technique is described in the following section.

2.6. Phase inversion process

Phase inversion technique was introduced for the first time by Leob and Sourirajan in the 1960's. This method is based on the research of Strathmann et al. describing the thermodynamics aspects of de-mixing in polymer solutions. De-mixing can be divided to two categories; as instantaneous de-mixing and delayed de-mixing processes, which lead to different types of membrane structure [22]. During the phase inversion process, a thermodynamically stable polymer solution is transferred to form a solid porous material. This process is preceded by a de-mixing process. The polymer solution undergoes liquid-liquid de-mixing and it converts into a polymer-rich and a polymer-lean phase. The polymer rich phase solidifies and forms the body of the membrane while the polymer lean phase will lead to pores in the solidified material. The solidification of the polymer rich material may occur through the processes such as gelation, verification, or crystallization [3]. Phase inversion technique is divided to several below listed categories based on their de-mixing process;

- Immersion precipitation

- Controlled evaporation (evaporation of the volatile solvent from the polymer solution, consisting of solvent/nonsolvent mixture)
- Thermal precipitation
- Precipitation from the vapor phase

Among these methods, immersion precipitation is the most widely used technique and membranes from a wide variety of polymers can be synthesized by this method. Any polymer that is soluble in a solvent or solvent mixture can be used in this technique. The phase inversion process is complicated and thermodynamics and kinetics of this process still is not fully understood. The fact that the whole phase inversion process finished in a few milliseconds, making it even more challenging [3]. Generally, the pore size and total porosity of the membrane determine by the rate of diffusion of solvent to the coagulation bath and diffusion of nonsolvent from to the polymer solution. Ternary phase diagram of polymer-solvent-nonsolvent usually use to discuss and describe the membrane precipitation process. The type of de-mixing can be instantaneous or delayed de-mixing, which greatly affects the morphology of the membrane. Typical diagrams for this two types of de-mixing is shown in Figure 2.8. The ternary system consists of a one phase region where all the components are miscible and a two-phase region where the systems is separated to a polymer lean and a polymer rich phase.

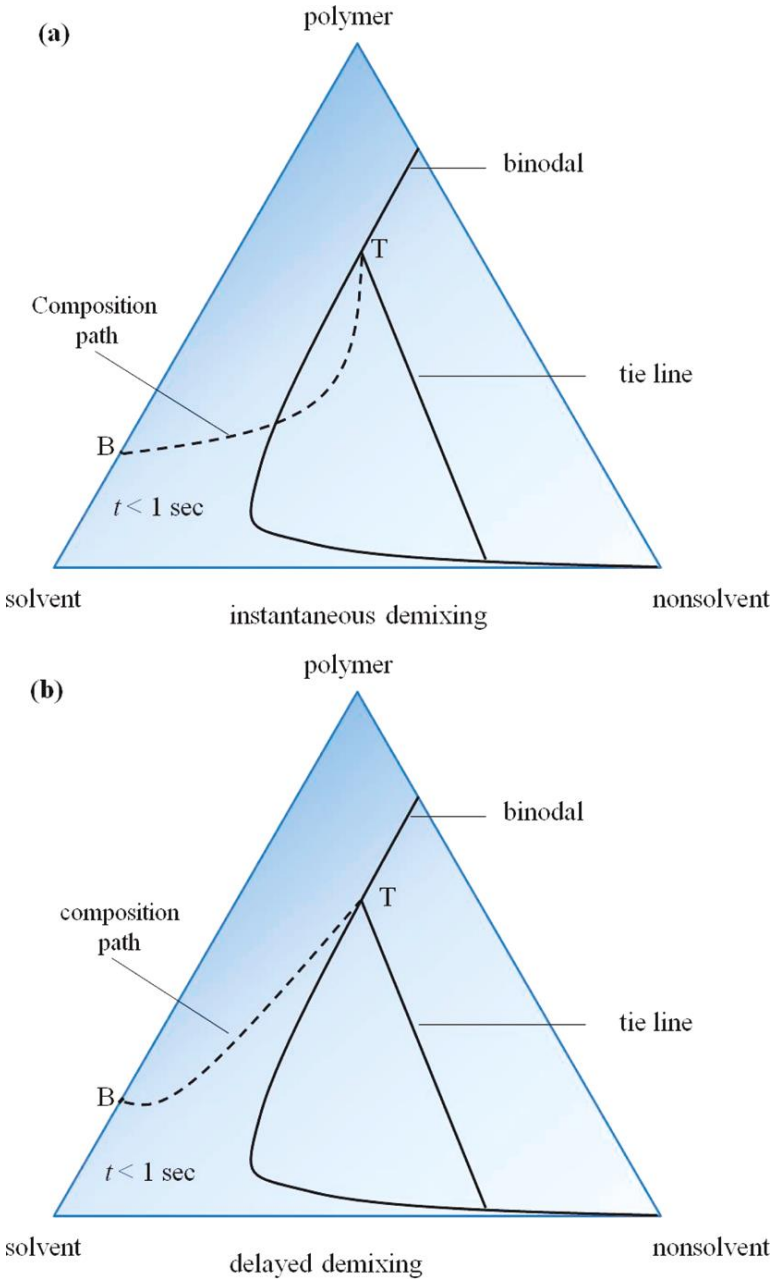

Figure 2. 8 Composition paths of a casting film demonstration a) instantaneous de0mixing and b) delayed de-mixing [22]

The liquid-liquid phase boundary is called binodal. Every composition inside the binodal region will de-mix into two different phases, which are in thermodynamic equilibrium with each other [22].

The composition of the film during the phase inversion process can be expressed using the ternary diagram. It can be seen in figure 2.8 (a) that at t<1, the composition path crosses the binodal line, which means the de-mixing starts immediately. Figure 2.8 (b) shows all the compositions blow the top layer remain in the single phase region. After a long time, the compositions below the cross line with cut the binodal and will have de-mixing. These two di-mixing processes lead to two distinctly distinguished membrane morphologies.

2.6.1. Processing parameters:

The membrane morphology and performance depend on several processing parameters. Composition of the casting solution including polymer concentration, type of the solvent, type of the support material, thickness of the cast film, and temperature of the casting are among the factors that affecting the final morphology of the membranes. Composition of the casting solution is the most important factor that influences the de-mixing process and eventually morphology of the membranes. The choice of the solvent and non-solvent is another factor that alter the phase precipitation. The miscibility of solvent and nonsolvent and the affinity between polymer and non-solvent affect the de-mixing process, and control the membrane structure. Moreover, different types of

additives can be added to polymer solution. High and low molecular weight additives can be added to improve the performance of the membranes. Frequently used additives include polyethylene glycol (PEG), propionic acid (PA), surfactants such as sorbitan monoleate (Span-80), alcohols, dialcohols, water, polyethylene oxide (PEO). Another factor that can affect the de-mixing process is the casting temperature. Temperature changes the viscosity of the casting solution and therefore the diffusion rate of solvent-nonsolvent [3, 22].

2.7. PES membranes incorporated with metal oxide nanoparticles

Using nanomaterials in the fabrication process of PES and PSf membranes has received lots of attention during recent years, particularly for membrane flux enhancement, fouling mitigation, antimicrobial functionalities, and introducing contaminant absorption capability to membranes [8]. In addition, incorporation of nanomaterials can also changes the pore structure of membranes and subsequently affects their water permeability and solute rejection [8]. Furthermore, it has been reported that membrane charge density also changes by adding nanoparticles due to the surface functional groups of the nanoparticles [8, 11]. Also, almost all of the different types of nanoparticles enhance mechanical stability of the membranes [8, 12]. The main drawback of incorporation of nanoparticles into polymeric membranes is the poor dispersibility of the nanoparticles in

the polymer matrices and aggregation of nanoparticles in polymeric solution due to surface interactions [7]. Ionic strength, applying surfactant, and pH of the solution are among the factors that affect the aggregation between particles [7, 42]. Modifying nanoparticles surface or using hybrid nanoparticles attracted a lot of attention recently to avoid particle agglomeration in polymeric nanocomposite membranes [8, 43-45]. The effect of incorporating nanoparticles into PES and PSf membranes on morphology and performance of the nanocomposite membranes would be discussed further in the following discussion. Table 2.1 summarizes the effects of adding metal oxide nanoparticles according to the improvement the functionality of nanocomposite membranes.

2.7.1. Membranes with silver nanoparticles

Adding silver nanoparticles to PES and PSf membranes has been investigated widely in order to overcome the fouling and biofouling properties of sulfone membranes [7]. Sulfone membranes are hydrophobic intrinsically and prone to fouling, which leads to a decrease in membrane flux, deteriorating the membrane structure, an increase in energy costs, higher cleaning frequency, and shorten membrane life [7, 29].

Table 2. 1 Effects of adding nanoparticles to polysulfone membranes (*: modified particles)

Main Performance	Polymer Matrix	Filler	Ref.
Fouling Mitigation	PSf	Ag	30,32,1,33
		TiO_2	48,27,29
		SiO_2 coated GO	60
		Modified ZrO_2	8,82
		ZnO	94
		Alumina	78,74,73,72
	PES	Ag	31,83*
		TiO2	51,49,38,46,10,43
		Modified Iron oxide	59(Magnetic Casting)
		Modified SiO_2	28
		Alumina	75,69,72
		ZrO_2	44,80,81
		Mangenese dioxide	84,85
		ZnO	14,91
		Se and Cu	101
Permeability	PSf	Ag	34
		TiO_2	45,41*, 29*
		SiO_2	64,65,60*
		Al_2O_3	78,74
	PES	Ag	83*
		TiO_2	40,53,49,38,46,43*
		SiO_2	66,28*
		boehmite	68,77*
		ZrO_2	80,81
		HMO	84,85
		ZnO	14
Improve Solute Rejection	PSf	Silver	34
		ZnO	91
		Modified SiO_2	60
		TiO_2	53, 41*, 27*
		Alumina	72
	PES	SiO_2	66
		boehmite	68, 77*
		Alumina	72
Anti-Bacterial and Anti-virual	PSf	Ag	30,32,1,4,34
	PES	Ag	35,36,83*
Heavy metal Ion Removal Ability	PES	Fe-Mn Binary oxide	
		Modified Iron oxide	20,55,22,57,58
		HMO	86
		Al_2O_3	19

Biofouling results from the accumulation of assimiable organics, biofilm formation, and attaching and growth of microorganisms on the membrane surface. It occurs most often during nanofiltration and reverse osmosis processes when membranes cannot be disinfected with chlorine in order to kill the bacteria [29]. Several studies have investigated improving anti-biofouling performance of the silver containing nanocomposite membranes by enhancing hydrophilicity of membranes surface, preventing of attaching microorganisms to the membrane surface, and/or growth inhabitation of bacteria as a result of presence of silver ions [21, 46-48]. J. Taurozzi et al successfully inhibited biofilm growth on the membrane surfaces by incorporating 1.98 and 3.84 wt.% of silver nanoparticles to the PES membranes [49]. They reported two different pathways to incorporate silver particles in the membrane structure, either by ex-situ synthesis of nanoparticles and then adding to the casting solution or via an in-situ reduction of ionic silver by the polymer solvent [49]. A similar study was carried out by P.F. Andrade et al incorporating 2 wt. % silver nanoparticles via ex-situ and in-situ method (using different polymeric solvent for reduction of ionic silver). They reported a preferential distribution of nanoparticles in the top and bottom of the membrane surface [46]. In both studies, a very strong anti-adhesion property of bacteria to the membrane surface and inhabitation of biofilm growth has been reported. In addition, in situ approach to synthesize nanocomposite membranes displayed improved anti-fouling property compared to those membranes prepared by ex situ methodology [46, 49]. M.

Zhang et al, reported that adding biogenic silver nanoparticles to PES nanocomposite membranes effectively inhibited formation of biofilms and showed good anti-fouling performance after 9 weeks of using membranes [47]. In another study, nanocomposite membranes containing silver ions have shown improved anti-biofouling properties and very low bovine serum albumin (BSA) surface adsorption by adding up to 2.5 wt. % of silver nanoparticles. This improvement attributed to the combination of antibacterial and anti-bacterial adhesion properties of silver contained membranes [18].

One of the most important factors that affect the biofouling of the sulfone membranes is the degree of hydrophilicity of the surface. The contaminants prefer to attach to more hydrophobic surfaces [18], and hydrophilic surfaces may prevent membrane from hydrophobic microorganism attachment which, in turn, demonstrate anti-fouling properties [28]. Studies have revealed that addition of silver nanoparticles to the PES and PSf membranes significantly decreases the static water contact angle and induces hydrophilicity to the membrane surface [18, 21, 28, 46, 47, 50, 51]. For example, A. Alpatova et al reported a decrease in membrane surface contact angle from 72 degrees to 61 degrees by adding 2.5 wt.% of silver nanoparticles [18]. In another study, water contact angle of 51 degrees has been reported by incorporating 1 wt.% of silver nanoparticles to polysulfone membranes [51]. Several researchers reported the increase in water flux through the membrane is due to increasing hydrophobicity, increasing porosity, and pore size by incorporating silver nanoparticles [18, 46, 47]. However, A. Alpatova et al reported

no change in average pore size of membranes by adding silver, and attributed the enhancement in permeate flux to the increase of the hydrophilicity of the membrane surface due to the introduction of silver nanoparticles to the casting mixture [18]. In another study, a decrease in the permeability of membranes because of the increase in the silver nanoparticles content has been reported. This phenomena explained by an increase in the number and size of the silver nanoparticles on the membrane surface due to agglomeration and an increase in the membrane surface roughness [50]. As the porous structure of the membranes has not been investigated in Alpatova's paper, the decrease in permeability might also attribute to the changing in the membrane porosity or pore blocking as a result of particle agglomeration.

Although membrane filtration is known as a disinfection alternative in water treatment, disinfection operations (via UV, ozonation, or chlorination) after the membrane filtration process are still recommended as a secondary bacteria control barrier [28, 29]. The other promising disinfection option is to incorporate an antibacterial nanoparticle such as silver ions into the polymeric membranes. Silver is believed to act as an antibacterial agent either upon contact to the bacteria or as released ion in the media [28, 52, 53]. Several studies have shown the significant antibacterial and antiviral properties of silver containing nanocomposite membranes. Furthermore, they reported the bacteriostatic (inhabitation of bacterial growth) and bactericidal (killing of inoculated bacteria) activities of PES or PSf silver containing nanocomposite membranes [18, 21, 28,

29, 46, 49-52, 54]. H. Basri et al improved the anti-bacterial performance of silver-containing PES nanocomposite membranes by changing the polyvinylpyrrolidone (PVP) and 2,4,6-triaminopyrimidine (TAP) content of the phase inversion casting solution. They showed 100% bacteria inhabitation after using the membrane in C. coli bacteria suspension filtration. Also, it was mentioned that nanocomposite membranes containing silver nanoparticles exhibit better antibacterial activity to gram-negative bacteria [52]. A. Mollahosseini et al have reported better anti-bacterial performance for smaller silver nanoparticles (30 nm particles compare to 70 nm particles) due to the higher silver release form nanocomposite membranes and higher surface to volume ration of smaller particles as well [51]. Also incorporation of silver nanoparticles to PES/PSf membranes significantly enhanced virus removal capability of the membranes [21]. Some possible mechanisms for virus removal including change in the membrane permeability, depth filtration, electrostatic adsorption, and inactivation of viruses by Ag^{+} ions have been reported [21].

Despite the extensive use of silver nanoparticles in synthesizing nanocomposite membranes, still there are some challenges which need more investigations [21]. According to World Health Organization (WHO) guideline, the Ag threshold in drinking water is limited to 100 ppb [55]. Therefore, leaching of silver ions from membranes to filtrated water must be investigated carefully. In addition, antibacterial and antiviral activities of membranes may be lost due to the rapid silver depletion [21]. This calls for

future research that leads to improved silver nanoparticle incorporation and controlled release. It can be done by concentrating the particles to the selective layer of the membrane using fabrication of functionally graded nanoconmposites and thin-film nanocomposites. In addition, encapsulating silver particles in a polymer and then covalently binding it to membrane polymers either directly or through the use of cross linkers can be utilized to improve nanoparticle incorporation in polymeric membranes [21]. Another challenge is the uniform distribution of silver nanoparticles in the polymeric matrix of the membranes. Using hybrid nanoparticles and surface modification of the nanoparticles have recently shown a great potential to address this challenge [56]. For example M. Zhang et al have embedded biogenic silver nanoparticles in PES membranes and reported very good antibacterial activity and silver leaching in the WHO accepted threshold. They reported the attachment of silver particles to a bacterial carrier to prevent them from aggregation and thus preserving their high surface area to mass ratio [47]. Additionally, it has been shown that using the in-situ approach via reduction of ionic silver by the polymer solvent results in better distribution of nanoparticles [46, 49].

2.7.2 Membranes with TiO_2 nanoparticles

TiO_2 nanoparticles as an additive to organic membranes have attracted considerable attentions because of good physical and chemical characteristics, antibacterial properties, commercial availability, as well as its potential antifouling abilities. However, most of the works carried out focus on the use of TiO_2 powder suspended in the water as a catalyst

[7, 13, 37, 57, 58]. Also, introduction of titanium oxide nanoparticles to the membrane structure enhances membrane water permeation and hydrophilicity of surface of the membranes due to nanoparticles' superhydrophilic properties and increasing nanocomposite material affinity to the water [28, 57].

The pore structure and morphology of the nanocomposite membranes are expected to depend on different variables such as viscosity of the polymer solution during casting, liquid-liquid de-mixing process , polymer chain packing, and the degree of agglomeration of the nanoparticles [59, 60]. Morphology of nanocomposite membranes changes significantly by introducing TiO_2 nanoparticles even in low concentrations. Several studies reported that the addition of TiO_2 nanoparticles results in the increase of the micro-void dimensions and more open structure in the membranes. Also, the sponge like structure of membranes will be suppressed [13, 57] even in very small amount of added nanoparticles [43] due to the hindrance effect of nanoparticles during the phase inversion process [57]. M. R. Esfahani reported that overall porosity and mean pore size of the nanocomposite membranes increased compared to pure polysulfone membranes as a result of disruption of polymer chains packing by nanoparticles [59, 61] which is in agreement with the results of other researchers [57, 62-65]. Fig. 2.9 shows that the TiO_2 addition results in the increase of skin layer pore number and micro-voids growth compared to PSf neat membranes [63]. The higher filler concentration (≥ 3%) induces

nanoparticles aggregation, and produces a considerable number of large surface pores mostly formed in the vicinity of TiO_2 aggregates [63].

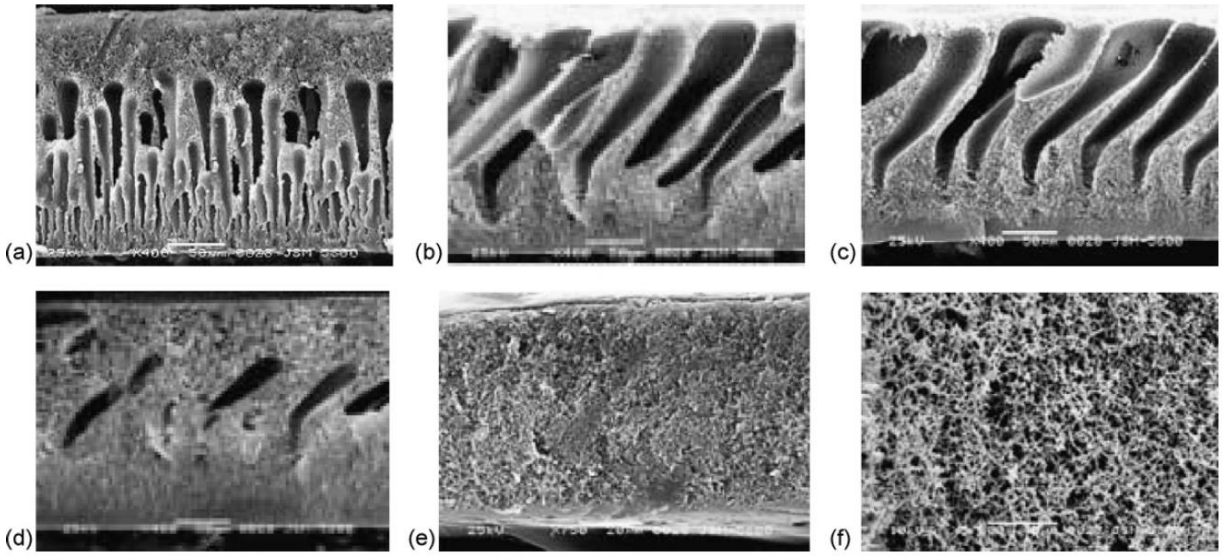

Figure 2. 9 SEM pictures of the morphology of PSf/TiO_2 membranes with a) 0 wt. % TiO_2, b) 1 wt.% TiO_2, c) 2 wt.% TiO_2, d) 3 wt.% TiO_2, e) 5 wt.% TiO_2 and f) e's local magnifying figure [45].

Increasing the hydrophilicity of the membrane surfaces and mitigation of fouling is one of the main advantages of adding TiO_2 nanoparticles to PES membranes [13, 24, 57-59, 62-68]. V. Vatanpour reported improving of the membrane hydrophilicity as a result of introducing hydrophilic –OH groups on the membrane surface [67]. In another study, the fouling performance of PES/TiO_2 (0, 0.3, 0.5 and o.7 wt. % TiO_2) nanocomposite membranes has been investigated using bovine serum albumin (BSA) solution. Results of this study showed that increasing TiO_2 content to 0.5 wt. % led to a decrease in the membrane fouling. However, increasing TiO_2 content to 0.7 wt.% decreased antifouling performance of the membrane [69]. This happened because of blockage and collapse of

the membrane pore structure by excessive amount of TiO_2 as the defective pore structure of the membranes was damaged easily by water pressure during filtration process and more of the BSA solute remained in the membrane pores [59, 69].

Permeability is another membrane property that improves significantly due to the combination effect of increasing the hydrophilicity of membrane surface, increasing porosity, and mean pore size of the membranes by adding TiO_2 nanoparticles [13, 26, 62, 64, 67]. A. Sotto et all have shown enhancing the permeability of the nanocomposite membranes by increasing TiO_2 concentration, which is in agreement with the observed trend for the membrane surface contact angle measurements. They mentioned that the higher water permeability of membranes containing nanoparticles compared to neat PES membranes might be associated with a higher affinity of nanoparticles to water in comparison with the hydrophobic polymer. This led to an increase in the pore size of the membranes during phase inversion process [64]. However, in another study by the same research group, a decrease in permeability by adding TiO_2 nanoparticles after an optimum concentration has been reported. This was explained as a result of pore blocking of membranes due to the nanoparticles aggregates and also larger size TiO_2 cluster formed, which cannot be entrapped by the polymer network during phase inversion process [57]. In another study by J. F. Li et al a decrease in nanocomposite membrane permeability by low loading amount of TiO_2 nanoparticles (1-2 wt. %) has been reported. This has been contributed to the formation of denser skin layer at the surface of the

nanocomposite membranes compared to neat PES membranes [58]. However, adding a higher amount of nanoparticles led to more loose membrane structure and enhancement of the membranes permeability significantly [58]. The rejection potential of nanocomposite membranes also is affected by adding the TiO_2 nanoparticles. Razmjo et al have reported the molecular weight cut off (MWCO) at the rejection of 90%, shifts from 100 kDa to 240 kDa for modified TiO_2 nanocomposite membranes in comparison with PES membranes. They attributed this phenomena to larger pore size of the nanocomposite membranes [13]. A slight decrease of rejection of organic compounds (BSA and methylene blue dye) by adding TiO_2 nanoparticles due to the formation of membranes with larger porosity and surface pore size is reported in other researchers' works as well [62, 64].

Some research have been carried out by loading low concentrations (less than 0.7 wt.%) of TiO_2 nanoparticles in nanocomposite membranes in order to decrease the aggregation issue of particles, improve the water permeability, and increase the fouling resistance of these membranes [57, 62, 64, 69]. A. Sotto et al investigated adding ultralow concentration of TiO_2 nanoparticles (0.035- 0.375 wt.%) and reported around 12% decrease of the nanocomposite membrane fouling rate [64]. V. Vatanpour et al also investigated the effect of size and types of TiO_2 nanoparticles on the structure and antifouling properties of PES membranes. The results of this study revealed that the particles with higher surface area (Millennium PC 500 TiO_2 nanoparticles compare to PC 105 type with 320 and 81.5 m^2/g

surface area, respectively) showed higher aggregation, which led to pore clogging and reduced the pure water flux of the membranes [67]. Several researchers reported that incorporating TiO_2 nanoparticles in the nanocomposite membranes led to better mechanical properties even in membranes with a higher amount of porosity [58, 63, 65]. This phenomena could be attributed to the interaction between the TiO_2 nanoparticles and the polymeric membranes, in which TiO_2 could act as a crosslinking point in the nanocomposite membranes to link the polymer chains and increase the rigidity of the polymer [58]. However, by loading a small amount of TiO_2 nanoparticles, the effect of increasing porosity may overcome the interaction between nanoparticles and polymer chains. As a result, mechanical properties of the nanocomposite membrane decrease [64]. Also uniform distribution of nanoparticles is another factor that can improve the mechanical properties of nanocomposite membranes [69]. Several studies have demonstrated the increase of thermal stability of nanocomposite membranes by adding TiO_2 nanoparticles [13, 57, 58, 62-65, 69-71]. A. Sotto et al have shown an increase in the rate of decomposition of the nanocomposite membranes by adding nanoparticles. This can be interpreted by the interaction of TiO_2 nanoparticles and polymeric chains, which led to an increase in the rigidity of the macromolecular chain and restrict the polymer chains movements during heating. As a result, the interaction between the nanoparticles and the polymer chains enhanced the energy needed by polymeric chain movement and breakage [57, 65].

Agglomeration of nanoparticles due to the attractive Van der Waals forces can increase the in-homogeneities and defects in the membrane morphology [62]. It is well known that the TiO_2 nanoparticles show a tendency to aggregation due to their high specific surface area and the hydroxyl groups on their surface [57]. J. Maria Arsuaga et al have reported an abrupt increase in the particle size of TiO_2 nanoparticles as a result of dispersion into the polymeric solution. They also reported further increase took place during the phase inversion process, and showed the particle size increases gradually during the entire membrane preparation route especially in higher amount of nanoparticles [62]. Some researchers applied modifications to avoid agglomeration and improve dispersion of TiO_2 nanoparticles [13, 57, 65, 72]. A. Razmjou et al used mechanical modification (grounding and sonication) and chemical modification (surface modification of TiO_2 nanoparticles with 3-aminopropyltriethoxysilane (APTES) as silane coupling agent). They reported a significant improvement in flux recovery from 57% for unmodified nanoparticles to 84% for chemically and mechanically modified particles, and 18% improvement in hydrophilicity at 2 wt.% TiO_2 loading [13]. Also, another study investigated the use of ethanol (EtOH) as an additional polymer co-solvent for the membrane synthesis to decrease particle agglomeration [57]. Although the particle dispersion was not enhanced, a structural change from a sponge-like to a finger-like structure and a significant improvement on fouling resistance of modified membranes was observed [57]. Surface modification of TiO_2 nanoparticles by the anionic surfactant

sodium dodecyl sulfate (SDS) is another method which has been used to improve dispersion of TiO_2 nanoparticles [65].

In summary, the presence of the TiO_2 nanoparticles in the PES and PSf nanocomposite membranes significantly increases fouling resistance and permeability. Incorporation of TiO_2 nanoparticles into the membranes also enhances the hydrophilicity and mechanical strength of the nanocomposite membranes. In addition, adding TiO_2 nanoparticles mostly increases the porosity and mean pore size of the membranes, which may lead to a reduction in their rejection potential. Therefore, more investigations are needed to maintain the desirable rejection performance of membranes by incorporating TiO_2 nanoparticles. In spite of some published works, which have been done to avoid aggregation of nanoparticles, further research is still needed to obtain better dispersion of nanoparticles and prevent agglomeration. Excessive nanoparticle agglomeration may deteriorate nanocomposite membrane functionality. Furthermore, considering the anti-bacterial properties of TiO_2 nanoparticles [7] there is no research in disinfection of water using TiO_2 incorporated PES and PSf nanocomposite membranes.

2.7.3 Membranes with Iron oxide nanoparticles

Iron is one of the most plentiful elements in the earth [7, 68]. The facileness of resources, ease in synthesis, and great affinity toward heavy metals made ferric oxides nanoparticles to be low-cost adsorbents for toxic metal sorption [38, 68, 73]. In addition to their intrinsic

adsorptive properties, it is also possible to improve iron oxide nanoparticle hydrophilicity and adsorption performance to obtain new properties and capabilities using nanoparticle modification by other chemicals and coupling with desired functional groups [38, 74-76]. Iron oxide nanoparticles have been utilized in PES and PSf membranes preparation to improve adsorptive removal of heavy metals and also improve the membrane properties such as permeability and fouling resistant. In 2012, P. Daraei et al incorporated iron oxide/polyaniline core-shell structure adsorbent in a PES matrix to obtain a new nanocomposite membrane with enhanced copper ion elimination capability and excellent reusability. They added 0.01, 0.1 and 1 wt. % of nanoparticles to the PES membranes, and reported 80% removal of copper ions from the feed with 10 mg/l of CU(II) after 2 h for the membrane containing 0.1 wt.% nanoparticles. It was also mentioned that the most probable adsorption isotherm was Redlich-Peterson isotherm which expresses a relatively complex adsorption mechanism. The unusual result of this study is decreasing water flux in the nanocomposite membranes compared to the pristine PES membranes, which has been described by facial pore blockage by nanoparticles and reduction of pore size in the nanocomposite membranes [74]. Fig. 2.10 shows the Cu(II) rejection results for nanocomposite membranes containing 0.01, 0.1, and 1 wt. % of modified iron oxide nanoparticles at two different feed concentration [74].

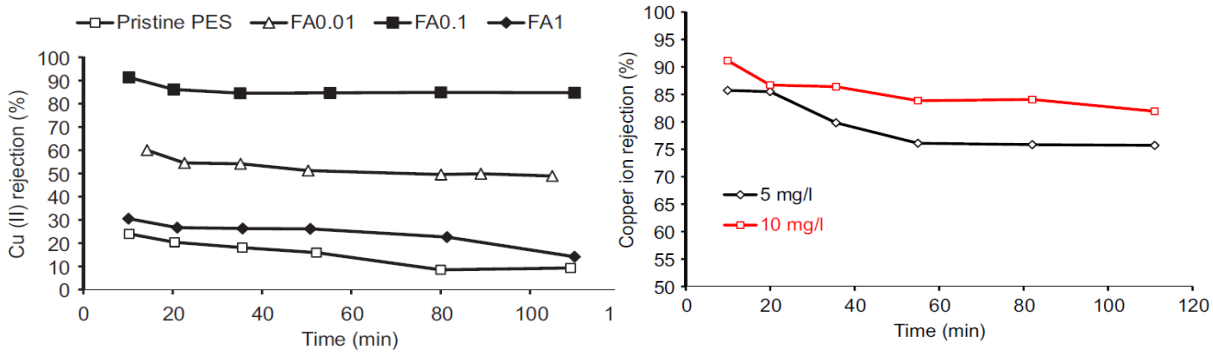

Figure 2. 10 a) Cu(II) ion rejection of the PES nanocomposite membranes with 0,0.01, and 0.1 wt.% of modified iron oxide nanoparticles at 4.5 bar of TM pressure using 20 mg/l of aqueous $Cu(NO_3)_2$ solution b) Rejection of copper ions versus time at low concentrations of feed solution for nanocomposite membranes containing 0.1 wt.% modified iron oxide nanoparticles [74]

In an another attempt to simultaneously increase the permeate water flux and Cu(II) removal of PES membranes, iron oxide nanoparticles have been modified by silica coating, metaformin-modified silica coating, and amine-modified silica coating. The result of this study showed that the membrane ability for removal of CU(II) in solutions containing low concentrations of copper ions (20 mg/l of aqueous $Cu(NO_3)_2$) increased to more than 92% after 90 min [38]. In addition, the water flux of the nanocomposite membranes was enhanced due to the surface treatment of nanoparticles. The enhancement of Cu(II) removal of nanocomposite membranes might be due to the more adsorption sites and nucleophile groups (N atoms) of the modified nanoparticles [38]. Moreover, more hydrophilicity of modified nanoparticles caused better dispersion of

them in the membrane matrix as well as on the membrane surface during phase inversion process. This increased available active sorption sites on the membrane surface. Meanwhile, growth in membrane sub-layer porosity, an increase in the mean pore size of the membranes, and an increase in the hydrophilicity of the membranes surface by incorporating modified iron oxide nanoparticles are three main factors responsible for improving the water permeability of the membranes. Additionally, the membranes usability results showed a reduction of about 4% was achieved after each run of copper removal/regeneration test. This showed a relatively acceptable reusability of the modified nanocomposite membranes to be applied for removal of copper ions after being used for several times [38]. It can be concluded that modifying iron oxide nanoparticles with higher hydrophilic modifiers such as metaformin, which contains nucleophile functional groups, is preferred to less hydrophilic modifier such as polyaniline [38, 74]. Polyethylene glycole (PEG) coated cobalt doped iron oxide (Co-Fe_2O_3)/ PES nanocomposite membranes have also been investigated and a 96% rejection of Cu(II) ions at pH 7 from 20 ppm copper aqueous solution and only a 7% drop in rejection performance even after 5 treatment cycles has been reported. The modified membranes exhibited their best removal performance at pH 7 since there is no competition between the Cu(II) ions and hydrogen ions for the active sites on the embedded nanoparticles. Furthermore, increasing the coated PEG nanoparticles concentration would help to increase the pore size of the

membrane and therefore increase the molecular weight cut-off (MWCO) and water flux of the nanocomposite membranes [39, 76].

Although all of the research on Iron oxide nanoparticles doped PES and PSf membranes have been concentrated on removal of copper ions from water, R. J. Gohari et al investigated the effect of the addition of Fe-Mn binary oxide (FMBO) nanoparticles to the PES membranes for removal of As(III) ions from contaminated water solutions. They reported a 75% of As(III) ions removal from a solution containing initial As(III) of 20 mg/L concentration after 2.5 hours. In this research, a very high amount of FMBO nanoparticles have been incorporated to the PES membranes, in which agglomeration was observed obviously in the nanocomposite membranes [77]. However, the results of As(III) ion removal tests of this study were not significant, but a 140% increase in water flux for the membranes containing nanoparticles was reported. The combination effects of a decreased contact angle, an increased porosity, and a greater surface roughness and contact area upon incorporation of nanoparticles were considered as the main reasons for high observed water flux [77]. In another study, three different self-synthesized magnetic iron oxide particles were mixed by PES and casted under magnetic field during phase inversion process of membrane fabrication [78]. Neat Fe_3O_4, polyaniline coated Fe_3O_4, and Fe_3O_4 coated multiwall carbon nanotube (MWCNT) were incorporated in the PES membranes, and it was revealed that adding the magnetic nanoparticles improved membranes antifouling property (reduced the irreversible fouling ratio). They also

reported that casting of the membranes under a magnetic field offered even better membrane performance [78]. This can be explained by lower agglomeration of the nanoparticles and preventing pore blockage caused by poorly dispersed nanoparticles [78].

In spite of the high potential of iron oxide nanoparticles in removing heavy metal ions from water due to their high affinity with most of heavy metals, incorporating of these nanoparticles in the PES and PSf membranes needs more investigation. Modification of iron oxide nanoparticles to enhance their dispersion in polymer matrices is the main challenge in fabrication of iron oxide containing nanocomposite membranes. Additionally, there is no study on the effects of using iron oxide nano-fillers in the PES or PSf nanocomposite membranes to remove Pb, Ni, or Cr ions from water and there are only very limed studies on As removal. Nanoparticle modification also can be investigated to achieve higher adsorption ability in order to increase the heavy metal removal capability of the nanocomposite membranes.

2.7.4. Membranes with Silica nanoparticles

Silica (SiO_2) nanoparticles have been investigated intensively and proven to improve the hydrophilicity and performance of the polymeric membranes [7]. Recent studies on silica containing PES and PSf nanocomposite membranes show that most of the properties of the membranes especially water permeability, hydrophilicity, and anti-

fouling ability are affected by incorporating the silica nanoparticles due to the hydrophilic groups on the surface of the particles [12, 79-81]. Different methods including interfacial polymerization, sole gel, and phase inversion have been used for fabrication of membranes containing silica nanoparticles [82-84]. In the year 2000, P. Aerts et al investigated the effect of adding 1-3 vol. % of aerosol to polysulfone membranes on formation process and membrane morphology [85]. They reported that the nanocomposite membrane thickness increased by adding more silica nanoparticles to the solution, which indicated a slower transport of solvent/nonsolvent during the membrane formation process. Incorporation of nanoparticles to the polymeric membranes also led to formation of macro-voids with a more irregular and round shape and overall decrease in macro-void porosity amount [85]. This research group also studied the performance of nano silica incorporated polysulfone membranes and showed that adding up to 2 vol.% of aerosol increased the membrane permeability without losing its rejection properties [86]. However, by loading a greater amount of nano-fillers, both permeability and rejection of the membranes decreased [86]. In another research, SiO_2 nanoparticles modified by sodium dodecyl sulfate (SDS) with the average size of 30 nm have been added to PES membranes by 0.5, 1, 2 and 4 wt. %. The fabricated nanocomposite membranes demonstrated an increase in the skin layer thickness, a decrease in the finger-like pore size, and an increase in the connectivity of the pores between the sub-layer and bottom layer in comparison with pure PES membranes [87]. An increase in the

hydrophilicity and permeability of the membranes and also 97% retention of bovine serum albumin (BSA) for the nanocomposite membranes contacting 2 wt.% of silica nanoparticles was also reported [87].

Recently, some studies have been conducted to improve the dispersion of silica nanoparticles in the polymeric membranes using hybrid nanoparticles [44, 79]. J. Yin et al added modified silica nanoparticles by poly(2-(dimethylamino)ethylmethacrylate-co-3-dimethyl(methacryloyloxyethyl)ammoniumpropanesulfonate) (PDMAEMA-co-PDMAPS) grafting to the PES membranes and reported a significant enhancement in the pure water permeability, oil in water emulsion permeability, and the anti-fouling property of membranes. Also, the modified nanoparticles showed better dispersibility in the organic solvent in comparison with the bare SiO_2 nanoparticles. On the other hand, improving in binding ability of modified nanoparticles and PES membrane matrix made the nanoparticles stably entrapped in the PES membrane for a long time [44]. In another study, SiO_2 coated graphene oxide (GO) nanoparticles have been synthesized and incorporated to the PSf membranes to enhance dispersion and take advantage of synergism between the characteristics of SiO_2 nanoparticles and GO to improve membrane performance. The results of this study showed that compared with SiO_2/PSf and GO/PSf membranes, SiO_2-GO/PSf membranes presented the best overall properties including water flux rate, protein rejection, and antifouling ability as a result of unique properties of SiO_2-GO nano-hybrid and a better dispersion of the nanoparticles in the

polymeric matrix as well. The optimum amount of loaded nanoparticles has been reported at 0.3 wt.% of SiO_2-GO, which the flux reached a maximum nearly twice of the PSf membrane, while the rejection to egg albumin maintained at more than 98% level [79].

Although quite large amount of studies have been done on the effect of adding silica nanoparticles on the morphology and performance of PES and PSf nanocomposite membranes, there are no study on the removing heavy metal ions capacity of such membranes from water while around 90% adsorption of Cu(II) ions from water containing 200 ppm of Cu_2SO_4 after 20 min by PES/SiO_2 nanocomposite powder has been reported [88].

2.7.5. Membranes with Aluminum Oxide nanoparticles

Aluminum oxides are one of the most stable inorganic materials which generally are inexpensive, non-toxic, and resistant to chemical cleaning agents [37, 89]. Due to the higher affinity of metal oxides to water, Al_2O_3 particles may incorporate into the polymeric membranes to induce hydrophilicity on the surface of membranes [89, 90]. Moreover, due to the considerable affinity of alumina nanoparticles in adsorption of contaminants specifically heavy metals from aqueous solution, these nanoparticles might be also employed as fillers in the nanocomposite membranes to enhance their ability in removal of heavy metals i.e. Ni^{2+}, Cu^{2+}, Zn^{2+} and Pb^{2+} from water [7, 37, 91, 92].

Most of the studies in incorporation of alumina nanoparticles in the PSf and PES membranes have focused on fouling mitigation of the nanocomposite membranes [93, 94]. M.R. Mehrnia et al reported that the Al_2O_3/PSf nanocomposite membranes showed a concentration threshold of 0.39 wt.% , in which optimum membrane performance for instance relatively high water flux (750 l/m^2.h at TMP = 300 KPa) has been obtained [95]. Maximous et al loaded PES membranes with 0.01 to 0.2 wt. % of alumina nanoparticles to improve the performance of the membranes in sludge filtration. They reported that Al_2O_3 entrapped membranes showed lower flux decline during activated sludge filtration compared to the neat PES membranes, with the pseudo-steady-state permeability increasing by 3.5 to 12 folds [90]. They also showed that fouling mitigation reached an optimum limit (for 0.05 wt.% of added alumina nanoparticles) above which pore plugging decreased the fouling resistance of the membranes dramatically [90]. These researchers also investigated the effect of solvent concentration and evaporation time of phase inversion process on the Al_2O_3/PES nanocomposite membranes performance. They found that within 5-20 wt.% polymer concentration, the 18 wt.% was the optimum and within the 15-120 seconds solvent evaporation times, the optimum was found to be 15 s in terms of permeability and fouling resistance of the membranes [96]. Boehmite (AlOOH) has the highest hydrated surface and hydrophilicity among the alumina compounds [97], which due to the extra hydroxyl groups on the surface on the nanoparticles can improve membrane hydrophilicity remarkably [89, 98]. V. Vatanpour et al reported a drastic

decrease in the water contact angle of the nanocomposite membranes surface from 66 degrees to 41 by adding 3 wt.% of boehmite nanoparticles. This can be attributed to the before mentioned extra hydroxyl groups of the nanoparticles surface. They also reported an increase in the pure water flux from 3.9 kg/m^2h for bare PES membrane to 5.24 kg/m^2h for nanocomposite membranes containing 0.5 wt. % boehmite nanoparticles using dead-end nanofiltration cell at the operation pressure of 5 bar. A decrease in the flux by adding more nanoparticles due to the plugging the membrane pore as a result of agglomeration of particles has also been observed [89]. It is worth mentioning that the rejection of whey protein was in the order of 98% for all of the nanocomposite membranes [89]. In addition, adding acrylic acid modified boehmite nanoparticles into the casting solution has been investigated to provide a support linking sites for an effective grafting of polyacrylic acid on the membranes in surface polymerization method of fabricating nanocomposite membranes [98].

The method of incorporating alumina nanoparticles into the nanocomposite membranes also can affect the membrane performance. Y. Mojtahedi et al were added Al_2O_3 nanoparticles to the PSf ultrafiltration membranes through two methods of nanoparticles entrapment in the structure. They used phase inversion method, and deposition of nanoparticles onto the surface of the pre-prepared PSf membrane via using photo-polymerization method. The results of this research showed that the water flux and the hydrophilicity are higher and fouling is lower in the nanocomposite membranes

with entrapped alumina nanoparticles by ultrasonic stirring and phase inversion than in nanocomposite membranes fabricated by Al_2O_3 surface deposition method [99]. Meanwhile, the nanocomposite membranes fabricated with surface deposition method have a higher rejection than the membranes with entrapped nanoparticles which can be due to a decrease in pore size through poly acrylic acid/ Al_2O_3 nanoparticle deposition on the membrane surface [99].

In spite of proven performance of alumina nanoparticles as an effective adsorbent for removal of the heavy metal ions such as Pb, Ni, Zn, and Cu from water [91, 92], there is only one published paper on the investigation of performance of the alumina /PES and PSf nanocomposite membranes. In the only one available study in the literature, N. Ghaemi reported an increase for Cu ion removal capability from water from 25% for the bare PES membrane to around 60% for the 1 wt.% containing γ-alumina nanoparticle membranes [37]. However, this amount of rejection is significantly less than the Cu removal of polyethylene glycol (PEG) coated cobalt doped iron oxide (Co-Fe_2O_3) PES nanocomposite membranes (96%) [76]. In addition, excessive adding of alumina nanoparticles to the polymeric membranes could lead to decline in membrane strength and performance due to agglomeration of the nanoparticles [7]. This needs more research by modifying nanoparticles or processing parameters to improve the nanoparticles dispersion in the polymeric matrix.

2.7.6. Membranes with ZrO_2 nanoparticles

At 1996, for the first time, ZrO_2 particles with the average size of 10 micrometer added to PSf membranes and better permeability for the composite membranes was reported [100]. J.M. Arsuaga et al fabricated nanocomposite PES membranes by dispersing 0.4 wt.% of TiO_2, Al_2O_3, and ZrO_2 nanoparticles in PES solution [62]. Using laser diffraction particle size analyzer, they showed that the average size of the as-received ZrO_2 nanoparticles increased form around 80 nm to 204 nm for nanoparticles dispersed in N-methyl-pyrrolidone (NMP) as a result of particle agglomeration. Also, pure water flux of ZrO_2/PES membranes increased slightly from around 180 l/m^{2}h to around 190 l/m^{2}h at 3 bar transmembrane pressure. This can be attributed to the increasing the hydrophilicity of the membrane surface as confirmed by the contact angle measurements and increasing the porosity of the membrane from 51% to 64% [62]. In another research, N. Maximous et al investigated the effect of adding ZrO_2 nanoparticles (average particle size 200 nm) with five different ratios of ZrO_2 to PES of 0.01, 0.03, 0.05, 0.07, and 0.1 for reducing fouling in membrane bioreactor (MBR) filtration. They reported 5% weight fraction of ZrO_2 with PES as an optimum load of adding ZrO_2 particles in terms of highest membrane permeability and lowest fouling rate. Their findings showed that ZrO_2 incorporated PES membranes during sludge filtration exhibited lower flux decline, total membrane resistance (R_t), cake resistance (R_c), and fouling resistance (R_f) compared to the neat polymeric membranes. Also the pseudo-steady-state permeability increased by 3-10 folds

[101]. The same research group compared adding ZrO_2 (average particle size 200 nm) and Al_2O_3 (average particle size 50 nm) to PES membranes and showed a higher deionized water (DIW) permeability of ZrO_2/PES membranes compared to Al_2O_3/PES membranes. This may be attributed to the higher percentage of finger structure porosity in ZrO_2 containing nanocomposite membranes [102]. In a study to reduce the flux decline of PES membranes in oil containing wastewater treatment, yttrium-doped zirconia nanoparticles sulfated by dipping in H_2SO_4 solution and then the optimized amount of sulfated yttrium-doped zirconia (SYZ) particles with the average size of 36 nm incorporated to the PSf membranes with 15% mass ratio of SYZ/PES [24, 103]. The tensile strength of membrane improved noticeably from 1.925 MPa for the bare PSF membrane to 3.315 MPa for the nanocomposite membranes as a result of relatively good dispersion of nanoparticles and polysulfone compatibility of SYZ particles. Additionally, flux decline of the membranes slightly decreased from 60% to 53% after 11 h filtration process, which can be related to the improvement of hydrophilicity of the nanocomposite membranes as a result of introducing more OH groups and Lewis acid sites to the surface of the membranes by adding the SYZ nanoparticles [103].

More complex compound of zirconium such as silver loaded sodium zirconium phosphate (AgZ nanoparticles) also has been incorporated to PES membranes. Incorporation of 1 wt.% of AgZ nanoparticles increased the pure water flux of the

membrane from around 80 l/m^2.h to 100 l/m^2.h at 0.1 MPa and also prevented the formation of biofilm and show anti-bacterial performances [104].

2.7.7. Membranes with MnO_2 nanoparticles

Recently, a number of studies have been reported on incorporating manganese dioxide nanoparticles to the PES and PSf membranes to improve their antifouling capability and heavy metal ions removal in water filtration [105-107]. R. J. Gohari et al in their two different published works have investigated the effect of incorporating hydrous manganese dioxide (HMO) nanoparticles into PES membranes to improve anti-fouling properties for oily wastewater treatment. The neat PES membranes loaded by 7, 13, 18, and 23 wt. % of HMO. It was reported that the addition of hydrophilic HMO nanoparticles plays a role in improving membrane hydrophilicity by drastically decreasing the membrane surface contact angle from 69 degrees for pristine PES membranes to 16 degrees for membranes containing 23wt. % HMO nanoparticles. Adding the nanoparticles into the polymeric membranes also enhanced the membrane water permeation rate and anti-fouling resistance against oil deposition and adsorption [105, 106]. Pure water flux of membranes increased from 39.2 L/m^2.h.bar of pristine PES membrane to 573.2 L/m^2.h.bar for the nanocomposite membranes as a result of increasing hydrophilicity of membranes due to superhydrophilic nature of HMO with many –OH functional groups [105, 108]. It should be mentioned that in spite of the high amount of HMO nanoparticles loading, a uniform dispersion of nanoparticles along the cross

section was reported. Also, it was indicated that sedimentation of the nanoparticles does not occurred during nanocomposite membrane preparation [105]. Moreover, the same researchers showed a significant increase in the separation performance of membranes in removing bovine serum albumin (BSA), Pepsin, and trypsin from feed solution containing 200 ppm solute [106].

In spite of numerous studies of the capability of manganese oxide nanoparticles in the removal of heavy metal ions such as lead, cadmium, zinc, and copper ions from water [70, 109-111], there is only one published work on investigation the removal of heavy metal ions from aqueous solution by PES/hydrated manganese oxide nanocomposite membranes [107]. In this research, HMO/PES nanocomposite membranes were tested for Pb(II) removal from water and showed a maximum adsorption capacity as high as 204.1 mg/g for 1 g/l lead ion solution. It was also indicated that among adsorption models, Langmuir model is better to be employed in describing the adsorption isotherm of Pb(II) for the nanocomposite membranes [107]. They reported that the optimum nanocomposite membrane (containing 23 wt.% HMO), operated at 0.5 bar, was able to maintain the concentration of Pb(II) using feed solution containing initial Pb(II) concentration of 148.5 ppb below the maximum contaminant level (MCL) of 15 microgram/L for nearly 6000 cm^3 of permeate collected, before failing to produce permeate of high quality [107]. Additionally, the results of the effect of the solution pH on the Pb(II) removal showed a higher amount of ion adsorption in the pH between 6 and 8, indicating the potential of

using these nanocomposite membranes to treat natural water without any pH adjustment. Also it was revealed that the leaching of manganese ions to permeate during filtration was negligible [107].

There are promising studies considering the improved functionalities of PES and PSf membranes containing manganese oxides nanoparticles in the water treatment. These nanocomposite membranes exhibit higher surface hydrophilicity, which may cause a higher flux, anti-fouling properties, and capacity of adsorbing heavy metal ions. However, there are limiting number of studies in investigation the effect of adding such nanoparticles on the morphology and performance of PES and PSf membranes. Moreover, to make manganese oxide nanoparticles/PES membranes applicable in water treatment, leaching of manganese ions into permeate should be investigated.

2.7.8. Membranes with ZnO nanoparticles

Nano-ZnO, similar to other metal oxide nanoparticles, can easily adsorb hydrophilic hydroxyl groups (-OH) to become hydrophilic [30]. In addition, ZnO is one of the most important multifunctional semiconductor materials and is very important for photo-catalysis, anti-bacterial, and antifungal application in water treatment [112-114]. To the best of our knowledge, few reports about the filtration performance of nano-ZnO/PES membranes have been published. In 2012, for the first time, Balta et al incorporated ZnO nanoparticles to PES membranes as an alternative of TiO_2 nanoparticles. They reported

ZnO nanoparticles are an excellent competitor to the TiO_2 nanoparticles as an anti-fouling material [112]. Adding ZnO to PES membranes significantly improved rejection of methylene blue from 47.5% for bare PES membranes to 82% for the nanocomposite membranes. Moreover, zinc oxide nanoparticles promoted micro-void formation and porosity of membranes due to a hindrance effect of nanoparticles during the phase-inversion process [112]. Another research group indicated that after a threshold of added amount of zinc oxide nanoparticles, the porosity of membranes declined. This was explained by high viscosity of casting suspension and a decrease of the exchange rate between water and solvent during the phase inversion process [30]. An increase in the permeability of zinc oxide containing nanocomposite membranes due to improvement in hydrophilicity and porosity of the membranes was observed [30, 112]. L. Shen et al reported up to 254% improvement in water flux for PES membranes, while the flux decrease for 0.5 g/L BSA solution of PES membrane after 25h filtration is 27% for bare PES membranes compared to 7.8% for the ZnO/PES nanocomposite membranes, which shows good antifouling performance of the fabricated membrane [112]. In another study, C.P. Leo et al incorporated 1-4 wt. % of nano zinc oxide with the size of around 20 nm to reduce fouling of PSf membranes. They reported maximum pure water permeability and minimum oleic acid fouling of membranes by adding 2 wt. % of ZnO nanoparticles as a result of higher porosity and more hydrophilicity of the nanocomposite membranes.

Increasing the amount of added nanoparticles more than 2wt.%, may deteriorate the nanocomposite membrane performance due to serious aggregation of particles [115].

Most of the studies on the zinc oxide containing PES and PSf nanocomposite membranes have addressed fouling issue of the membranes. Despite the reported potential of ZnO nanoparticles as a promising adsorbents of heavy metal ions like Cu(II) and Pb ions [116, 117], there is no published research on removal capability of heavy metal ions from water using nano zinc oxide/PES or PSf nanocomposite membranes. Moreover, antimicrobial properties of ZnO, make it a good candidate for fabricating antibacterial and anti-bio filming membranes which need more attention and research [113, 114].

2.7.9. Other metal nanoparticles

Selenium is an indirect elemental semiconductor and exhibits good photoelectrical properties and catalytic activities toward organic hydration and oxidation reactions [118]. Moreover, new studies have introduced selenium as an antimicrobial agent which inhibits the development of bacterial biofilm on a surface by acting as a catalyst for redox reactions involving reactive oxygen species [119, 120]. Anti-bacterial and anti-fungal properties have also been reported for copper nanoparticles [121]. Recently, the addition of selenium and copper nanoparticles to PES membranes to improve bio-fouling properties of the membranes has been investigated [122]. Increasing up to 0.05 wt.% of copper and selenium nanoparticles content of PES membrane, decreased the permeability

of the PES membranes from 231 L/m^2.h.bar for neat membrane to 58, and 69 L/m^2.h.bar for selenium/PES and copper/PES nanocomposite membranes, respectively. In addition, the water contact angle of the membranes did not change significantly by loading selenium and copper membrane. Although, no pore size study is reported in this study, but pore dispersion of nanoparticles and pore size decrease of membranes as a result of adding nanoparticles reported as an explanation for declining permeability of the nanocomposite membranes [122]. In other hand, antifouling properties for the nanocomposite membranes improved, and BSA rejection performance increased significantly from around 50% for pristine membranes to 80-85 % for the nanocomposite membranes [122]. Further research is needed to investigate morphology and performance of the copper and selenium containing nanocomposite membranes including anti-bacterial properties.

Chapter 3) Experimental work

3.1. Research Methodology

A comprehensive designed set of experiments followed by theoretical discussions were utilized in this research in order to systematically achieve the research goal. The research methodology of this project is shown schematically in the figure 3.1.

The design of experiments (DOE) is divided into two sections; first section is a set of experiments to optimize the synthesizing of PES ultrafiltration membranes, and the second section is to investigate the morphology and performance of the membranes by incorporating nanoparticles. For both sections full factorial design of experiments was used.

I. Synthesize and optimize PES ultrafiltration membranes

Factors: Polymer concentration and temperature of the casting solution are chosen as the controllable variables. Polymer concentration was chosen as it is the main thermodynamic factor that influences the membrane morphology and characteristics. Temperature of the casting solution which altering the kinetics of the phase inversion process was also chosen as the second factor. The range of the factors were chosen considering the literature and feasibility of the experiments.

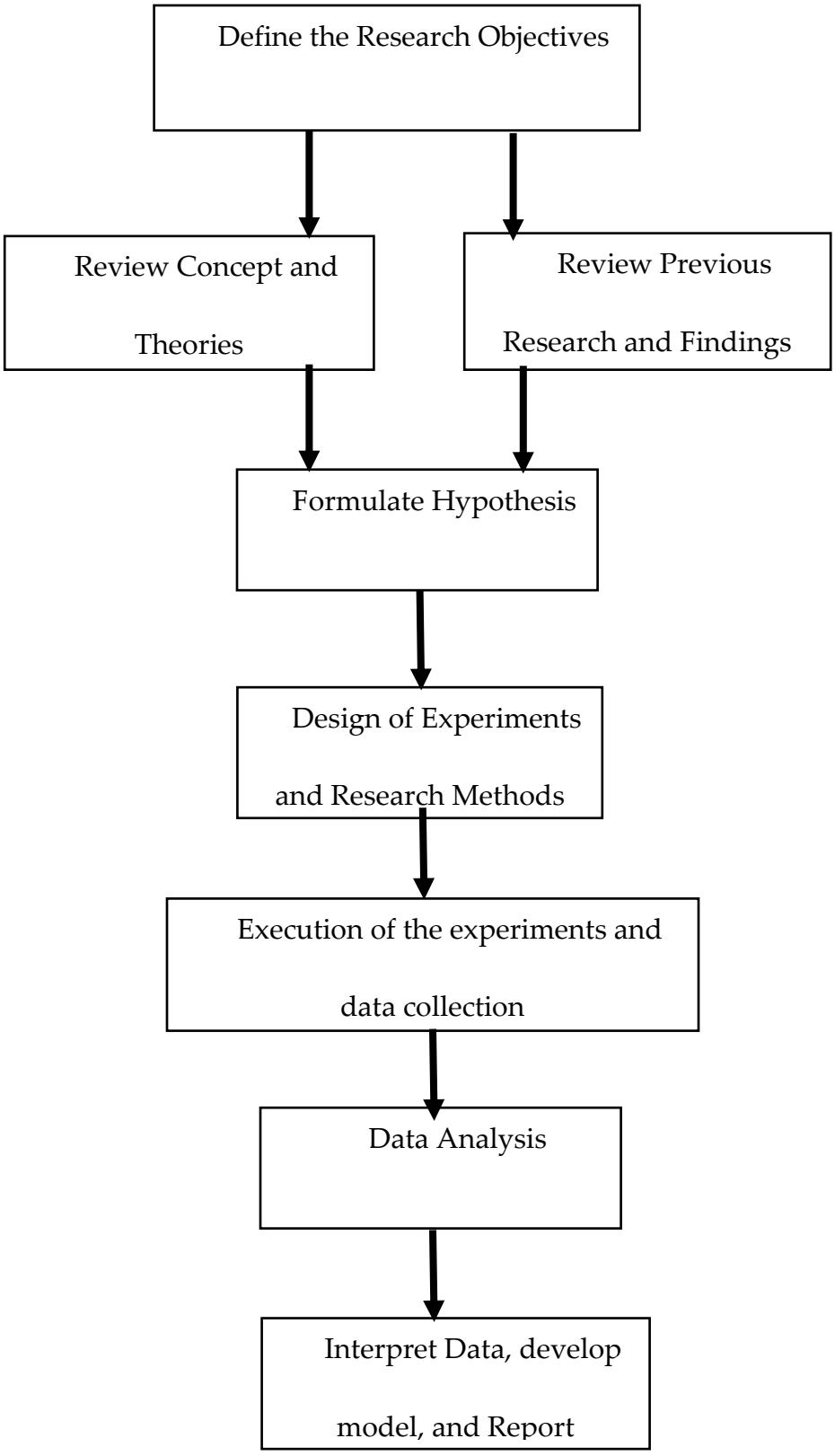

Figure 3. 1. Research methodology

Levels: 3 levels were chosen for each factor. The chosen levels were based on the literature review, feedback from initial experiments, and limitation of the process factors. Considering the solvent-nonsolvent-water ternary diagram, the PES concentration in the casting solution was chosen as 16-18-20 wt. %. The temperature of the casting solution was also chosen as 30 and 50° C.

Responses: The responses and outputs of this phase of the project were chosen as pure water flux and tensile strength of the membranes.

Table 3. 1 Design of experiments for synthesizing polymeric membranes

Experiment Numbers	Factor 1 (Polymer concentration, wt. %)	Factor 2 (Temperature of the casting solution, Centigrade)
1	16	30
2	16	50
3	18	30
4	18	50

5	20	30
6	20	50

II. Synthesize and optimize PES nanocomposite membranes

Factors: Amount of added nanoparticles was chosen as the first factor as it plays a significant role in the morphology and performance of the nanocomposite membranes. Surface treatment of the nanoparticles in another factor that was investigated in this research. Incorporated nanoparticles are treated or untreated.

Levels: The amount of nanoparticles was selected considering the previous published works and by getting feedback from the initial experiments. Six levels (1, 2, 3, 4, 5, 6 wt. %) were chosen for the amount of incorporated nanoparticles. Also there are two levels for the surface treatment factor (treated and untreated). Table 3.2 shows the designed experiments for this stage.

Table 3. 2 Design of experiments for synthesizing nanocomposite membranes

Experiment Number	Factor 1 (amount of nanoparticles wt. %)	Factor 2 (Surface Treatment)
1	1	Treated
2	1	Untreated
3	2	Treated
4	2	Untreated
5	3	Treated
6	3	Untreated
7	4	Treated
8	4	Untreated
9	5	Treated
10	5	Untreated
11	6	Treated
12	6	Untreated

3.3.3. Assumptions:

Below assumptions are made in conducting the experiments and collecting the test data:

1. Nanoparticles have the same size, morphology, and surface area.

2. Variation of the phase inversion process is negligible and process in under control.

3. Presence of nanoparticles does not alter the phase inversion process.

4. Modeling assumptions are listed in section 4.4.2 and 4.4.3.

3.2. Materials

γ-Al_2O_3 nanoparticles with the size of 80 nm and surface area of 58 m^2/gr were purchased from US Research nanomaterials (Texas, USA). Polyethersulfone (Ultrason E6020P, 58,000 g/mol, BASF Company, Germany) was used as the base polymer. Polyvinyl pyrrolidone (PVP) with a 25,000 g/mol molecular weight and dimethylacetamide (DMAc) were purchased from Sigma-Aldrich. The solvent, DMAC, was used without purification. Copper nitrate was purchased from Sigma-Aldrich and used to prepare feed solution containing specific concentration of copper ions. Necessary dilutions were performed with Milli-Q water having resistivity higher than 18 MΩ.cm. Nitric acid (HNO_3) used for preparing the standard solutions for filtration experiments.

99% nitric acid was purchased from Sigma-Aldrich. High purity anhydrous ethanol and acetone which were used for necessary dilution and washing were purchased from Sigma-Aldrich.

3-Aminopropyltriethoxysilane (APTES) is an aminosilane that is frequently used in the process of silanization, the functionalization of surfaces with alkoxysilane molecules. In this work APTES is purchased from Sigma-Aldrich and used to functionalize the nanoparticles surface. Table 3.3 summarizes the materials used in the experiments.

Table 3. 3 Materials used in the research

Material	Description
Polyethersulfone (PES)	Ultrason E6020P, 58,000 g/mol, BASF Company, Germany
dimethylacetamide (DMAc)	Sigma-Aldrich
Polyvinyl pyrrolidone (PVP)	25,000 g/mol molecular weight, Sigma-Aldrich

Copper nitrate, ($Cu(NO_3)_2$	Sigma-Aldrich
Nitric acid (HNO_3)	Sigma-Aldrich
Anhydrous Ethanol	Sigma-Aldrich
Acetone	Sigma-Aldrich
Sodium dodecyl sulfate (SDS)	288.38 g/mol molecular weight , Sigma-Aldrich
(3-Aminopropyl)triethoxysilane (APTES)	Sigma-Aldrich

3.3. Modification of Nanoparticles

Surface modification of nanoparticles is used in this research to improve the polymer-nanoparticles interaction in nanocomposite membranes. Modification of the nanoparticles by a silane agent (APTES) is used in this research.

To modify the γ-Alumina nanoparticles by SDS First, the alumina nanoparticles were modified using SDS solution according to Muhamad et al. work [123]. In the modification

process, 3 vol% SDS solutions was prepared in 1,000 mL deionized water. Then, 5.0 g γ-alumina nanoparticles was added to the solution. After that the mixture was ultra-sonicated for 1 h and then mixed with magnetic stirrer for 6 h. Then, nanoparticles were separated from the mixture by a centrifuge at 12000 rpm for 30 min. The obtained powder air-dried for 24 h and were used to prepare nanocomposite membranes. Figure 3.2 shows the schematic of the SDS modification of the nanoparticles.

The modified nanoparticles then were used in the next steps to fabricate the nanocomposite membranes.

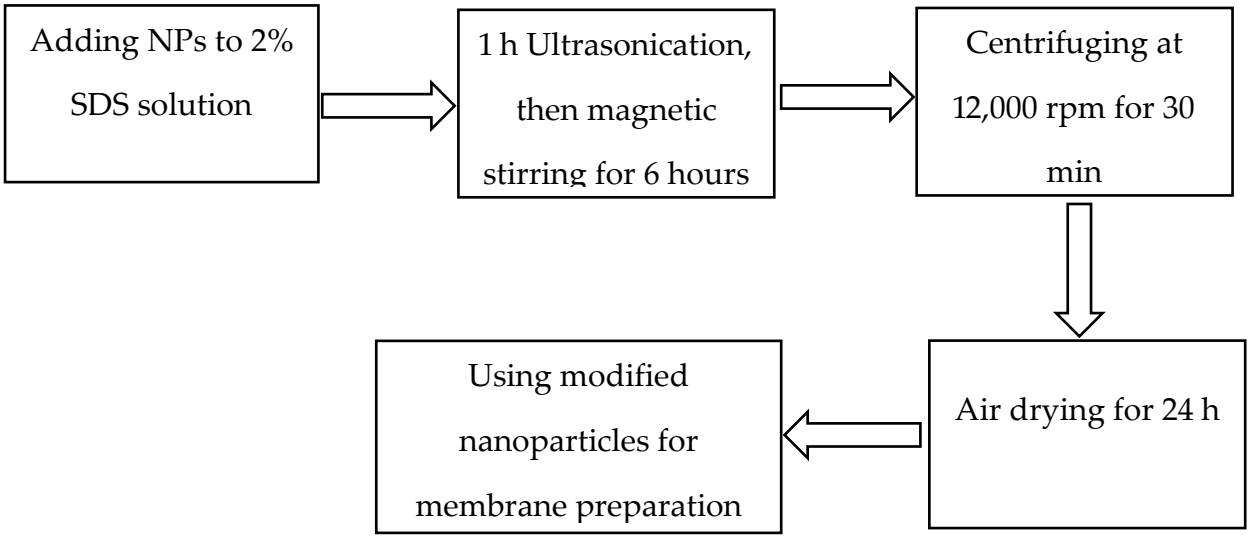

Figure 3. 2 Schematic of modification of the nanoparticles by SDS

In the second modification method, silane coupling agent was used to optimize the performance of nanocomposite membranes. The silane modification of the alumina

nanoparticles was carried out using 3-Aminopropyltriethoxysilane (APTES). In this process, nanoparticles were dispersed in anhydrous ethanol using 30 min ultra-sonication. After that APTES (2 wt. %) was added drop-wise to the mixture under nitrogen purging and was stirred for 2 hours at 75 °C. Finally, the particles were isolated from the solution by centrifuging and were dried in an oven for 24 hours at 50 °C. Figure 3.3 shows the schematic of silane modification process.

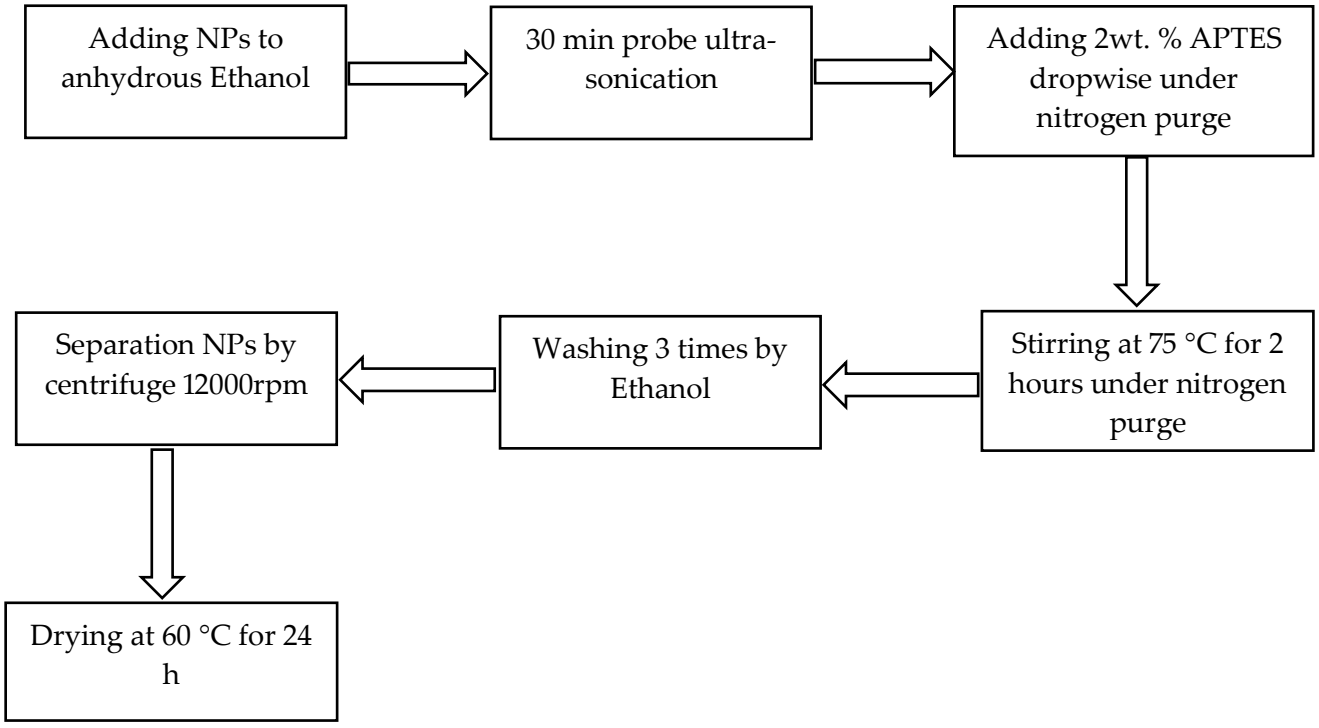

Figure 3. 3 Schematic of silane treatment process of the nanoparticles

3.4. Synthesizing of the polymeric and nanocomposite membranes

PES flat membranes were synthesized by phase inversion via immersion precipitation method. Figure 3.4 shows the schematic of the phase inversion process.

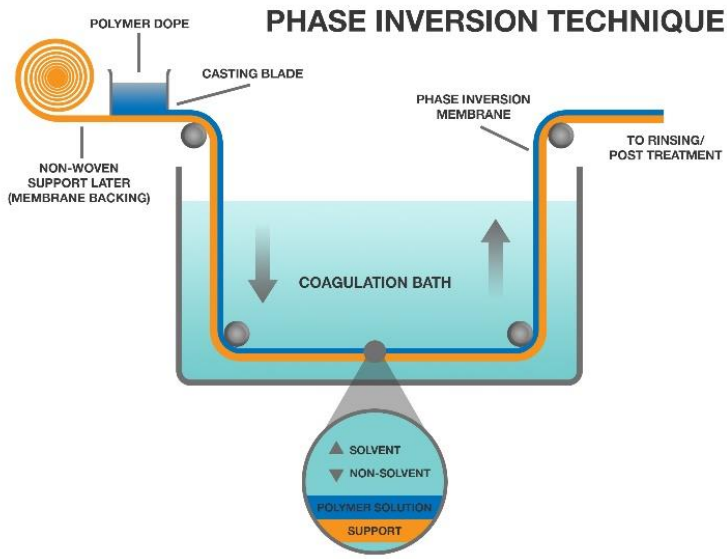

Figure 3. 4 Schematic of the phase inversion process

To prepare PES membranes, a casting solution containing different concentration of PES dissolved in the solvent (DMAc) was prepared using 1 wt. % PVP as pore former and stirred for 24 h. High power ultra-sonication was utilized to remove the bubbles, and the membranes were cast by doctor blade and automatic film applicator at a speed of 60 mm/s and thickness of 200 μm. The homogenous solution was cast at room temperatures and then moved into the distilled water bath at the same casting temperature. The prepared membranes were then washed and stored in distilled water for 24 h to leach out the residual solvents. Finally, the membranes were dried between two sheets of filter paper

and then vacuum dried for 24 h at 50° C. The schematic of the synthesizing procedure is shown in figure 3.5.

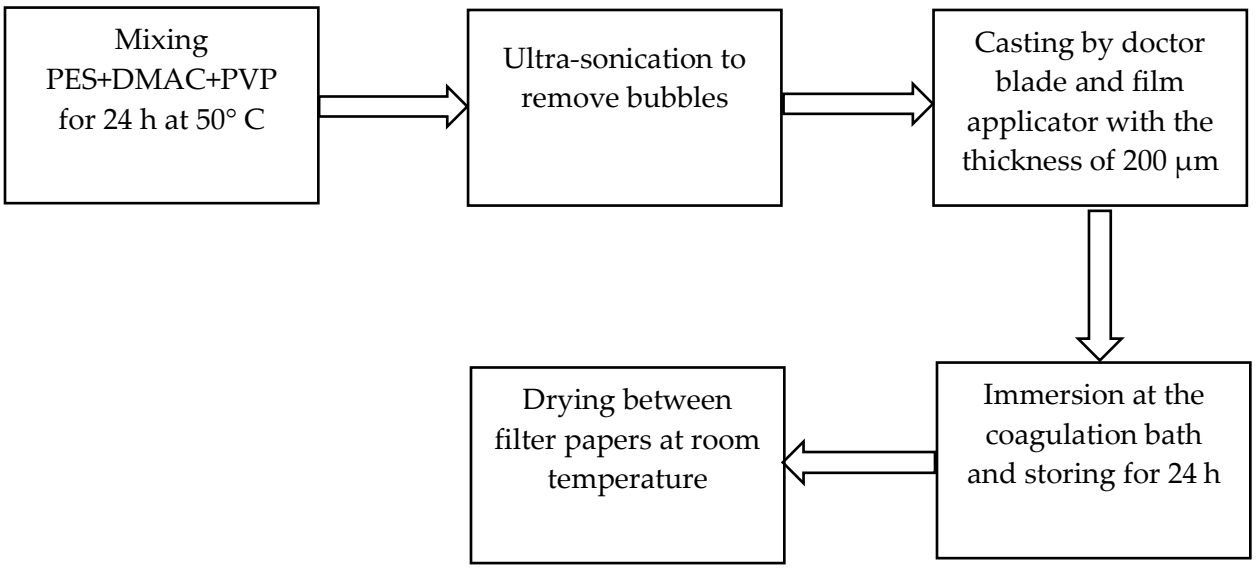

Figure 3. 5 Schematic of the membrane fabrication process

To synthesize the nanocomposite membranes, a homogenous mixture of alumina nanoparticles and DMAc was prepared by adding predetermined amount of alumina nanoparticles into the DMAc and sonication for 1 h. Afterward, measured amounts of PES and PVP were dissolved into the mixture while stirring at 400 rpm for 24 h. The rest of the process is identical to the method to synthesize polymeric membranes which is described before.

3.4. Characterization of the membranes

3.4.1. Viscosity measurement

Viscosity of the casting solution can impede the exchange rate of solvent and non-solvent during phase inversion process, and therefore it is an important parameter to affect the formation of resulting membrane morphology. The casting solution viscosity was measured with a rotational rheometer connected to a furnace to control the temperature. The casting solutions were placed in the cylinder and sufficient time was allowed for it to reach thermal equilibrium. Viscosity of the solutions were measured using the shear rate of 10-120 s^{-1}.

3.4.2. Determination of coagulation value

Coagulation value can be used as a measure of thermodynamic stability of the casting solution. It is defined as the added amount of water in a casting solution, when remarkable coagulation is visually observed. DMAc solutions with different polymer contents (16, 18, 20 wt. %) were placed in Erlenmeyer flasks at room temperature. Using a precise pipet, small volumes of distilled water were added to the solutions until turbidity detected by visual observation. As the phases separate locally at the spot when non-solvent (water) hits the polymer solution, the samples were heated to 70° C to dissolve the formed phase and then cool down to room temperature. If the system does not become limpid after the heating-cooling sequence, then another volume of water was

added to the polymer solution and the temperature sequence was repeated until observation a persistent turbidity [18]. The cloud point composition was calculated from the mass balance in the system at which turbidity started to observe upon cooling.

3.4.3. Contact angle measurements

To study the hydrophilicity and surface wetting characteristic of membranes as a function of polymer concentration and casting temperature, water contact angle was measured for membrane using a contact angle measuring instrument (goniometer 500 Rame-Hart). The equilibrium water contact angle was measured at room temperature by sessile droplet method and image analysis of the droplet on the surface. For each sample, 6 microliter water droplet was deposited on the membrane surface and contact angle measured after 5 s. Contact angle was measured at three different points of the membrane surface and the results were reported as an average.

3.4.4. Equilibrium water content (EWC)

Equilibrium water content (EWC) was used to measure the porosity of membranes. The membrane samples were cut and the dry weight was recorded. Then, they were soaked in distilled water for 24 h. The surface of the membrane samples was wiped with filter paper and the samples immediately weighted. After that, the membranes were dried in a vacuum oven at 50 °C for 24 h and weighted again. The equilibrium water content at room temperature was calculated as follows:

$$\text{Water content (\%)} = \frac{Ww - Wd}{Wd} * 100 \qquad \text{Equation 3. 1}$$

Where W_w and W_d are wet and dry membrane weights (g), respectively. Moreover, the average porosity of the synthesized membranes was determined by the following equations:

$$\text{Porosity (\%)} = \frac{Ww - Wd}{\rho f - Vm} * 100 \qquad \text{Equation 3. 2}$$

Where P_f and V_m are water density (g/cm^3) and membrane pieces volume (cm^3), respectively. The results were reported as an average of three experiments for each membrane sample.

3.4.5. Scanning electron microscopy

Field emission scanning electron microscopy (FESEM, Hitachi, S-8400) was used to analyze morphology of the membranes. A modified freeze fracture method (Cryo-snap), where the specimen is embedded in ice before cleaving, was developed to minimize the stresses put on the sample during fracturing, thereby reducing the distortion to the membrane cross-section and increasing the resulting detailed resolution [124] . The dried cut samples were iridium sputtered and they were views with the microscope at 3 kV. To measure the top-layer thickness of membrane, four or five casual points on top-layer were selected and the average value was reported as the membrane skin-layer thickness.

3.4.6. Pore size distribution and surface area

The gas adsorption-desorption technique was operated to obtain information about the overall morphology variation of synthesized membranes. Nitrogen sorption analyses were obtained with a surface-area and pore-volume analyzer (ASAP 2020, Micromeritics) using standard continuous procedures at 77.15 °K on membrane samples that had been degassed at 333 °K under high vacuum for at 6 h. The surface area was calculated according to the Brunauer–Emmett–Teller (BET) model over a relative pressure range of 0.05–0.90.

3.4.7. Static adsorption analysis

Batch adsorption experiments were conducted to calculate the static adsorption of heavy metal ions on the alumina/PES membranes mixed matrix membranes. Copper solutions with different initial concentrations in a range of 20-80 ppm, were prepared by dissolving $Cu(NO_3)_2$ in deionized (DI) water. Batch adsorption tests were conducted by adding 0.1 gram of sliced membranes into vessels containing 100 ml of heavy metal ion solutions. The vessels were then placed in a shaker and agitated at room temperature for 48 h. The equilibrium concentration of the heavy metal ion in the solutions was determined by a flame atomic adsorption spectrometer (AAS) (ICE 3000 ThermoFisher). The lead ion adsorption of the membranes (mg/g) were calculated by equation 3.3:

$$q_e = \frac{(C_0 - C_e)V}{M_m} \qquad \text{Equation 3. 3}$$

Where q_e is the equilibrium adsorbed amount of copper ions per membrane weight (mg/g), C_0 and C_e are initial and equilibrium concentrations (mg/L) of heavy metal ion in the solution, V is the volume of the copper solution (L), and M_m is the mass of the membrane (g).

Langmuir and Freundlich equilibrium adsorption isotherms were applied on the adsorption data for the alumina/PES membranes. Langmuir isotherm, which indicates a monolayer adsorption on the homogenous adsorption sites, is expressed as shown in equation 3.4:

$$q_e = \frac{q_{max}\, b\, C_e}{1+bC_e} \qquad \text{Equation 3. 4}$$

where q_e is the equilibrium adsorption (mg/g), C_e is the equilibrium concentration in the aqueous phase (g/L), q_{max} is the adsorption capacity (mg/g), and b in the equilibrium constant (L/mg).

Meanwhile, Freundlich isotherm corresponds to a multilayer adsorption on a heterogeneous surface and is formulated by equation 3.5:

$$q_e = k\,.\,Ce^n \qquad \text{Equation 3. 5}$$

where k and m are the relative adsorption constant and adsorption intensity parameter.

3.4.8. Water flux of the membranes

Water flux of the membranes was measured using a dead end stirred ultrafiltration (UF) cell (Millipore, Model 8050) at fixed speed of 400 rpm. Effective area of the membrane in the filtration cell was 13.4 cm^2. The stirred cell was pressurized with nitrogen gas to pass the liquid through the membrane. To compact the membranes before the pure water flux measurement, they were pressurized at 70 psi for 1 h. After compaction, transmembrane pressure was set to 65 psi and the permeate flux was calculated as follows:

$$\text{Permeate flux (Kg/m}^2\text{h)} = \frac{Q}{A\Delta t} \qquad \text{Equation 3. 6}$$

Where Q, A and Δt are quantity of permeate (Kg), membrane area (m^2) and sampling time (h), respectively. Figure 3.6 shows the ultrafiltration set up.

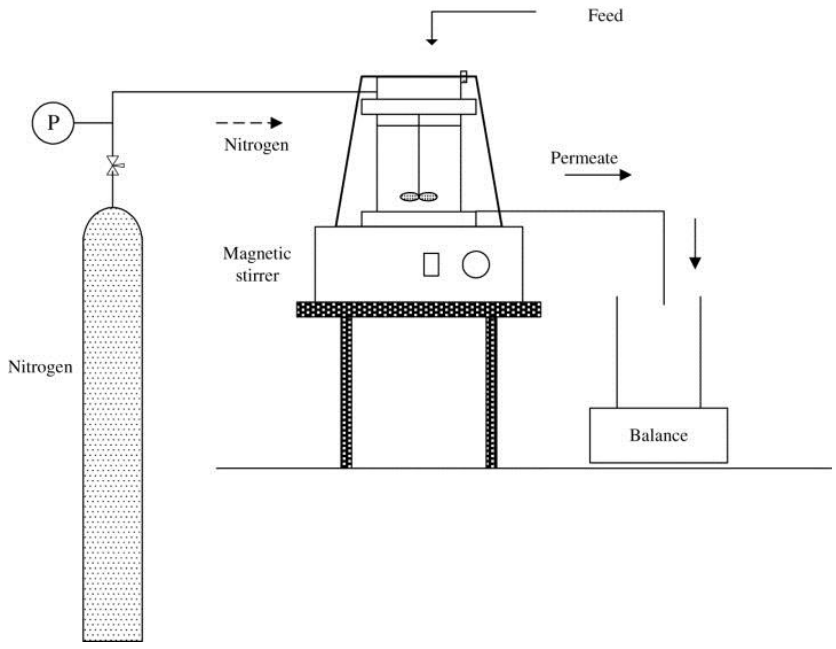

Figure 3. 6 Schematic of the ultrafiltration test

3.4.9. Solute rejection performance

In this study, the membrane potential for copper removal from water will be investigated. First using a dead-end filtration cell, the prepared membranes will be tested in terms of Cu (II) rejection using 20 mg/l of aqueous $Cu(NO_3)_2$ solution as feed. Ion removal will be monitored by atomic absorption spectroscopy. Rejection (R) percent can be calculated as:

$$R\% = \frac{Cf - Cp}{Cf} * 100 \qquad \text{Equation 3. 7}$$

C_f and C_P are ion concentration (mg/l) in feed and permeate, respectively. The efficiency of synthesized membranes is investigated by applying relatively low concentration feeds. Each experiment was repeated 5 times and the average was reported.

Chapter 4) Results and Discussion

4.1. Effect of casting temperature and polymer concentration on the characteristics and performance of the PES membranes

4.1.1 Introduction:

Membrane filtration has proven to be an effective tool in water and wastewater treatment [18-20]. Membrane filtration technologies such as; ultrafiltration, nanofiltration, and reverse osmosis provide reliable and energy effective methods for treating water [18, 20, 21]. Many different synthetic materials such as metals, ceramics, glasses, and polymers can be used for membrane fabrication [22]. Polymers are the most widely used materials for membrane synthesis due to their straightforward pore forming mechanism, good mechanical properties, compatibility, and relatively lower cost compared to inorganic membranes [8, 22, 23, 125]. Polyethersulfone (PES) is one of the most common polymers used in the preparation of commercial and laboratory membranes because of its commercial availability, ease of processing, and favorable selectivity-permeability characteristics. PES polymers also possess good mechanical, chemical, and thermal properties [27-29]. Polysulfone polymers consist of aromatic units bridged with sulfone as well as isopropylidene or ether moieties [27, 30, 31].

Polymeric membranes can be fabricated by a variety of different techniques of which the phase inversion (PI) method is the most commonly used [8, 22]. Dry or wet phase inversion processes; such as solvent evaporation, precipitation from vapor phase, thermal

precipitation, and immersion precipitation are used to prepare asymmetric membranes with a very thin, and dense, skin layer [22]. Among these phase inversion techniques, immersion precipitation is one of the most commercially explored membrane formation methods because it allows to obtain membranes with different morphology and properties [22].

To synthesize membranes using this method, a polymer solution is cast onto a suitable support using a film applicator. Afterwards, it is immersed into a nonsolvent (coagulation) bath, which consists of a weak solvent and may contain some additives [27, 32, 126, 127]. Subsequently, phase separation takes place by the exchange of solvent and nonsolvent, leading to solidification of an asymmetric polymeric membrane with a dense top layer [8, 22, 27, 32]. The varying morphology and separation performance of the prepared membranes can be controlled by several key factors; such as the choice of solvent-nonsolvent system, the composition of the polymer solution, additives in the polymer solution, the composition of the coagulation bath, and the film casting conditions (i.e. temperature) [3, 22, 32, 128-131].

Several researchers have investigated the influence of using additives in the polymer solution, choice and composition of the nonsolvent system, and the casting temperature on the performance and properties of PES membranes [132-139]. Temperature is an important factor which influences the viscosity of the casting solution and subsequently

the solvent and nonsolvent exchange rate during the phase inversion process [22]. Tsai et al. reported that the higher coagulation bath temperature inhibits the formation of micro-voids [140]. In contrast, Zheng et al. showed that increasing the coagulation bath temperature leads to an increase in the size of finger-like macro-voids [141]. Moreover, it has been reported that increasing the casting solution temperature decreases the solution viscosity while also increases the miscibility of the solvent-nonsolvent [142].

In this work, the morphology and structure of PES membranes, fabricated by the immersion precipitation phase inversion method at different casting temperatures and polymer concentrations, are investigated. Different PES concentrations in the casting solution (16, 18, 20 wt. %) as well as casting temperatures (30 °C and 50 °C) were chosen to synthesize the membranes. The effect of these parameters on the physiochemical characteristics of the membranes was analyzed. The results of this study highlight the relationship between the composition, processing conditions, and properties of PES membranes.

4.1.2. Membrane preparation and characterization

PES flat membranes were fabricated by phase inversion via the immersion precipitation method. In preparing the PES membranes, a casting solution containing different concentrations of PES (16, 18, 20 wt. %), solvent (DMAc), and PVP as a pore former were stirred for 24 hours at 50 °C. Table 4.1 shows the composition and viscosity

of the casting solutions as well as the casting temperature. The bubbles were removed from the solution using high power ultrasonication, and the membranes were cast by a doctor blade with a gap of 200 μm and automatic film applicator at a speed of 60 mm/s. The homogenous solution was cast at different temperatures (30 °C and 50 °C) and then moved into a distilled water bath at the same casting temperature. The prepared membranes were then washed and stored in distilled water for 24 hours to leach out the residual solvents. Finally, the membranes were dried between two sheets of filter paper for 24 hours. Samples that were used for SEM and contact angle measurement test, were vacuum dried for 24 hours at 50 °C.

Table 4. 1 Compositions, casting temperature, and viscosities of the casting solutions

Membrane Name	PES (wt. %)	PVP (wt. %)	DMAc (wt. %)	Casting Temp.	Viscosity (cps)
PES 1630	16	1	83	30	249
PES 1650	16	1	83	50	149
PES 1830	18	1	81	30	659
PES 1850	18	1	81	50	358
PES 2030	20	1	79	30	839
PES 2050	20	1	79	50	474

The synthesized membranes are characterized in terms of morphology and performance using field emission scanning electron microscopy (FESEM), viscosity measurements,

water contact angle, porosity measurements, pure water flux, and tensile strength. The materials and the description the characterization method is described in chapter 3.

4.1.3. Results and Discussion

4.1.3.1 Thermodynamics of membrane-forming system

In order to better understand the membrane forming mechanism during the phase inversion process, the coagulation value can be used as a measure of the thermodynamic stability of the casting solution [143]. Table 4.2 shows the coagulation value of the casting solution versus the polymer concentration at 30 °C. A ternary solution with 16 wt. % PES, 1 wt. % PVP, and 83 wt. % DMAc became cloudy with 8.3 wt. % addition of water. By increasing the polymer concentration of the casting solution, a slightly lower amount of non-solvent was required for the solution to become cloudy. This is indicated by the 7.8 and 6.8 wt. % addition of water for the solutions containing 18 and 20 wt. % PES, respectively. This trend indicates that solutions with a higher concentration of polymer are thermodynamically less stable. In addition, Table 4.2 shows the viscosity of the casting solutions, which increases with increasing the polymer (PES) concentration. It can be inferred that the overall diffusion taking place during the phase inversion process (the exchange between solvent and non-solvent) can be hindered as a result of higher viscosity.

Table 4. 2 Cloud point and viscosity data of casting solution at 30 °C

Solution composition (wt. %)			Water content at cloud point* (g/wt. %)	Viscosity (cps)
PES	PVP	DMAc		
16	1	83	2.83/8.3	249
18	1	80	2.64/7.8	659
20	1	79	2.31/6.8	839

*Solution composition is based on 5 g PES

Thermodynamically less stable solutions enhance the precipitation rate leading to more porous structures [144]. The rheological behavior of the casting solution is another factor that determines the de-mixing and morphology of the formed membranes. De-mixing of the cast solution during coagulation can be controlled by the diffusion rate between the solvent and non-solvent. Stability (thermodynamic factor) and viscosity (kinetic factor) of the casting solution are among the key factors that determine the pore structure of the prepared membranes [22].

As it can be seen in Table 4.2, the membranes with 16 wt.% polymer show a higher stability and lower viscosity compared to 18 and 20 wt.%. This is in accordance with the total porosity data which shows an increase in porosity of the membranes with lower polymer concentrations. This can be explained by the competition between the kinetic factor (viscosity of the casting solution) and the thermodynamic factor (stability of the solution). The lower viscosity of the solutions with less PES concentration counteracts the

thermodynamic factor (higher stability) and lead to the formation of more porous membranes.

4.1.3.2 Morphological analysis

SEM analysis is known as a very useful technique to study membrane morphologies. Fig. 4.1 shows SEM images of the cross section of the membranes prepared with different polymer concentrations and casting temperatures. The fabricated membranes exhibit a typical asymmetric structure and fully developed macro-pores, irrespective of the polymer concentration and casting temperature. Overall, membranes consist of a thin top layer supported by a porous sub-layer containing large finger-like macro-voids. The high mutual affinity of DMAc for water results in instantaneous de-mixing, leading to the formation of finger like pores in the sub-layer of the prepared membranes [3]. It also can be concluded that by changing the polymer concentration and casting temperature in the range of 16-20 wt. % and 30-50 °C, instantaneous de-mixing is still maintained.

As it can be seen in the SEM images, which is also confirmed by the total porosity results (Table 4.2), the samples cast at higher temperatures and lower polymer concentrations contain higher amounts of macro-voids and hence more porosity. The formation of macro-voids was promoted due to the faster precipitation at elevated temperatures [145]. Therefore, at higher temperatures and/or lower polymer concentrations (when the viscosity is lower), the diffusion rate between the solvent and

non-solvent is higher and the macro-void growth is promoted. On the other hand, the nuclei, which are formed after immersion of the cast film in the water bath, grow at a slower rate at lower temperatures, which result in a denser top layer and the suppression of macro-void formation. These observations are in close agreement with the literature [143, 146].

	Casting Temperature : 30 °C	Casting temperature : 50 °C
16 wt.% PES	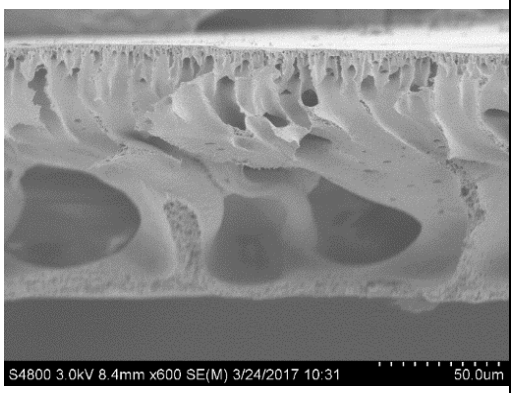	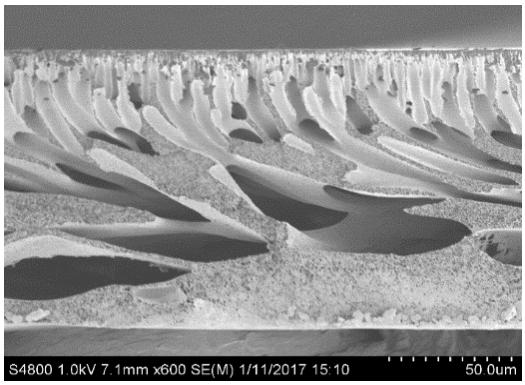
18 wt.% PES	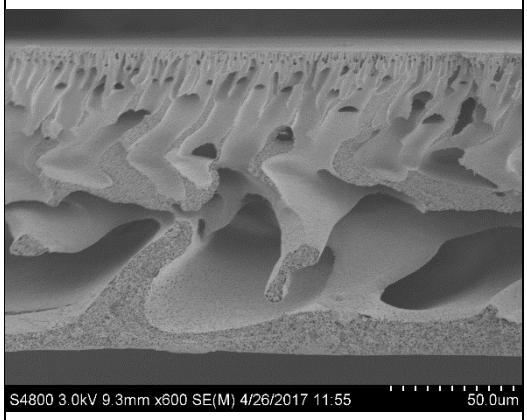	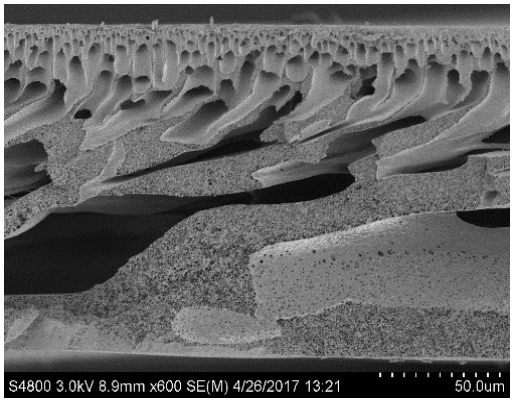

20 wt.% PES	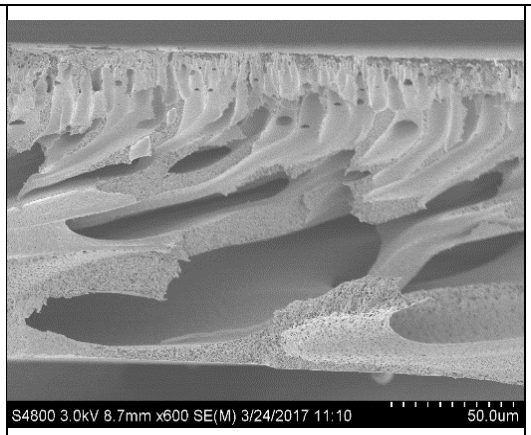	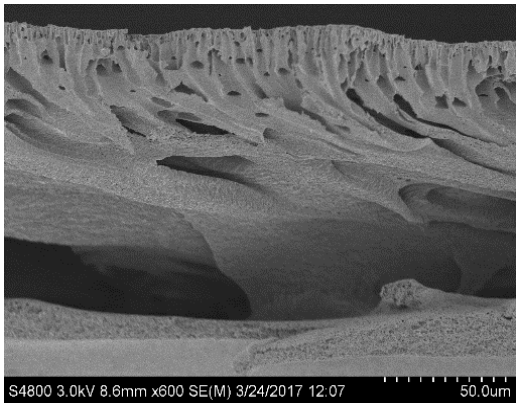

Figure 4. 1 SEM cross-section images of the PES membranes

Moreover, increased polymer concentration in the casting solution leads to a higher polymer concentration at the nonsolvent interface as well as a lower possibility of solvent extraction from the surrounding polymer solution to the polymer-lean phase during the formation of micro-voids [146]. This led to a decrease in the overall porosity and the mean pore size of the prepared membranes. It has also been reported when the polymer concentration is increased beyond a certain value, the resulting membrane has a lower porosity and the pure water flux may approach zero even with the occurrence of instantaneous de-mixing [22, 147]. The average thickness of the prepared membranes was measured to be 114 μm ± 3 μm regardless of the fabrication.

4.1.3.3 Hydrophilicity and porosity

The average static water contact angle and total porosity are two important factors that determine the permeability of the membranes [148]. The water contact angle is often used

to represent the surface hydrophilicity of the membranes. The contact angle of the membranes are reported in figure 4.2.

Although there is no significant change in the contact angle of the membranes which were cast at the same PES concentration, increasing the casting temperature from 30to 50 °C decreased the contact angle. This might be due to the change in the surface roughness of the membranes since the chemistry of the surface remains unchanged in all the membrane samples. Since all the membranes have similar chemical composition, the change in the surface pore size and surface roughness of the membranes may be the main reason for the variation of the contact angle of the membranes. The membranes which were cast at a higher temperature, display larger pore size of the top dense layer (Table 4.3) and higher surface roughness, which resulted in a lower contact angle.

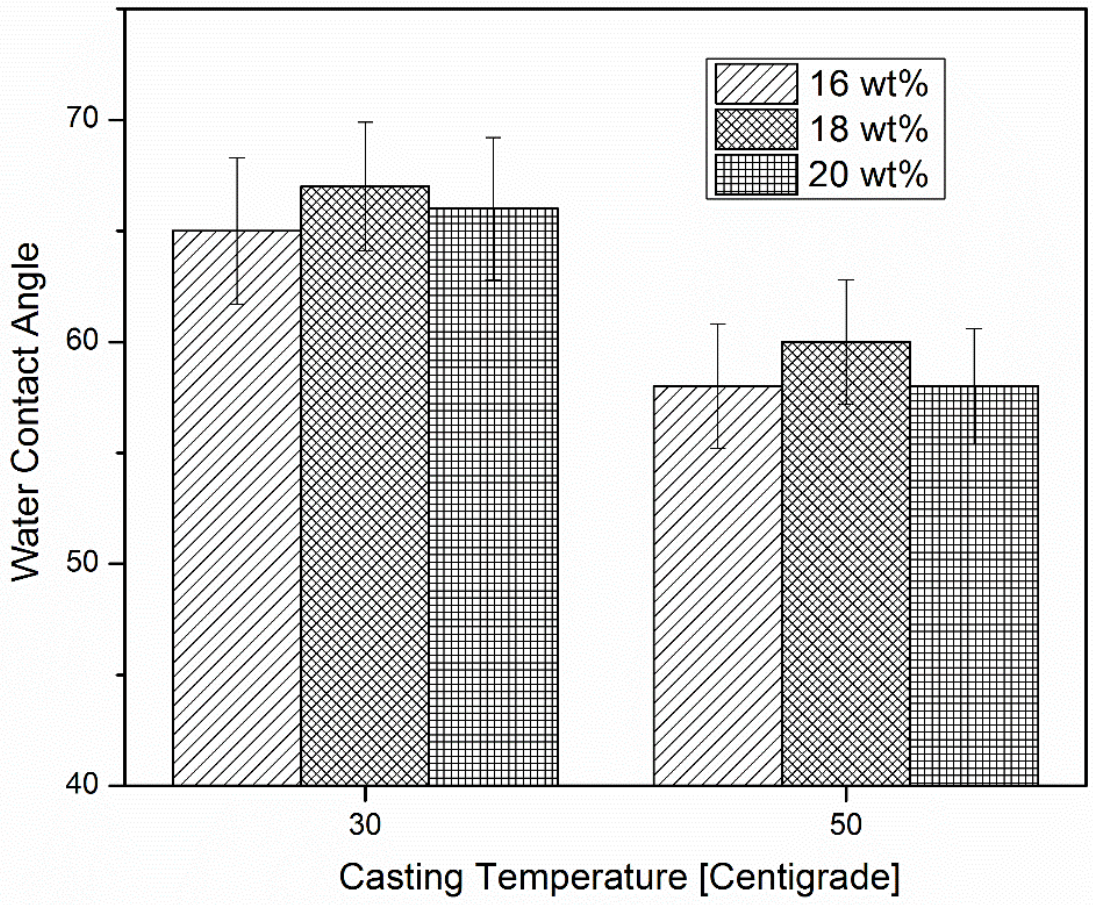

Figure 4. 2 Water contact angle for the membrane prepared with 16, 18, 20 wt. % PES

Table 4.3 shows the total porosity of the prepared membranes. The overall porosity increased with the casting temperature for all of the prepared membranes; meanwhile, it declined by increasing the polymer concentration in the casting solutions. As discussed previously, the higher rate of diffusion between the solvent and non-solvent in the polymer films at elevated temperatures may facilitate the formation of pores, and hence lead to an increase in the total porosity. Moreover, casting solutions with higher polymer

concentrations displayed higher viscosity which dominated its lower thermodynamic stability and led to an overall lower porosity [149].

Table 4.3 shows the mean pore radius of the top dense layer of the membranes measured by the Guerout-Elford-Ferry equation. The average pore radius of the dense layer of the membranes is in the range of 3.3-7.3 nanometers. The samples which were cast at 50 °C, with lower polymer concentrations, showed larger pore radii. Pore size of the membranes is influenced by two competing factors; de-mixing of the solutions and the diffusion rate between the solvent and non-solvent [144]. Decreasing the de-mixing of the polymer solution, by increasing the temperature, may lead to smaller pore sizes; but a higher rate of diffusion between the solvent and non-solvent facilitates the pore formation and leads to an increase in the average pore size. Therefore, it can be inferred that the effect of the higher temperature dominated the decrease in the de-mixing tendency; which led to an increase in the total porosity and the average pore size of the membranes.

Membranes with 18 wt. % PES in the casting solution, show a slightly higher pore size than the membranes cast with 16 wt. % concentration. This observation can be explained by the competition between temperature of the casting solution (kinetic factor) and polymer concentration in the casting solution (thermodynamic factor). By increasing the polymer concentration from 16 wt. % to 18 wt. %, the increase in the de-mixing rate of the

solution dominated the effect of increased viscosity and lower diffusion rate. This led to higher pore size of the membranes cast with 18 wt. % PES.

Table 4.3. Total porosity, mean pore size, and surface are of the membranes

Membrane Name	Total Porosity (%)	Mean Pore Size (nm)	Surface area (cm^2/g)
PES 1630	73	4.7	21
PES 1650	81	5.6	16
PES 1830	69	5.7	20
PES 1850	70	7.3	17.5
PES 2030	67	3.3	19.2
PES 2050	73	4.4	18.1

The surface area of the membranes measured by the BET method are also presented in Table 4.3. It can be seen that the membranes prepared at a lower casting temperature (30 °C) have large surface areas, which is in agreement with previous studies [150]. The surface area of the membranes decreased by increasing the casting temperature from around 19, 20 and 21 m^2/g to 16, 17 and 18 m^2/g for membranes containing 16, 18, and 20 wt.% PES in the casting solution; respectively. The higher rate of de-mixing, occurring at elevated temperatures, led to a higher amount of macro-voids as well as a larger mean pore size, which is the main cause for the reduced surface area of the membranes.

It has also been reported that the nodular structure plays a major role in the high values of surface area for polysulfone membranes [150]. Fig. 4.3 shows SEM image of the nodular

structure of the fabricated membranes which contributes to the observed large surface areas.

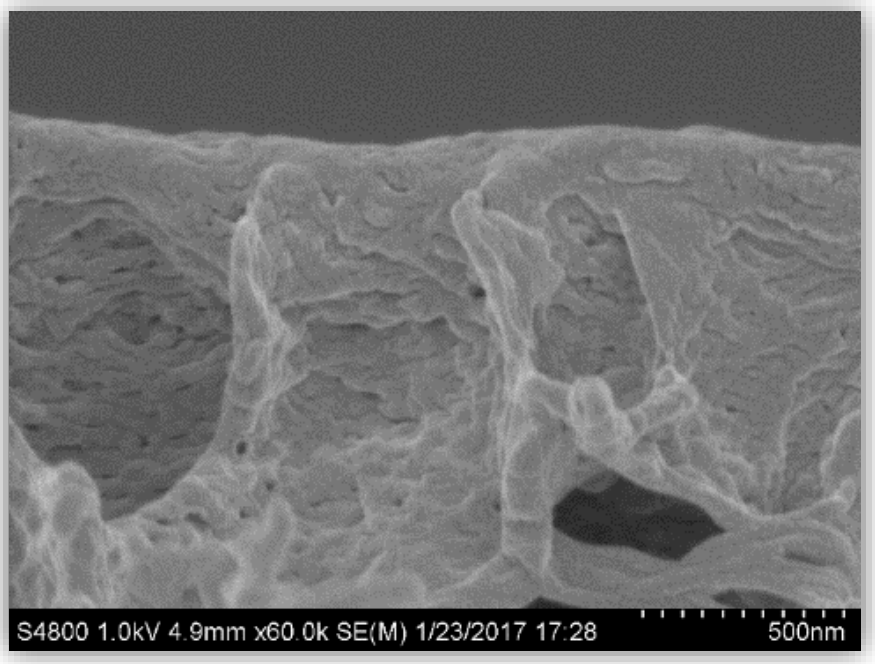

Figure 4. 3 Nodular structure of the PES membranes at high magnification

4.1.3.4 Permeability (Pure water flux)

Fig. 4.4 shows the average pure water flux (measured and averaged for three samples) of all the prepared membranes. The temperature of the casting solution has a significant effect on the pure water flux of the membranes. The pure water flux of the membranes containing 16 wt.% PES, increased from 62 to 110 kg/m^2.h while the membranes containing 20 wt.% showed an increase from 22 to 48 kg/m^2.h when the casting temperature was

decreased from 50 °C to 30 °C. Overall, the permeability of the membranes nearly doubled with increasing the casting temperature. The lower hydrophilicity and higher pore content of the membranes, at lower PES concentration, are the main contributors to the increase in permeability for these membranes.

The membranes with lower PES concentration cast at same temperature displayed higher water flux. Since the water contact angle of these samples does not show a considerable variation, the higher pore content and larger pore size of the membranes cast with lower PES concentration is the main reason for their higher pure water flux. Therefore, the change in the polymer concentration and temperature of the casting solution strongly influence the pore structure and hydrophilicity of the membranes; and hence affecting their overall permeability.

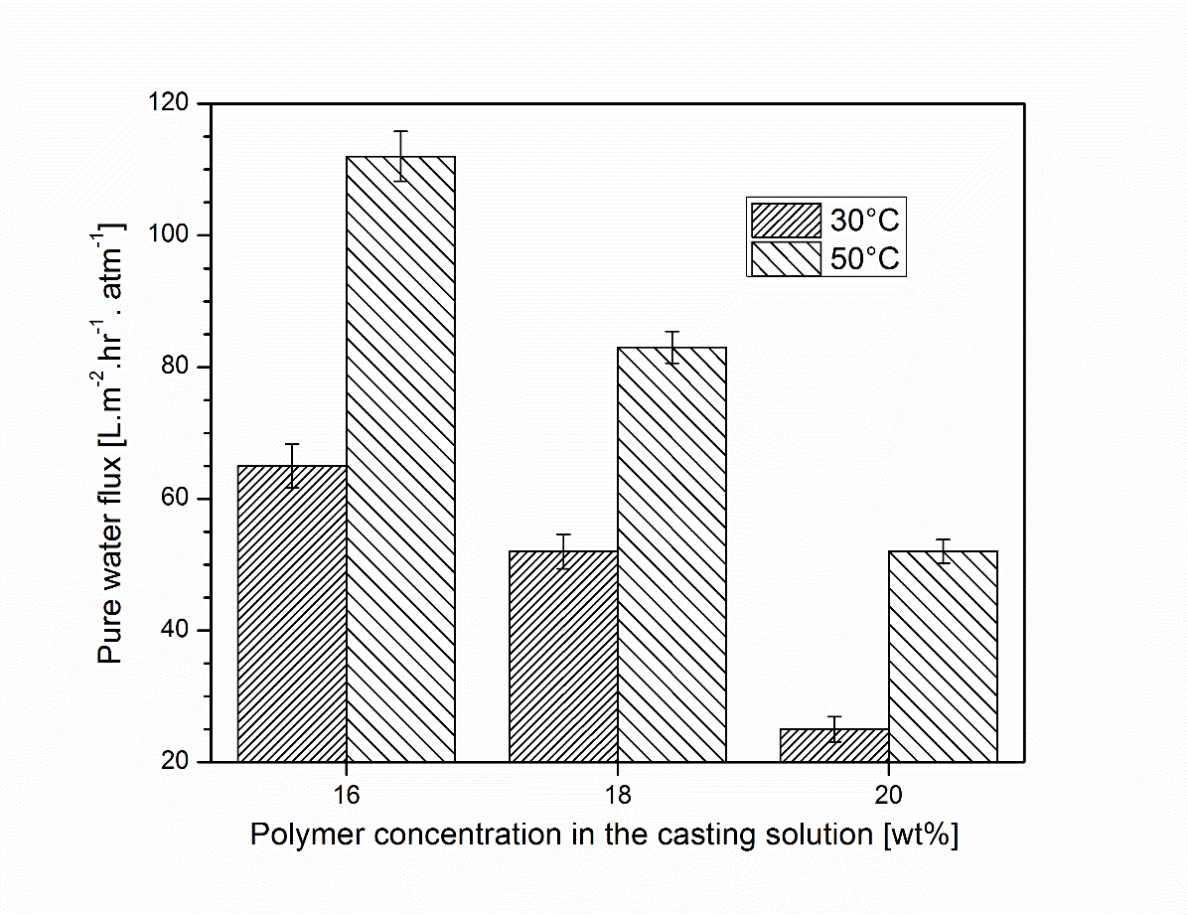

Figure 4. 4 Permeability of the membranes prepared with 16, 18, and 20 wt% PES

4.1.3.5. Tensile strength

Fig. 4.5 shows the tensile strength of the prepared samples. The sample with 20 wt. % cast at 30 °C displayed the highest tensile strength while the 16 wt. % polymer concentration sample casted at 50 °C show the lowest tensile strength. Among the membranes cast at the same temperature, the samples with higher polymer concentration show higher tensile strength. This may be due to the greater amount of micro-voids in

the membrane structure. The presence of macro-voids in the membranes has advantages and disadvantages. Macro-voids could result in decreased mechanical properties of the membranes and limit their application in the filtration process. On the other hand, macro-voids provide better permeability due to their larger size. Moreover, by increasing the temperature from 30 to 50 °C, the tensile strength decreased which can be contributed to the higher total porosity of the membranes cast at 50 °C.

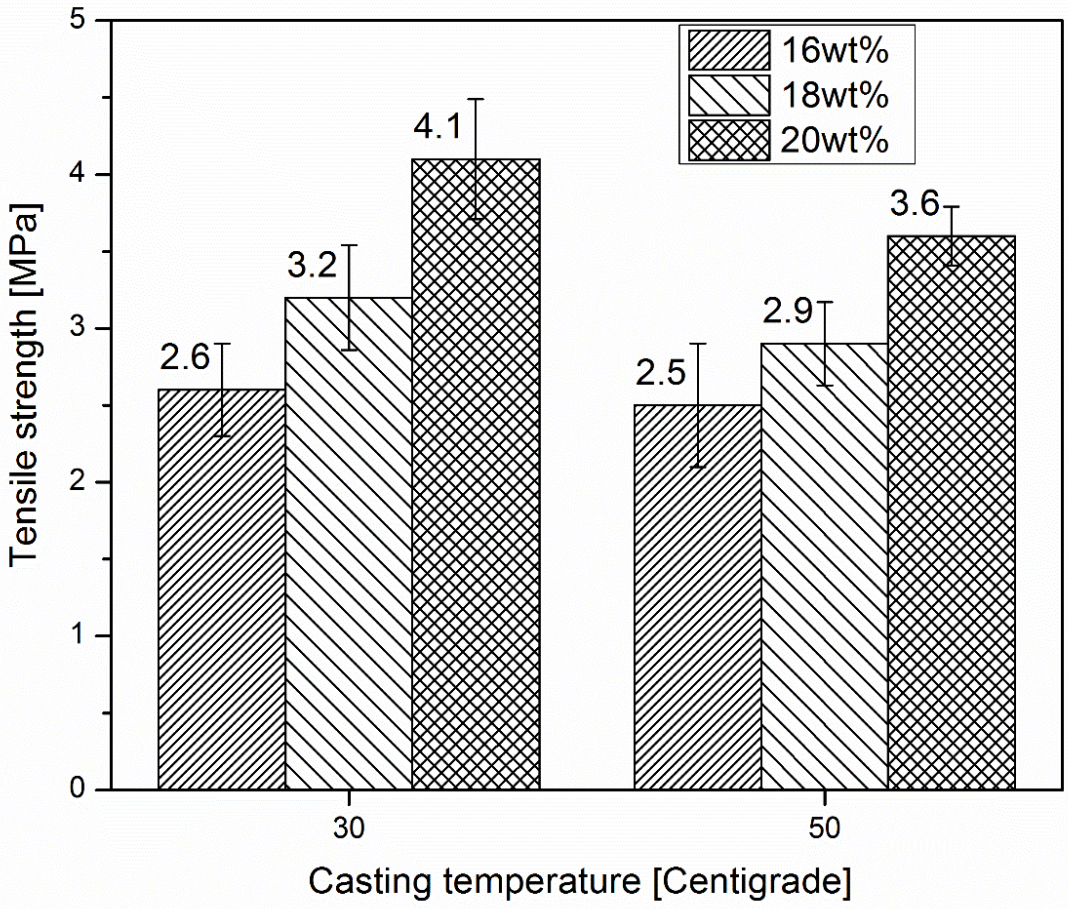

Figure 4. 5 Tensile strength of the membranes prepared with 16, 18, and 20 wt% PES

4.1.3.6 Conclusion

PES asymmetric membranes were prepared from casting solutions containing 16, 18, and 20 wt. % PES using the immersion precipitation method, at 30 and 50 °C. The casting parameters (polymer concentration and temperature of the casting solution) greatly influenced the morphology and performance of the membranes. All the membranes demonstrated a typical asymmetric structure with fully developed macro-pores due to the instantaneous de-mixing, irrespective of polymer concentration and temperature of the casting solution. Membranes prepared with higher amounts of polymer (PES) exhibited lower total porosity, smaller mean pore size, lower permeability, and less surface area. Whereas, membranes prepared with a higher solution temperature, exhibited larger pore size, higher hydrophilicity, and higher water flux. In addition, increasing the casting temperature led to a decrease in the tensile strength of the membranes. The results of this study show that the polymer concentration and casting temperature can be used to custom tailor PES membranes for various specific applications.

Considering the pure water flux and tensile strength of PES membranes, membranes with 18wt% polymer in the casting solution casted at 30 °C was to use as the matrix to prepare

nanocomposite membranes. Membranes with 16 wt. % PES in the casting solution, showed decreased mechanical properties. These membranes got wrinkled in the handling and drying process. Moreover, membranes with 20 wt. % PES exhibited low power flux. Therefore, membranes with 18 wt. % polymer in the casting solution were selected.

4.2. Synthesizing and characterization of nanocomposite membrane

4.2.1. Introduction

Despite the abundant number of water filtration technologies and products available in the market today, new products and technologies are continuously being introduced to the global markets. This can be attributed to several reasons: (1) the practical uses of the majority of the available products and technologies are often limited to a narrow set of conditions, therefore lacking versatility even within a specific type of contaminants; (2) their performance continues to lag behind the recommendations of various world health organization's due to concurrent new research and discoveries of the serious health risks of these contaminants on the human organs, and the continuously evolving nature and forms of generating contaminants (existing and new) and delivering them into our eco system; (3) the material and manufacturing costs of the majority of commercial products present one of the main constraints to alleviating the aforementioned limitations. It is possible to design water filtration systems with far superior flexibility and performance than the existing systems, however, the cost of such systems hinders their commercialization potentials and competitiveness in the global markets.

Heavy metal ions are among the most dangerous water pollutants, even at low concentration [151]. Lead is one of the most hazardous heavy metals due to its toxicity

and potential carcinogenicity toward human and other organisms [152]. Exposure to lead through drinking water is attributed to different health problems; such as kidney damage, anemia, learning disabilities, hypertension, mental retardation, and sterility [153]. Therefore, there is of the utmost importance to improve the methods of removing lead ions from water [154, 155]. Currently, several physio-chemical and biological approaches such as precipitation, coagulation, adsorption, ion-exchange, biological treatment, and membrane processes are employed to remove lead from polluted waters [156-158]. Among these methods adsorption is one of the most widely used processes since it is very effective, economical and versatile [159, 160]. Meanwhile nanostructured materials usually in the form of inorganic nanoparticles, are known as efficient adsorbents due to their high specific surface area and high chemical affinity toward heavy metals [70]. However, difficulty in regeneration and separation of the nano-adsorbents from treated water remains a challenging issue [37, 159].

Incorporating of nanoparticles into polymeric membranes has been shown to be a promising method to improve the physio-chemical properties as well as heavy metal ions removal efficiency of such membranes [8, 37, 39, 161-165]. The membranes themselves might also act as the auxiliary adsorbent in enhancing the overall adsorption capacity [37]. Different types of nanoparticles have been utilized to improve the heavy metal ions removal performance of membranes [8, 166]; of which, metal oxide nanoparticles have shown unique and promising results [74, 167]. Metal oxide nanoparticles such as MnO_2

[157, 167], ZrO_2 [62] and Fe_3O_4 [38, 39, 74, 76] have been successfully utilized in polymer nanocomposite membranes and foams for the removal of heavy metal ions from water. Aluminum oxide is regarded as one of the most promising nano-adsorbents due to its high affinity toward heavy metal ions in aqueous solutions [92, 159, 168-172].

In this section, γ-alumina nanoparticles are used to synthesize PES nanocomposite membranes with enhanced removal capability of copper from water. Alumina/PES membranes with different amounts of alumina nanoparticles in the polymer matrix, were fabricated using a phase inversion process. The morphology and performance of the membranes were characterized using field emission scanning electron microscopy (FESEM), X-ray diffraction (XRD), water contact angle, porosity measurements, and tensile strength. The water flux, lead ion removal, and copper ions adsorption capacity of the membranes were also studied. The Experimental results showed that the addition of nanoparticles increases the hydrophilicity, total porosity, BET surface area, and tensile strength of the membranes. In addition, water permeation of the membranes increased significantly by adding alumina nanoparticles. Based on rejection performance test, the membrane with 1 wt. % nanoparticles exhibited the highest rejection for lead ions of 61%. Langmuir and Freundlich isotherm analysis were tested for adsorption, where Freundlich isotherm resulted in the best fitting indicating the presence of heterogeneous adsorption surfaces.

4.2.2. Membrane preparation and characterization

The PES and PES/Alumina membranes were prepared and characterized as described previously in chapter three. Briefly, PES flat membranes were synthesized by phase inversion method via the immersion precipitation. A homogenous mixture of alumina nanoparticles and DMAc was prepared by adding predetermined amount of alumina nanoparticles into the DMAc and sonication for 1 h. Afterward, measured amounts of PES and PVP were dissolved into the mixture while stirring at 400 rpm for 24 h. Finally, the doped solutions were mixed by an acoustic mixer for 1 h before casting. The solutions were cast on a glass plate at room temperature with a thickness of 200 μm using a doctor blade apparatus and an automatic film applicator at a speed of 60 mm/s. The cast was subsequently moved into the distilled water and stored for 24 h. Finally, the prepared membranes were washed and were dried between two sheets of filter paper and vacuum dried for 24 h at 50 °C. Table 4.4 shows the compositions of the solutions that were used to fabricate the PES/Alumina membranes. Nanoparticle contents more than 2wt. % were not chosen, as the synthesized membranes in preliminary experiments showed high agglomeration and high variation in the flux and rejection.

4.2.3. Static Cu(II) adsorption analysis

Batch adsorption experiments were conducted to calculate the static adsorption of Cu(II ions on the alumina/PES membranes mixed matrix membranes. Copper solutions with

Table 4.4 Compositions of the casting solutions

Sample	Al_2O_3 (wt. %)	PES (wt. %)	PVP (wt. %)	DMAc (wt. %)
M 0	0	18	1	81
M 0.5	0.5	18	1	80.5
M 1	1	18	1	80
M 2	2	18	1	79

different initial concentrations in a range of 20-80 ppm, were prepared by dissolving $Cu(NO_3)_2$ in deionized (DI) water. Batch adsorption tests were conducted by adding 0.1 gr of sliced membranes into vessels containing 100 ml of Cu(II) solutions. The vessels were then placed in a shaker and agitated at room temperature for 48 h. The equilibrium concentration of copper in the solutions was determined by a flame atomic adsorption spectrometer (AAS) (ICE 3000 ThermoFisher). The lead ion adsorption of the membranes (mg/g) were calculated by equation 4.1:

$$q_e = \frac{(C_0 - C_e)V}{M_m} \qquad \text{Equation 4. 1}$$

Where q_e is the equilibrium adsorbed amount of lead ions per membrane weight (mg/g), C_0 and C_e are initial and equilibrium concentrations (mg/L) of Cu(II) in the solution, V is the volume of the lead solution (L), and M_m is the mass of the membrane (g).

4.2.4. Results and Discussion

4.2.4.1. Membrane characterization

The presence of alumina nanoparticles in the membrane structure was confirmed by XRD analysis. The XRD spectra of γ-alumina nanoparticles, neat PES membrane and alumina/PES nanocomposite membranes are shown in Fig. 4.6. The pattern for alumina nanoparticles presented three main characteristic peaks at about 2θ = 38° , 46° and 68° which is in agreement with the characteristic peaks of γ-alumina [173, 174]. It can also be seen that the PES polymer is primarily amorphous and shows one main peak at 2θ = 18.2°, which is similar to the reported peak for pure polyethersulfone polymer [175].

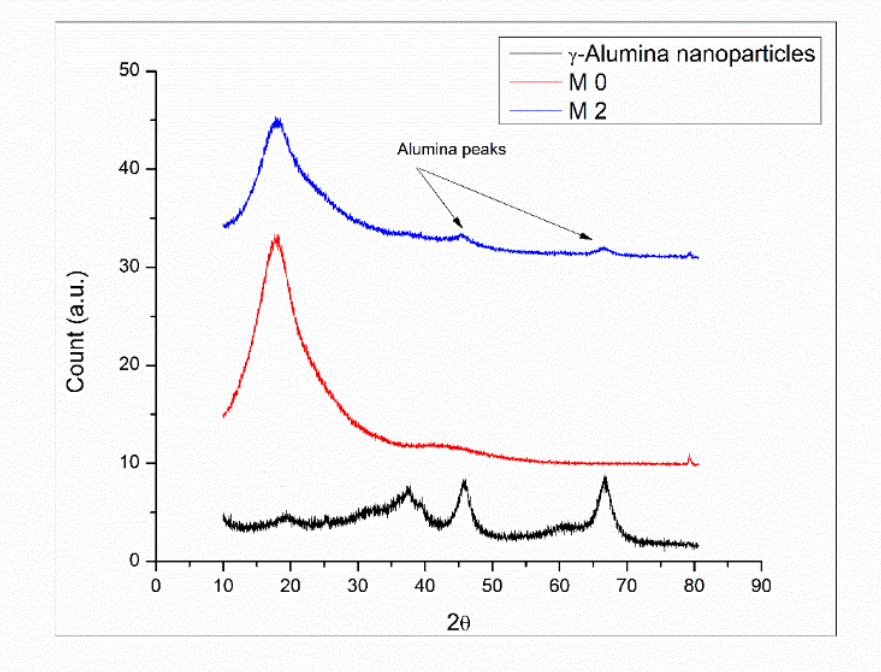

Figure 4. 6 X-ray diffraction patterns of γ-alumina nanoparticles, neat PES membranes and alumina/PES nanocomposite membranes

For the alumina/PES nano-enhanced membranes, two new peaks at $2\theta = 46°$ and 68° appeared on the spectrum, which indicated the presence of γ-alumina nanoparticles in the PES membrane matrix. The results show that the γ-alumina nanoparticles are distributed into the polymer matrix, while the membranes maintained their amorphous structure.

FESEM images of the cross section of the synthesized membranes are presented in Fig. 4.7. The cross section of the membranes shows a typical asymmetric structure consisting of a dense top layer supported by large finger like pores and macro voids. This structure contributes to the higher flux properties of the membrane while maintaining its salute rejection, which will be discussed in the following sections. It can also be seen that the nanocomposite membranes contain larger macro-voids in the sub layer compared to neat PES membrane, which is in accordance with the total porosity and BET surface area numbers presented in Table 4.5. Generally, the growth of sublayer macro voids lead to higher porosity and higher amount of available surface area.

The nanocomposite membranes possess higher total porosity and surface area compared to neat PES membranes as presented in Table 4.4. The total porosity increased with increasing the nanoparticles amounts in the matrix from 66% for neat polymeric membranes to 79% for membranes with 2% nanoparticles (M 2). It has been reported that the interaction between nanoparticles and the polymer solution leads to easier diffusion

of solvent molecules from the polymer matrix to the coagulation bath [38, 67]. In addition, the diffusion rate of the solvent (DMAc) from the membrane into the coagulation bath can also increase through the addition of nanoparticles [66]. As a result, the nanocomposite membranes have a higher amount of total porosity and BET surface area compared to the neat polymeric membrane.

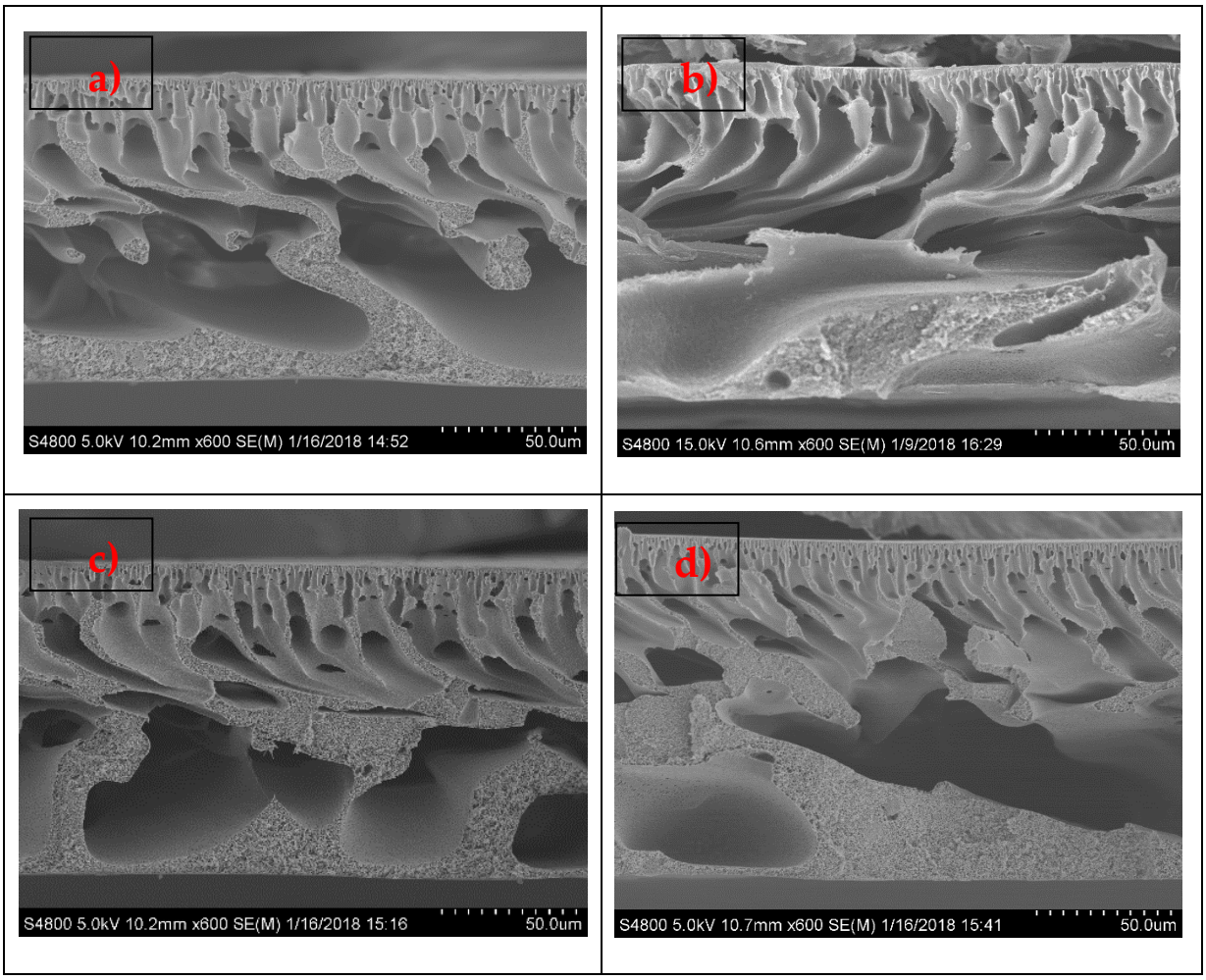

Figure 4. 7 SEM cross-section images of a) M 0, b) M 0.5, c) M 1, and M 2 membranes

Table 4.5 Total porosity, water contact angle, BET surface area, and pure water flux of the membranes

Membrane Samples	Porosity (%)	Water contact angle	Pure water flux ($Kg/m^2.h$)	BET Surface area (m^2/g)	Tensile Strength (MPa)
M 0	66	68	38.3	20.8	2.8
M 0.5	71	59	46.8	26.3	3.2
M 1	74	53	56.1	28.4	3.6
M 2	79	50	57.3	31.5	3.9

Contact angle measurement is a common method to characterize the hydrophobicity and hydrophilicity of membranes [28, 76]. A high contact angle indicates the membrane is more hydrophobic, and vice versa. Table 4.4 shows the contact angle measurements for the synthesized membrane samples. Water contact angle of PES membrane decreases from 68° to 50° with increasing the nanoparticle content in the matrix. The hydroxyl content of the membrane surface increases due to the incorporation of alumina nanoparticles into the membrane surface leading to increased hydrophilicity of the membrane surface [26].

The tensile strength of the nanocomposite membranes is also presented in table 4.4. The tensile strength of the membranes increased from 2.8 MPa to 3.9 MPa with the addition of nanoparticles to the polymer matrix. This can be attributed to restricting the movement of polymeric chains due to intermolecular forces between the polymeric chains and alumina nanoparticles [24].

4.2.4.2. Adsorption study

Figure 4.8 shows the static adsorption of Cu(II) versus time for the synthesized alumina/PES membranes at an initial lead concentration = 20 ppm. The results show that the adsorption capacity of Cu(II) in the nanocomposite membranes has improved significantly compared to the neat PES membrane. It can also be seen that by increasing the alumina concentration in the membranes, the adsorption capacity increases. The highest Cu(II) adsorption capacity for each membrane, was 6.5, 11.4, and 11.9 mg/g for M 0.5, M 1, and M 2 membranes, respectively. The increase in the adsorption capacity can be attributed to the higher number of active sites (alumina nanoparticles) available for the adsorption of Cu(II) ions in the membranes.

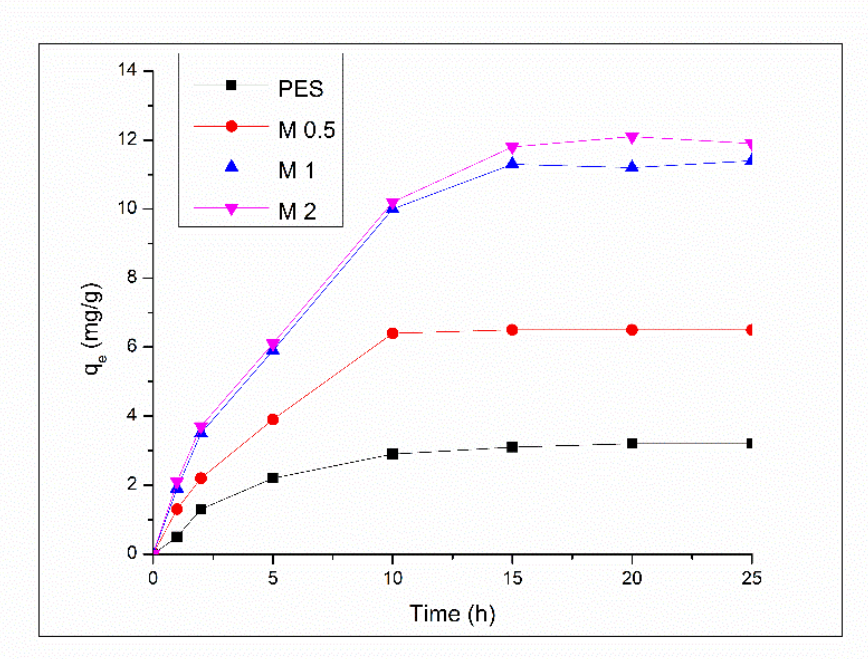

Figure 4. 8 Adsorption capacity of the membranes (initial copper concentration= 20 ppm)

Langmuir and Freundlich equilibrium adsorption isotherms were applied on the Cu(II) adsorption data for the alumina/PES membranes. Table 4.6 presents the Langmuir and Freundlich isotherm parameters. Langmuir isotherm, which indicates a monolayer adsorption on the homogenous adsorption sites, is expressed as shown in equation 4.2:

$$q_e = \frac{q_{max}\, b\, C_e}{1+bC_e} \qquad \text{Equation 4.2}$$

Where q_e is the equilibrium adsorption (mg/g), C_e is the equilibrium concentration in the aqueous phase (g/L), q_{max} is the adsorption capacity (mg/g), and b in the equilibrium constant (L/mg).

Meanwhile, Freundlich isotherm corresponds to a multilayer adsorption on a heterogeneous surface and is formulated by equation 4.3:

$$q_e = k\,.\,Ce^n \qquad \text{Equation 4. 3}$$

Where k and m are the relative adsorption constant and adsorption intensity parameter.

Both equilibrium models show strong data fittings with close to a 99% correlation coefficient (R^2). The slightly higher correlation coefficient in the case of the Freundlich model indicates a multilayer adsorption coverage on the membrane surface to be dominant. In addition, the fitness of equilibrium data to the Freundlich model indicates that the adsorption of lead ions is heterogeneous in nature.

Table 4. 6 Equilibrium constants of Langmuir and Freundlich isotherms

Membrane Sample	Langmuir Model			Freundlich model		
	q_m (mg/g)	b (L/mg)	R^2	K_F (mg/g)	n	R^2
M 0.5	18.08	0.057	0.985	3.135	0.359	0.994
M 1	23.36	0.021	0.981	5.942	0.291	0.993
M 2	25.91	0.018	0.983	6.051	0.312	0.995

4.2.4.3. Filtration performance of the membranes

The copper rejection capability of the synthesized alumina/PES membranes is shown in Fig. 4.9. Neat PES membranes exhibited the lowest amount of lead removal while the membranes containing 1 wt. % of alumina nanoparticles (M 1) revealed the highest copper removal of 61%. Alumina nanoparticles, dispersed in the polymer matrix of the nanocomposite membranes, act as active adsorption sites thus preventing copper ions from passing through the membranes [37, 91, 92, 176, 177]. This is compatible with the BET surface area and static adsorption results, presented earlier in Tables 4.4. The higher BET surface area of the nanocomposite membranes due to presence of alumina nanoparticles in the matrix of nanocomposite membranes provide more available active sites for copper adsorption.

Although M 2 membranes (2 wt. % alumina) showed the highest static adsorption capacity, the rejection rate for these membranes in the filtration cell was slightly less than M 1. This can be attributed to an agglomeration of the nanoparticles as shown in Fig. 4.10.

Agglomeration of the nanoparticles decreases the effectiveness of lead removal by decreasing the available surface area of the nanoparticles and hence the rejection rate.

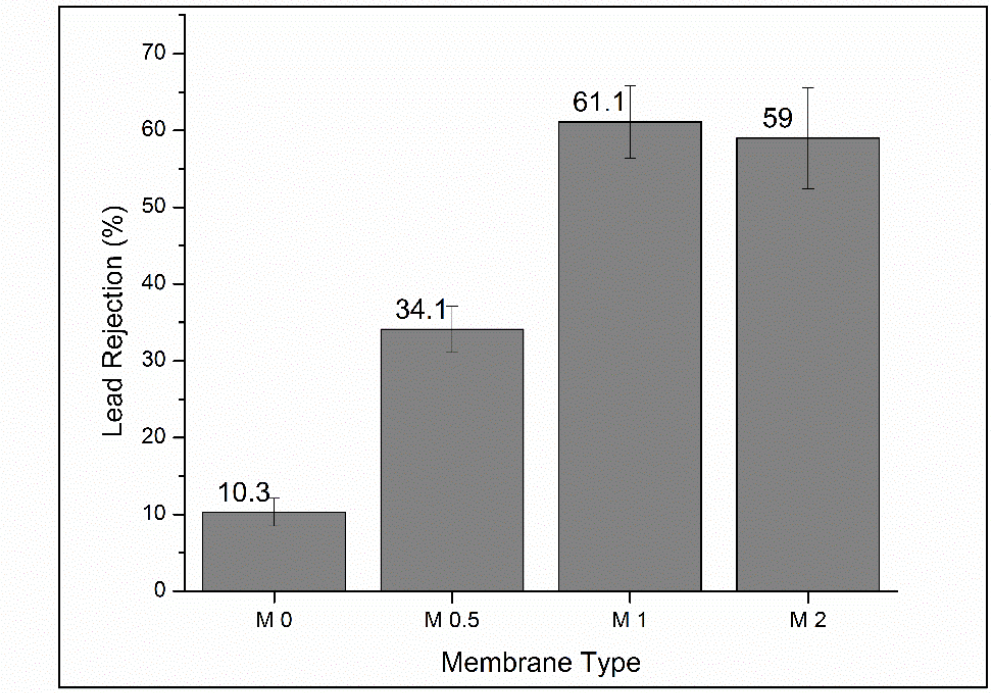

Figure 4. 9 Copper removal (%) from aqueous solution

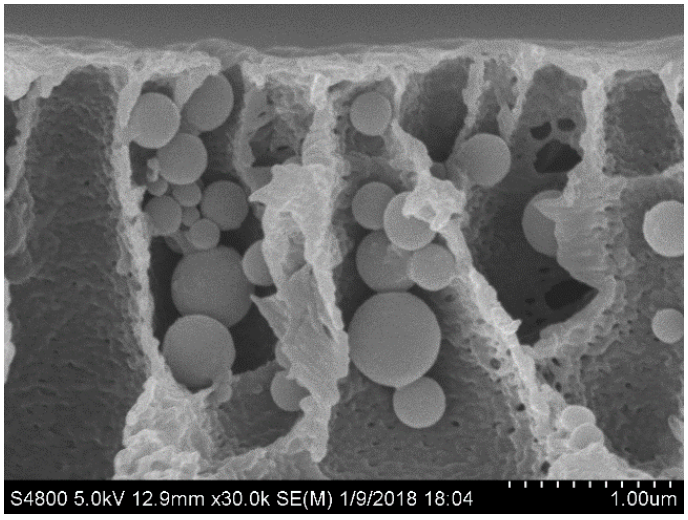

Figure 4. 10 SEM cross-section image of M 2 membrane at higher magnification which shows the embedded nanoparticles in the membrane matrix

The pure water flux along with water contact angles of the membranes are shown in Fig. 4.11. Membranes with higher amount of nanoparticles show a higher flux as well as lower water contact angle. This can be attributed to the higher hydrophilicity of surface and the higher porosity of the membranes containing higher nanoparticles amount [18, 62, 64, 104]. However, increasing the nanoparticles amount from 1 to 2 wt. % does not lead to a significant change in the water flux. This observation can be attributed to the agglomeration of the nanoparticles. It has been reported that the agglomeration of the nanoparticles can lead to the blocking of the surface pores of the membranes and result in lower permeability, which is in accordance with the result of other researchers [37, 57, 74]. Therefore, there is a maximum limit on the content of nanoparticles for optimum performance. Passing this threshold may lead to a decrease in the water flux due to pore clocking as a result of the agglomeration of the nanoparticles.

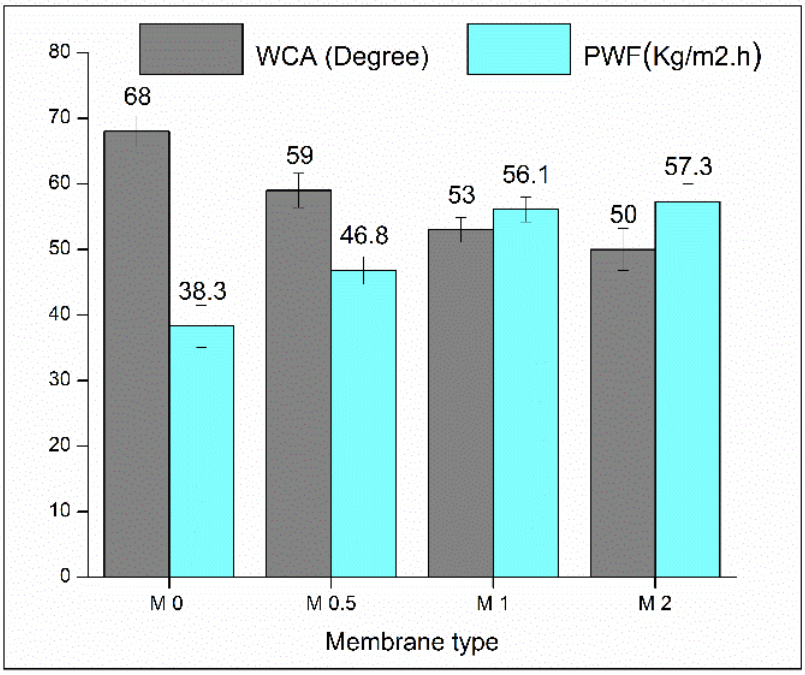

Figure 4. 11 Pure water flux (PWF) and water contact angle (WCA) of the synthesized membranes

4.2.4.4. Conclusion

Different concentrations of γ-Al_2O_3 nanoparticles were incorporated in PES membranes for the removal of copper ions from aqueous solutions. The morphology and performance of the nanocomposite membranes were analyzed. It was revealed that adding the alumina nanoparticles enhanced the membranes' hydrophilicity by decreasing the water contact angle from 68° to 57°; enhanced tensile strength of the membranes by 40% (2.8 to 3.9 MPa); enhanced the overall porosity and the BET surface area, and hence the permeability and water flux of the membranes. Consequently, the copper ion removal increased from 10%, in the case of pure PES membranes, to 61% for

nanocomposite membranes containing 1wt. % of alumina nanoparticles. Static adsorption study showed that Freundlich model better represents the adsorption of lead ions on the membranes which corresponds to the heterogeneous adsorption sites.

As the adsorption of heavy metal ions on the surface of alumina nanoparticles is the main mechanism of heavy metal ions rejection, increasing the amount of nanoparticles improves the heavy metal rejection of nanocomposite membranes. However, as shown in this section, practically it is not possible to add more than 2 wt. % alumina nanoparticles, and severe agglomeration happens in higher amount of nanoparticles. Following the designed set of experiments, in the next chapter, alumina nanoparticles were treated to decrease the agglomeration and to improve the heavy metal ions rejection performance of the nanocomposite membranes.

4.3. Polyethersulfone Membranes Prepared with 3-Aminopropyltriethoxysilane Modified Alumina Nanoparticles for Cu(II) Removal from Water

4.3.1. Introduction

Heavy metal ions are among the most dangerous water pollutants, even at low concentrations. Although copper is considered to be a vital micronutrient for humans, excess accumulation of copper in the human body poses a dangerous health risk and may cause headache, depression, nausea, learning problems, kidney and liver damage [76, 178]. Currently, several physio-chemical and biological approaches; such as precipitation, coagulation, adsorption, ion-exchange, biological treatment, and membrane processes are employed to remove heavy metals from polluted waters [157]. Among these methods, adsorption is the most widely used mechanism due to its high effectiveness, low cost, and versatility [159, 160].

Nanostructured materials, usually in the form of inorganic nanoparticles, are known as efficient adsorbents due to their high specific surface area and high chemical affinity toward heavy metals [70]. However, difficulty in regeneration and separation of nano-adsorbents from treated water remains a challenging issue [37, 159]. Incorporating nano-adsorbents into porous polymeric materials has been shown to be a promising approach to address the aforementioned issue and improve the removal efficiency of the

membranes [37, 39, 162]. The membranes themselves might also act as the auxiliary adsorbent in enhancing the overall adsorption capacity [37].

Different types of nanoparticles have been utilized to improve the heavy metal ions removal performance of membranes [8]; of which, metal oxide nanoparticles have shown the most promising results [43, 74, 167]. Metal oxide nanoparticles; such as MnO_2 [157, 167], ZrO_2 [62] and Fe_3O_4 [38, 39, 74, 76] have been extensively utilized to synthesize nanocomposite membranes in order to improve the membrane performance for the removal of heavy metal ions from water. Among these nanoparticles, aluminum oxide (alumina) is one of the most promising adsorbents due to its high affinity toward heavy metal ions in aqueous solutions [92, 159, 168, 171]. A majority of the research on impregnating polymeric membranes with alumina nanoparticles has been focused on flux improvement and fouling mitigation [62, 93-95]. Although few studies investigated the use of alumina nanoparticles in PES membranes for the removal of contaminants; such as dye and nitrate [90, 96, 179], very few studies investigated the use of alumina/PES membranes for the removal of heavy metal ions from water [37].

Recently, the incorporation of modified nanoparticles into polymeric materials has attracted great interests. One common method to modify the nanoparticles is treating them by silane coupling agents; such as MMDES, and 3-Aminopropyltriethoxysilane (APTES) [13, 14]. Silane coupling agents are extensively used in inorganic polymer composites such as mineral filled polymer composites [15, 16]. Choosing the appropriate

silane group can modify the surface of an inorganic material from hydrophilic to hydrophobic and increase its affinity to the functional groups of the polymer matrix [1, 2], and decrease the agglomeration of nanoparticles [180].

In this study, alumina nanoparticles, treated by APTES, are used to fabricate novel PES membranes to remove Cu(II) ions from water. The morphology and physio-chemical properties of the modified nanoparticles and membranes were characterized by FTIR, XRD, FESEM, DMA, porosity, and water contact angle. The performance of the membranes was tested in terms of Cu(II) ion removal from water as well as pure water flux measurements.

4.3.2. Experimental

4.3.2.1. Surface modification of alumina nanoparticles

To increase the stability of the nanoparticles in the casting solution, surface modification of alumina nanoparticles with APTES coupling agent was carried out. Certain amounts of alumina nanoparticles were added to anhydrous ethanol under nitrogen purging followed by 60 and 30 minutes bath and probe sonication. Subsequently, 4 wt. % of APTES was added to the mixture under nitrogen atmosphere. After stirring for 6 h at 70 °C, the particles were separated from the solution by centrifuging at 10,000 rpm for 20 min. Finally, the Al_2O_3 particles were dried in an oven for 24 h at 50 °C.

4.3.2.2. FTIR Study

FTIR spectroscopy was used to confirm the chemical modification of alumina nanoparticles. FTIR spectra of APTES modified alumina nanoparticles and non-modified alumina nanoparticles were measured using Bruker ECO-ATR spectrophotometer from 4000 to 400 cm^{-1}. Each spectrum was captured by averaging 400 scans with a resolution of 2 cm^{-1}.

4.3.2.3. Preparation of PES/alumina mixed matrix membranes

Table 4.7 shows the compositions of doped solutions prepared to fabricate nanocomposite membranes. PES flat membranes were synthesized by phase inversion via the immersion precipitation method. A homogenous mixture of alumina nanoparticles and DMAc was prepared by adding predetermined amounts of nanoparticles into the DMAc and sonication for 1 h. Afterward, measured amounts of PES and PVP were dissolved into the mixture while stirring at 400 rpm for 24 h. Finally the solutions were mixed by an acoustic mixer for 1 h before casting.

The solutions were cast onto a glass substrate at room temperature with a thickness of 200 μm using doctor blade technique and an automatic film applicator at a speed of 60 mm/s. The casting was subsequently moved into distilled water and stored for 24 h. The prepared membranes were washed and dried between two sheets of filter paper and subsequently vacuum dried for 24 h at 50 °C.

Table 4. 7 Compositions of the casting solutions

Membrane Sample	PES (wt.%)	PVP (wt.%)	DMAc (wt.%)	Al_2O_3 (wt.%)
M 0	18	1	81	0
M 3	18	1	78	3
M 4	18	1	77	4
M 5	18	1	76	5

4.3.2.4. Static Cu(II) adsorption study

Batch adsorption tests were performed to calculate the static adsorption of Cu(II) ions on the PES/alumina mixed matrix membranes. Copper solutions with different initial concentrations in the range of 20-80 mg/L were prepared by dissolving $Cu(NO_3)_2$ in DI water. The tests were carried out by adding 0.05 g of sliced membranes into vessels containing 100 ml of Cu(II) solutions. The vessels were then placed in a shaker and agitated at room temperature for 48 h. The equilibrium concentration of Cu(II) in the solutions was determined by a flame atomic adsorption spectrometer (AAS) (ICE 3000 ThermoFisher). The copper ion adsorption of the membranes (mg/g) were calculated by equation 4.4;

$$q_e = \frac{(C_0 - C_e)V}{M_m} \qquad \text{Equation 4. 4}$$

where q_e is the equilibrium adsorbed amount of copper ion per membrane weight (mg/g), C_0 and C_e are the initial and equilibrium concentrations (mg/L) of Cu(II) in the solution, V is the volume of the copper solution (L), and M_m is the mass of the membrane (g).

4.3.3. Nanocomposite membranes characterization

4.3.3.1. XRD analysis

To determine the crystal phase composition of the alumina nanoparticles, PES, and alumina/PES membranes, X-ray diffraction (XRD) analysis was conducted using an Advance Bruker-D8 Discover diffractometer ($K_{\alpha 1}$ = 1.5406 Å, 2θ range from 5° to 80°). The detector was LYNXEYE-XE operating at accelerating voltage of 40.0 kV and emission current of 40.0 mA.

4.3.3.2. Dynamic mechanical analysis

Dynamic mechanical analysis (DMA) is a useful technique to measure the glass transition temperature of the membranes. Neat polymeric and nanocomposite membranes were investigated using a TA Instrument Q800 dynamic mechanical analyzer. A preload of 0.005 N was applied to keep the samples flat during the test. The membrane samples were heated at the rate of 3 °C min^{-1} from 25 to 280 °C while oscillating at a frequency of 1 Hz at an amplitude of 10 μm. Glass transition temperature of the synthesized membranes were determined from the peak of the loss modulus.

4.3.3.3. TGA Thermal Analysis

To investigate the thermal stability and dispersion of the alumina nanoparticles in the membranes, thermogravimetric analysis (TGA) was conducted under air atmosphere over a temperature range of 25-1000 °C at a heating rate of 10 °C min^{-1}.

4.3.3.4. Contact angle measurements

The contact angle of the prepared membranes was measured using a contact angle measuring instrument (Rame-Hart goniometer model 250). Sessile droplet method and image analysis of the droplet on the surface were used to measure the equilibrium water contact angle. A 6 μL water droplet was deposited on the membrane surface and the contact angle was measured after 5 s. The contact angle was measured at three different points on the membrane surface and the average value was reported.

4.3.3.5. Membrane porosity

In order to determine the total porosity of the synthesized membranes, membrane samples were cut to a certain dimension and soaked in distilled water for 24 h. The surface of the membrane samples was wiped with filter paper and the samples were immediately weighed. After that, the membranes were dried in a vacuum oven at 50 °C for 24 h and weighed again.

The total porosity of the synthesized membranes was determined by the following equation;

$$\text{Porosity (\%)} = \frac{W_w - W_d}{\rho w \times V} \qquad \text{Equation 4. 5}$$

where W_w and W_d are the weights of wet and dry membranes (g), ρ_w and V are water density (g/cm^3) and membrane pieces volume (cm^3); respectively. The results were reported as an average number of three measurements for each membrane sample.

4.3.3.6. BET Surface area

The gas adsorption-desorption technique was used to measure the surface area of the synthesized membranes. Nitrogen sorption analyses were obtained with a surface-area analyzer (Micromeritics ASAP 2020) using standard continuous procedures at 77.15 °K on the membrane samples that had been degassed at 333 °K under a high vacuum for 6 h. The surface area was calculated according to the Brunauer–Emmett–Teller (BET) model over a relative pressure range of 0.05–0.90.

4.3.3.7. Scanning electron microscopy

Field emission scanning electron microscopy (FESEM, Hitachi, S-8400) was used to analyze the morphology of the membranes. In order to minimize the stress on the sample and prevent deformation of the membrane cross-section and pore structure during fracturing, a modified freeze fracture method (Cryo-snap method) was used to break the samples. In this method, the specimen is embedded into ice before breaking [124]. The dried cut samples were iridium sputtered and were investigated under the microscope at 5 kV.

4.3.3.8. Filtration process

Water flux of the membranes was measured using a batch type dead end stirred cell (Millipore, UFSC05001) at a fixed speed of 400 rpm. Effective area of the membrane in the filtration cell was 13.4 cm^2. Prior to the water flux determination, the membrane sample was first pressurized at 4 bar for 1 h to minimize compaction effects. After compaction,

transmembrane pressure was set to 3.5 bar and the permeate flux was calculated by equation 4.6;

$$\text{Pure water flux (Kg/m}^2\text{h)} = \frac{Q}{A \times \Delta t} \qquad \text{Equation 4. 6}$$

Where Q, A and Δt are the quantity of permeate (kg), membrane area (m^2) and sampling time (h); respectively.

In order to evaluate the membrane performance in removing Cu (II) from water, feed solutions containing initial Cu (II) concentration of 20 mg/l were employed. The permeate was collected every 10 min and its concentration was measured. Copper ion removal was calculated using equation 4.7;

$$\text{Copper removal (\%)} = \left(1 - \frac{C_p}{C_F}\right) \times 100 \qquad \text{Equation 4. 7}$$

where C_p and C_F are the copper ion concentrations (mg/l) in the permeate and feed; respectively.

4.3.3.9. Membrane Usability

The membrane with the best performance was chosen for reusability test. The membrane used for copper removal test was regenerated by dipping and stirring for 1 h in the 10 mM EDTA solution [74]. Then the membrane was washed with plenty of deionized water and reused for the filtration test. This procedure were repeated for four times with the duration of 100 min for each filtration cycle.

4.3.4. Result and Discussion

4.3.4.1. IR Spectroscopy (FTIR)

The modification of alumina with APTES occurs by the reaction of the hydroxyl groups of Al_2O_3 nanoparticles with the silane functional group of APTES [13]. To investigate the modification efficiency of the nanoparticles, FTIR spectroscopy was used. The IR spectra of non-modified γ-alumina nanoparticles and APTES modified nanoparticles are shown in Figure 4.12. The broad adsorption peak in the range of 980-1220 cm^{-1} corresponds to Al-O-Si and Si-O-Si bonds of silane coupling agent. The frequency of Al-O-Al bonds in the alumina structure is also in this range [15].The wide peak at the range of 3000-3550 cm^{-1} can be assigned to O-H bond and adsorbed water on Al_2O_3 surface [13, 15, 181]. APTES modified nanoparticles display two additional bands at 1600 cm^{-1} and 2950 cm^{-1}. The peak at 1600 cm^{-1} can be attributed to the N-H vibrations, indicating the presence of $R\text{-}NH_2$ groups at the surface of modified nanoparticles [181]. Also the peak at 2950 cm^{-1} can be assigned to C-H stretching vibrations [182]. These results confirm the presence of silane coupling agent at the surface of the treated nanoparticles.

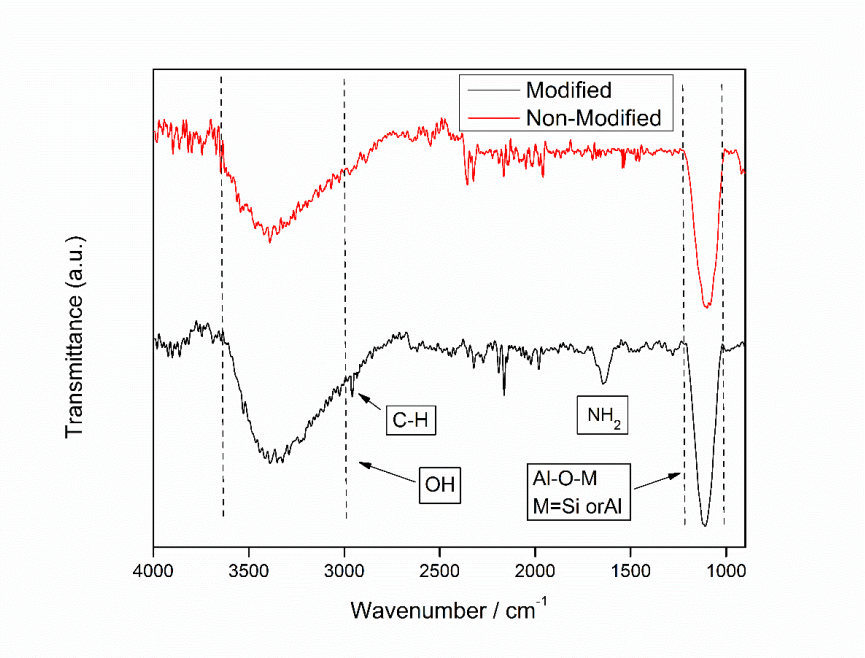

Figure 4. 12 FTIR spectra of the modified and non-modified alumina nanoparticles

4.3.4.2. Membrane characterization

The presence of alumina nanoparticles in the membrane structure was confirmed by XRD analysis. The XRD spectra of neat PES membrane and PES/alumina nanocomposite membranes are shown in Figure 4.13. As it can be seen, the PES polymer is primarily amorphous and shows one main peak at $2\theta = 18.2°$, which is similar to the reported peak for pure polyethersulfone [175]. For the alumina/PES nanocomposite membranes, two new peaks at $2\theta = 46°$ and 68° were observed. These peaks are the characteristic peaks of γ-alumina [173]. This proves the presence of γ-alumina nanoparticles in the PES membrane matrix. These results show that the γ-alumina nanoparticles have been distributed into the polymer matrix and also with the addition of nanoparticles the nano-enhanced membranes remained amorphous.

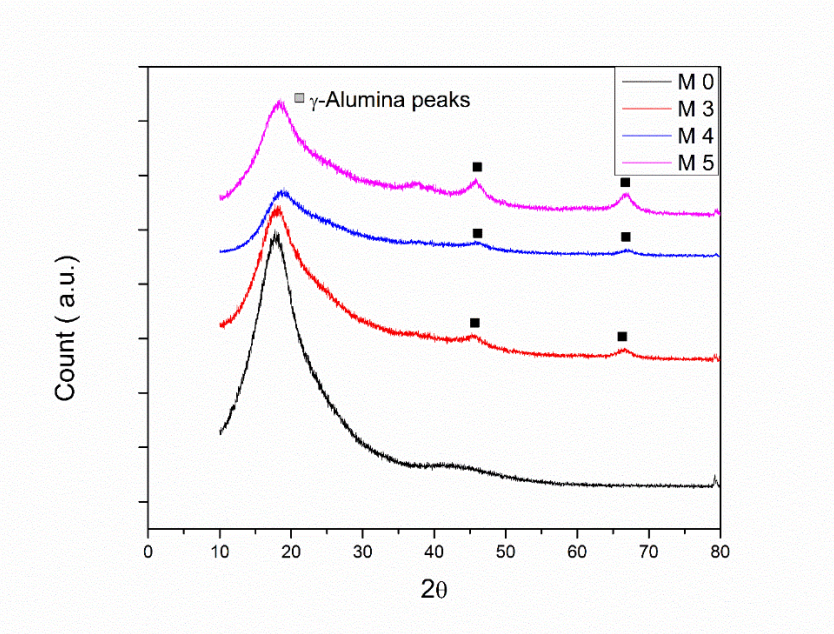

Figure 4. 13 X-ray diffraction patterns of neat PES membranes and PES/alumina nanocomposite membranes

The glass transition temperature of the membranes (T_g) was measured using a Dynamic Mechanical Analyzer (DMA).The glass transition temperature depicts the transition of the polymer from glassy behavior to rubbery state, which results in a considerable decrease in the stiffness of the polymer [183]. The T_g of the membranes can be determined form the peak of the loss modulus. As it can be seen in Figure 4.14, adding nanoparticles into the polymer membranes shifts the maximum peak of the loss modulus to higher temperatures. For the neat polymeric membrane (M 0), the glass-transition temperature was determined as 218 °C. The nanocomposite membranes showed significantly higher glass-transition temperatures, which were 224, 233, and 244 °C for M 3, M 4, and M 5 samples; respectively. The presence of the modified nanoparticles in the polymer matrix make interfacial strong bonds between the polymer matrix and the

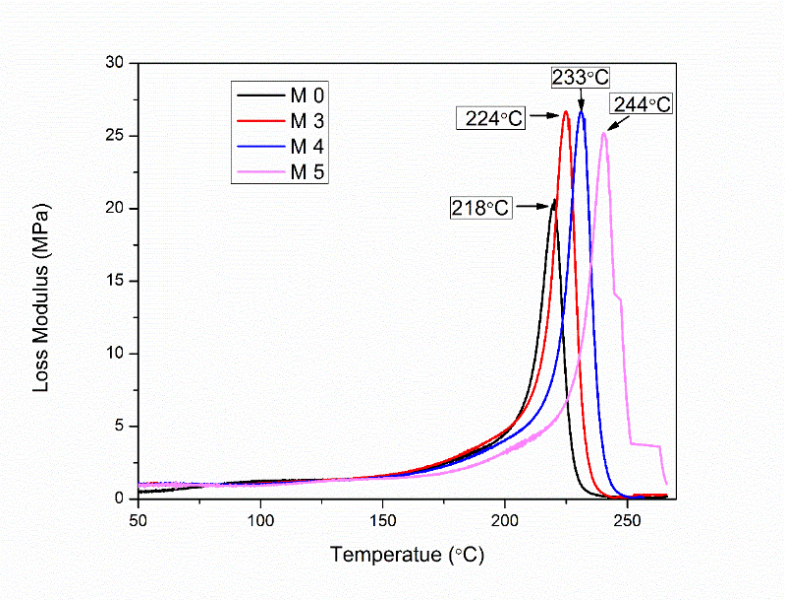

Figure 4. 14 Loss modulus versus temperature for the control and nanocomposite membranes

nanoparticles and also restrict the movement of polymeric chain [183]. This explains the increase in the glass-transition temperature by incorporating nanoparticles.

TGA analysis was used to confirm the distribution of the alumina nanoparticles and evaluate the thermal stability of the fabricated membranes. Figure 4.15 shows the TGA curves for neat polymeric and composite membranes. TGA curves for the composite membranes show a small shift compared to neat PES membranes, which indicates that the thermal stability of PES membranes containing alumina nanoparticles was enhanced. The residual weight ratios for M 3, M 4, and M 5 samples are 9.8%, 14.2%, and 17.5%; respectively. Comparing the residual weight ratios with the nominal concentration of nanoparticles in the membranes; i.e., 14% (M 3), 18% (M 4), and 21% (M 5), indicates that the nanoparticles were reasonably distributed in the polymer matrix [184]. However,

some amount of alumina particles leached out to the coagulation bath during the membrane formation.

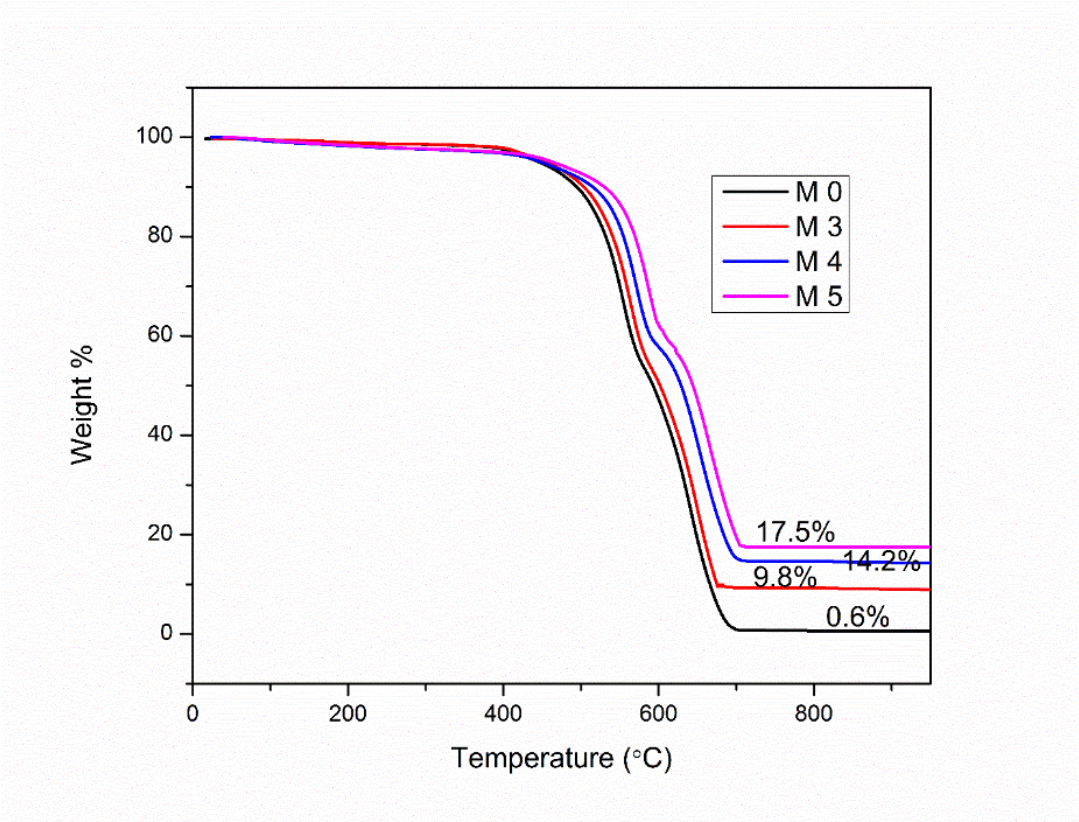

Figure 4. 15 Thermogravimetric (TGA) curves of the nanocomposite and neat polymer membranes

Figure 4.16 presents the FESEM images of the cross-section of the synthesized membranes. The cross-sections of the membranes show a typical asymmetric structure consisting of a thin dense layer supported by a large finger-like sublayer. Also, large macro-voids are formed beneath the finger-like pores. This structure contributes to the higher flux of the membrane while also maintaining its salute rejection as discussed in the following sections. In addition, it can be seen that the nanocomposite membranes

contain slightly larger macro-voids in the sub layer compared to neat PES membranes which is in accordance with the total porosity and BET surface area results.

The total porosity, presented in Table 4.7, shows that the nanocomposite membranes possess higher total porosity compared to neat PES membranes. The membrane porosity increased with increasing the nanoparticles amounts in the matrix from 66% for neat polymeric membranes to 82% in the case of M 5 samples. It has been reported that the interaction between nanoparticles and the polymer solution leads to easier diffusion of solvent molecules from the polymer matrix to the coagulation bath [38, 67]. In addition, the diffusion rate of the solvent (DMAc) from the membrane into the coagulation bath can also increase through the addition of nanoparticles [66]. As a result, the nanocomposite membranes have a higher amount of total porosity as well as BET surface area compared to the neat polymeric membrane.

The BET surface area of the membranes, shown in Table 4.8, increased from 20.6 cm^2/g for neat polymeric membrane to 35.5 cm^2/gr for M 3 Samples. This can be explained by the presence and dispersion of nanoparticles with high surface area in the membrane structure. Figure 4.17(c) confirms the suitable dispersion of alumina nanoparticles in the matrix of the membranes. The uniform distribution of the nanoparticles is favorable since it increases the contact area of the passing water through the membrane and the surface

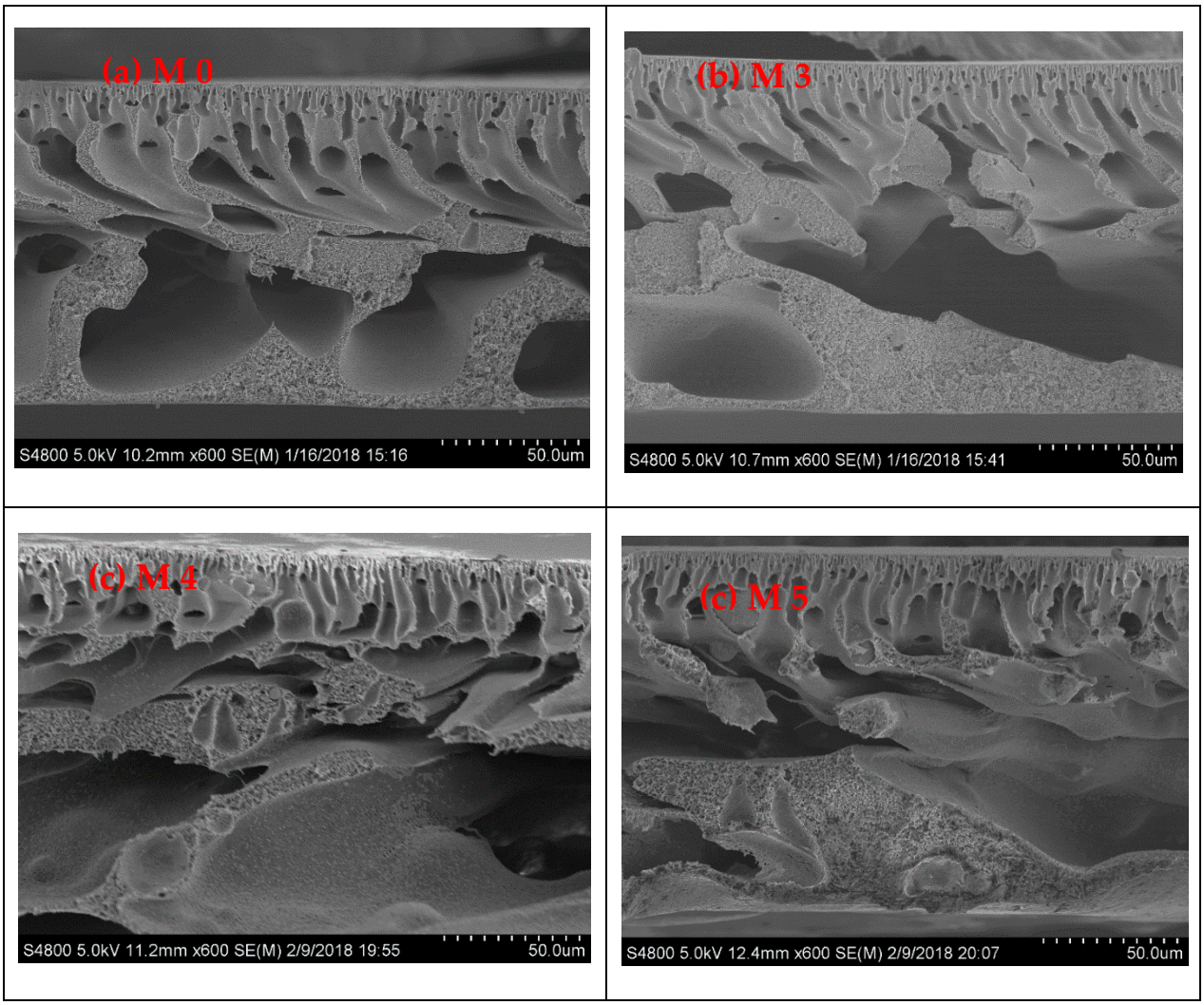

Figure 4. 16 SEM cross-section images of (a) M 0, (b) M 3, (c) M 4, (d) M 5 membranes

of the particles, which subsequently increases the surface adsorption of the copper ions. Interestingly, M 5 samples exhibit less amount of surface area compared to the M 4 and M 3 samples. This can be attributed to the agglomeration of the nanoparticles, as depicted in Figure 4.17(b). Agglomeration may also lead to blocking of some pores in the structure and consequently lowering the available surface area of the membranes.

Table 4. 8 Total porosity, water contact angle, surface area, and pure water flux of the membranes

Membrane Sample	Porosity (%)	Water contact angle	Pure water flux (Kg/m^2h)	Surface area (m^2/g)
M 0	68	69	29.1	20.6
M 3	73	54	44.1	32.3
M 4	78	47	54.3	35.5
M 5	81	44	48.6	29.1
γ-Al_2O_3 nanoparticles	–	–	–	58.1

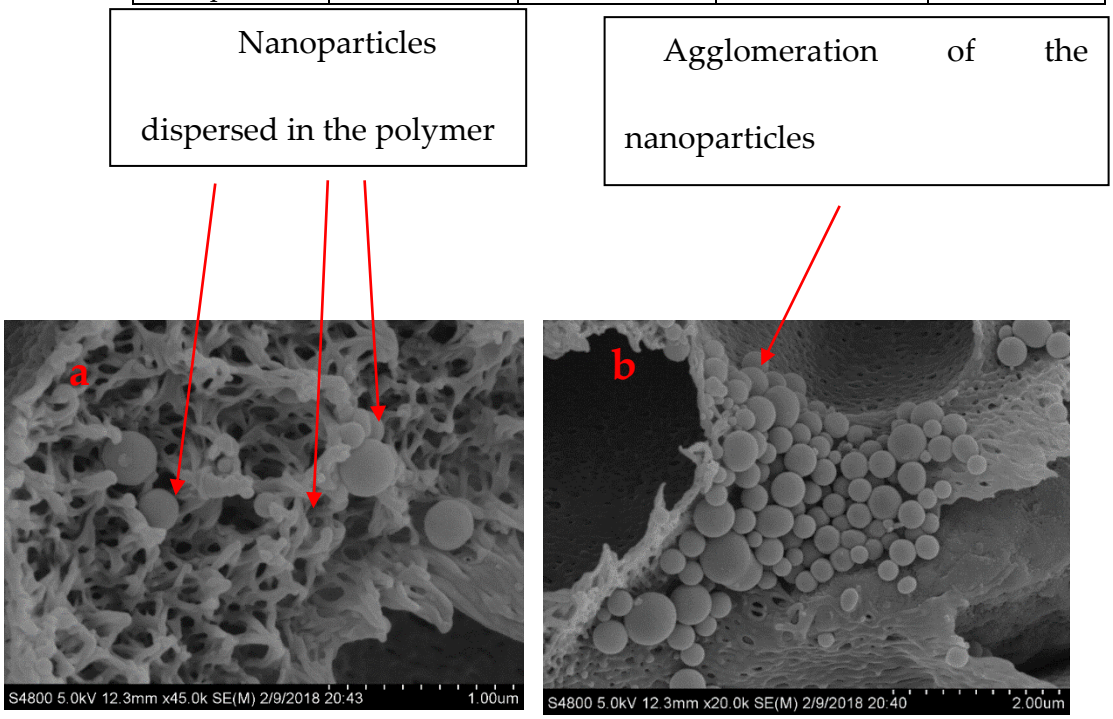

Figure 4.17 Higher magnification SEM cross-section image of a) M 4 membrane showing incorporation of the nanoparticles in the polymer matrix b) M 5 showing the agglomeration of nanoparticles c) EDX map scanning spectra for the cross section of M 4 sample.

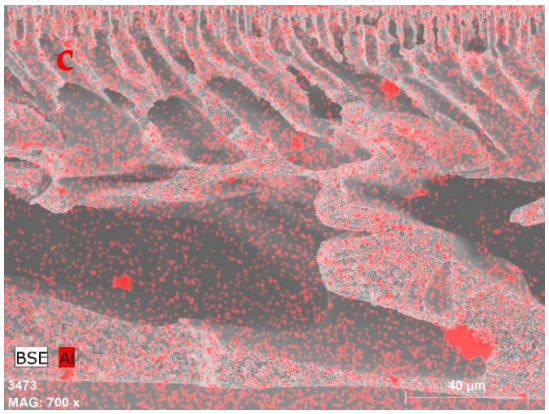

Contact angle measurement is a commonly used method to characterize the hydrophobicity and hydrophilicity of membranes [76]. High contact angle indicates that the membrane is more hydrophobic and vice versa for lower contact angle. Table 4.8 shows the water contact angle of the PES membranes decreasing from 69° to 44° with increasing the nanoparticle amount in the matrix. The hydroxyl content of the membrane surface increases due to the incorporation of alumina nanoparticles into the membrane surface leading to increased hydrophilicity of the membrane surface [26].

4.3.4.3.Adsorption study

Figure 4.18 shows the equilibrium adsorption of Cu(II) versus time for the membranes synthesized in this work. The results show that by increasing the alumina concentration in the membranes, the adsorption capacity increases significantly. The highest Cu(II) adsorption capacity of each membrane, was 18.7, 24.7, and 31.8 mg/g for M 3, M 4, and M 5 membranes; respectively. The increase in the adsorption capacity of the membranes could be attributed to the increased number of active sites for adsorption of copper ions as a result of increasing the amount of alumina in the membranes, as well as the increased surface area of the membranes.

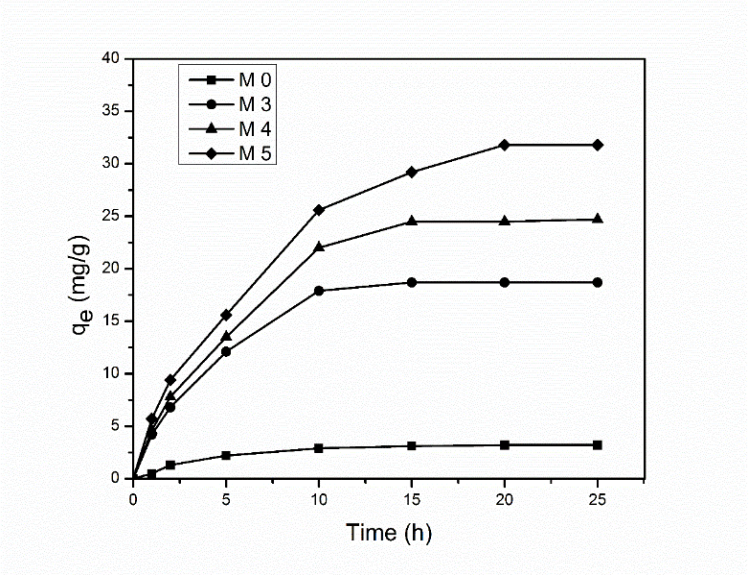

Figure 4. 18 Equilibrium adsorption of the membranes as a function of time (initial copper concentration= mg/L)

Langmuir and Freundlich equilibrium adsorption isotherms were applied to the adsorption data. Table 4.9 presents the Langmuir and Freundlich isotherm parameters for Cu(II) adsorption on the nano-enhanced membranes. Langmuir isotherm, which indicates a monolayer adsorption on homogenous adsorption sites, is expressed by equation 4.8;

$$q_e = \frac{q_{max}\, b\, C_e}{1+bC_e} \qquad \text{Equation 4. 8}$$

where q_e is the equilibrium adsorption (mg/g), C_e is the equilibrium concentration in the aqueous phase (g/L), q_{max} is the adsorption capacity (mg/g), and b in the equilibrium constant (L/mg).

The Freundlich isotherm corresponds to a multilayer adsorption on a heterogeneous surface and is formulated by equation 4.9;

$$q_e = k\,.\,Ce^n \qquad \text{Equation 4. 9}$$

where k and n are the relative adsorption constant and adsorption intensity parameter; respectively. Based on the obtained data, Freundlich model showed a better fit with the equilibrium data (R^2 = 0.99), which indicates a multilayer coverage and heterogeneous adsorption on the membrane surface.

Table 4. 9 Equilibrium constants of Langmuir and Freundlich isotherms for Cu(II) adsorption.

Membrane Sample	Langmuir Model			Freundlich model		
	q_m (mg/g)	b (L/mg)	R^2	K_F (mg/g)	n	R^2
M 3	34.01	0.068	0.972	6.68	0.426	0.994
M 4	39.37	0.168	0.961	16.88	0.183	0.991
M 5	44.84	0.401	0.974	26.99	0.1149	0.996

4.3.4.4. Filtration performance

The results of membrane performance to remove Cu(II) are shown in figure 4.19. It can be seen that neat PES membranes exhibit the lowest amount of copper removal while the membranes containing 4 wt. % of alumina nanoparticles (M 4) exhibit the highest Cu(II) at 87%. The dispersed modified alumina nanoparticles in the polymer matrix act as active sites to adsorb copper ions and prevent copper ions from passing through the membrane [37, 92, 176].

However, the nanocomposite membranes with the highest content of nanoparticles (M 5) showed lower copper removal compared to M 4, due to the agglomeration of the

nanoparticles, discussed earlier. Since the adsorption of the copper ions on the surface of alumina nanoparticles is the main mechanism for the copper removal, dispersion of the nanoparticles in the polymer matrix plays an important role in the membrane performance. Agglomeration of nanoparticles decreases the effectiveness of the nano-enhanced membranes by decreasing the available surface area of the nanoparticles leading to the lower rejection performance [37, 74]. This is in accordance with the decreased available BET surface area of M 5 sample.

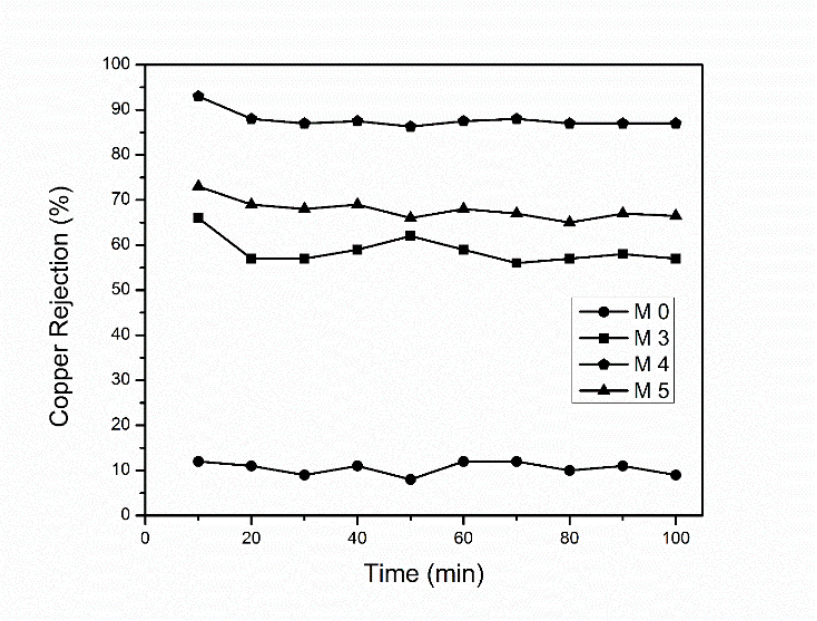

Figure 4. 19 Copper removal (%) from aqueous solution for PES and nano-enhanced membranes

The pure water flux along with water contact angles of the membranes are shown in Figure 4.20. It can be seen that the membranes with higher amount of nanoparticles exhibit higher flux and lower water contact angle. This can be explained by the

combination of the increased hydrophilicity of the surface at lower surface contact angles, and the higher porosity of the membranes with higher nanoparticles content. Several studies have reported an increase in water flux through the membranes due to the increased hydrophilicity, porosity, and the mean pore size of membranes incorporating nanoparticles [18, 62, 64]. However, by increasing the nanoparticles amount from 4 to 5 wt. % the pure water flux decreased due to the agglomeration of the nanoparticles. Agglomeration of nanoparticles in the membranes can lead to the blocking of the surface pores and result in lower permeability in accordance with similar results reported by others [37, 57, 74].

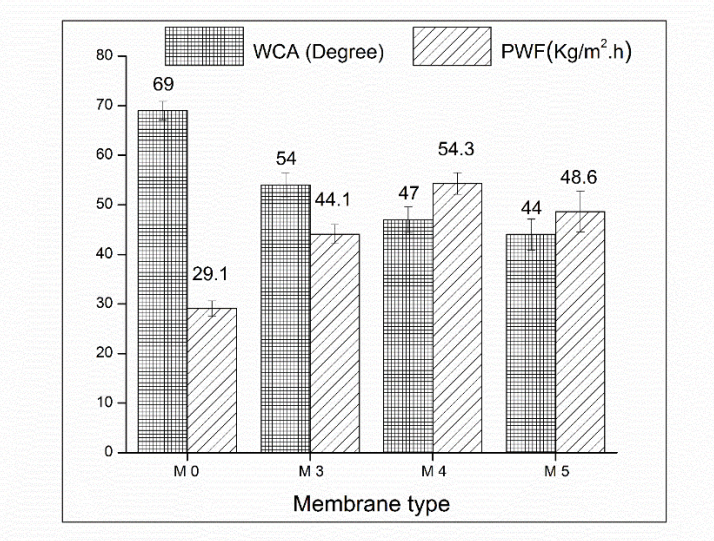

Figure 4. 20 Pure water flux (PWF) and water contact angle (WCA) of the synthesized membranes

It should be noted that reverse osmosis and nanofiltration have been investigated and used extensively to remove heavy metals ions from water. Although these techniques are able to remove heavy metals from water very efficiently, high operational pressure, high

energy consumption, and low flux are the main drawbacks of these systems [185]. The developed nanocomposite membrane in this study, is an attempt to mitigate these issues. The synthesized membranes combine adsorption and membrane technology, and since the pore size is bigger than nanofiltration and reverse osmosis, the operational pressure (transmembrane pressure) is lower and the water flux is higher.

4.3.4.5. Reusability

The membrane with the best performance of copper removal in the filtration experiment (M 4) was chosen for the usability study. Ethylenediaminetetraacetic acid (EDTA) was utilized as a cleaning agent since It has been reported that the EDTA is able to permanently remove copper ions form membrane adsorption sites due to the high formation constant of $[Cu(EDTA)]^{-2}$ [37]. As it can be seen in Figure 4.21, the M 4 membrane can be reused after 4 cycles with only 5 % reduction of copper removal (compared to initial copper removal capability). This confirms that performance of synthesized membranes in copper removal was not reduced significantly, even after four cycles of filtration process.

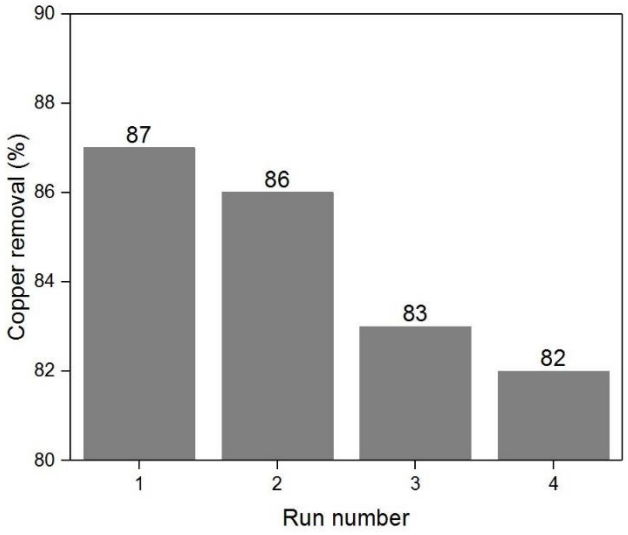

Figure 4. 21 Reusability of M 4 membrane for four sequential runs

4.3.5. Analyzing the adsorption capacity of the nanocomposite membranes

It has been reported in several studies that one of the main separation mechanisms for inorganic/organic nanocomposite membranes is adsorption. The results of adsorption isotherms of the synthesized nanocomposite membranes in this work also confirmed this. The samples that contain higher amount of nanoparticles in their structure show higher adsorption capacity. Meanwhile these samples also show enhanced copper ion rejection from the water. In this section composite theory is utilized to predict the adsorption capacity of the synthesized nanocomposite membranes.

A composites material consisting of two (or more) different phases designated as phases 1 and 2. Classic composite theory states that the overall properties of the composite materials can be calculated by two well-known following equations:

$$k_e = k_1\emptyset_1 + k_2\emptyset_2 \qquad \text{Equation 4. 10}$$

$$k_e = \frac{k_1 k_2}{k_1\emptyset_1 + k_2\emptyset_2} \qquad \text{Equation 4. 11}$$

where Ki is the properties of phase I, and $\emptyset_i$ is the volume fraction of phase i. Depending upon the physical context, the ith phase can be either solid, liquid, or void, and is characterized by a set of physical properties (elastic moduli, strength, conductivity, etc.). The volume fraction is the simplest but most important piece of microstructural information. Phase volume fractions in both the arithmetic average (equation 4.10) and the harmonic average (equation 4.11), not only was used to estimate linear properties of composites, such as elastic moduli and conductivity, but nonlinear properties, such as strength.

Studies have shown that arithmetic average better predict the adsorption in multi-phase adsorbents. In this section the composite theory is applied on the synthesized nanocomposite membranes in order to predict the overall adsorption capacity of the composite membrane. To be able to apply the above equations, we assume that the dispersion of the nanoparticles in the matrix is uniform. Fig 4.17(c) shows the EDX plot of the M 4 membrane which indicates the good dispersion of nanoparticles in the polymer matrix.

Using the arithmetic mean, adsorption capacity of a composite system can be calculated by the following equation:

$$q_{total} = (q_f \times f\ wt.\%) + (qm \times m\ wt.\%) \qquad \text{Equation 4. 12}$$

Where q_f and q_m are the adsorption capacity of the filler (f) and matrix (m) phase in the composite membranes.

To measure the actual amount of the filler (alumina nanoparticles) in the polymer matrix, TGA results has been used. Figure 4.15 shows the TGA graph of membrane samples with 3, 4, 5 wt. % of alumina in the cast solution. As it can be seen in the picture, M 3, M 4, and M 5 membranes contain 9.8, 14.2, and 17.5 wt. % nanoparticles.

Table 4.10 shows the experimental and calculated adsorption capacity of the nanocomposite membranes. As it can be seen in the table, the adsorption capacity of the composite membrane samples predicted by the composite theory, suitably match the experimental data. The difference between the predicted data and the experimental data is in the range of 12 to 25 %. Below reasons are the main reasons for this difference:

1. Agglomeration of the nanoparticles; agglomeration reduces the effectiveness of the particles and decreases the adsorption capacity of the nanoparticles.
2. Covering nanoparticles by polymer material; only nanoparticles that exposed to the passed water are considered as active sites, and contribute in the adsorption of the heavy metal ions. Some of the nanoparticles are not exposed (or fully exposed) as they are embedded in the polymer matrix.
3. Non-uniform distribution of the nanoparticles in the polymer matrix.

Table 4. 10 Predicted and experimental adsorption capacity of nanocomposite membranes

Membrane	Alumina (wt. %)	PES (wt. %)	$q_{Alumina}$ (mg/g)	q_{PES} (mg/g)	q_{total} (Predicted)	$Q_{Experimental}$	Error (%)
M 3	9.8	90.2	156	12.1	24.1	19.3	7.8
M 4	14.2	85.8	156	12.1	31.3	26.2	9.1
M 5	17.5	82.5	156	12.1	27.2	33.2	6.4

Therefore, it can be concluded that the composite theory and arithmetic mean equation can be used efficiently to predict the adsorption capacity of the nanocomposite membranes.

4.3.6. Prediction of Rejection of the nanocomposite membranes using Spiegler-Katchalsky- Kedem and Steric hindrance pore models

4.3.6.1. Modeling approach:

The development of models to predict the performance of the nanocomposite membranes in the removal of heavy metal ions is very beneficial for the optimal design and understanding the removal mechanisms of these membranes [186, 187]. To model the solvent and solute transport through the membrane, it can be assumed that the top dense layer of the membrane is responsible for solute rejection [188]. In this approach, the membrane top layer is considered as bundles of capillary tubes, and Hagen-Poiseuille type equation can describe the relationship between the solvent flux and applied

pressure. It is also assumed that this layer consists of parallel cylindrical pores. This active layer is so thin that it cannot be under pressure on its own, so the membrane has a support layer (finger-like pores and macro-pores) which is much thicker. The mass transfer of this layer is small and could be neglected. Figure 4.22 shows the schematic of the approach.

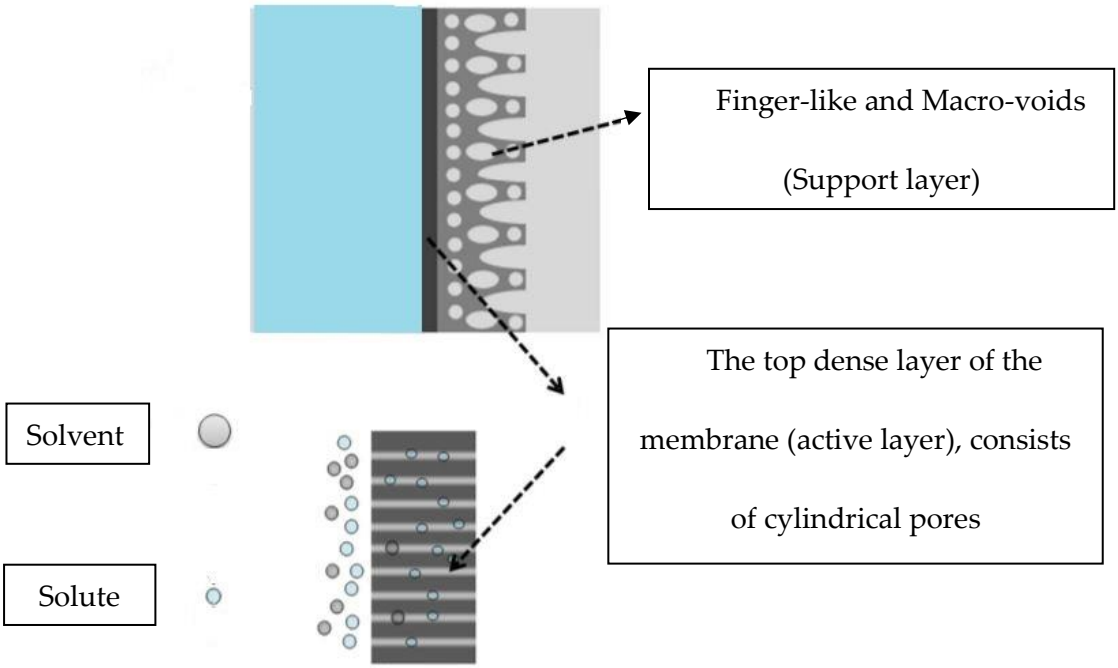

Figure 4. 22. Schematic representation of nanocomposite membrane

Spiegler-Katchalsky-Kedem (SKK) model was used to model the rejection of the membranes. The model is validated on its ability to reproduce observed water flux and heavy metal ion rejection. SKK model which is a mass transfer-based model relates flux

to the concentration difference of a solute for a given membrane and solvent properties , and has been successfully utilized by several researchers to analyze the nanofiltration and ultrafiltration membrane processes [187]. The model requires structural parameters which was estimated using Steric the Hindrance Model (SHP).

The Spiegler-Katchalsky-Kedem model is based on irreversible thermodynamics to explain the membrane transport when the transport mechanism and membrane structure is not fully understood [189]. The Spiegler-Katchalsky-Kedem model is typically applied when there is no electrostatic interactions between solute and membranes such as in case of uncharged membranes or neutral solutes. However, many researchers have used this model with charged membranes and charged solutes such as ions [190]. They suggested that reflection coefficient and solute flux depend on the effective membrane charge.

To establish the model, membrane performance was calculated in terms of permeate flux (Jp) and membrane rejection (R) by the following equations:

$$R = 100(1 - \frac{C_p}{C_f}) \qquad \text{Equation 4. 13}$$

$$J_p = \frac{Q_p}{S} \qquad \text{Equation 4. 14}$$

Where C_p and C_f are the solute concentration in the permeate and feed, respectively. Q_p is the volumetric permeate flux (m^3/ h) and S is the membrane active area (m^2).

According to this model, the transport phenomena of membranes in the pressure driven can be described by irreversible thermodynamics. Transport equations for the flow of a solute through a membrane consists of two terms, the diffusion component and the convection term. For a separation process involving a single solute in aqueous solution, solute retention can be formulated by three transport coefficients:

1. Specific hydraulic permeability (L_P)
2. Local solute permeability (P_s)
3. Reflection coefficient (σ)

Permeability is defined as the flux of solvent or solute per unite driving force (trans-membrane pressure). The reflection coefficient is exhibits the degree of semi-permeability of the membranes [191].

Transport equation in the Spiegler-Kedem-Katchalsky model formulated as [187]:

$$J_w = L_p(\frac{dp}{dx} - \sigma \frac{d\pi}{dx}) \qquad \text{Equation 4. 15}$$

and

$$J_s = P_s \frac{dC_s}{dx} + (1 - \sigma) J_w C_m \qquad \text{Equation 4. 16}$$

First term of equation 4.15 represents the diffusion and the second term represents the contribution of concoction in transport. These equation can be simplified using below assumptions:

- The SKK model predicts the transport of solute and solvent, regardless of the type and charge of the solvent, the membrane, and solute.
- The driving forces for the membrane process are pressure and concentration gradients.
- L_p, P_s , $and\ \sigma$ are constants.
- The solute concentration at membrane surface Cm is equals to solute concentration in the feed Cf.

The simplified version of transport equations can be written as [187];

$$J_w = L_p(\Delta P - \sigma\Delta\pi) \qquad \text{Equation 4. 17}$$

$$J_s = P_s\Delta C_s + (1-\sigma)J_w C_m \qquad \text{Equation 4. 18}$$

where $J_w\ and\ J_s$ are solvent flux and solute flux respectively. $\Delta C_s = C_m - C_p$, and C_p and C_m are the permeate concentration and solute concentration at the membrane surface. ΔP is the pressure difference between the feed and permeate, and $\Delta\pi$ is the osmotic pressure difference of feed and permeate. As it can be seen in the equation 4.18, the solute flux in the sum of diffusive and convective terms. Transfer of the solute by convection as a result of an applied external pressure gradient across the membrane. The difference of the concentration on the feed side and permeate side results in transport by diffusion.

According to this model, the rejection of the membrane is a function of structural characteristics of the membranes and can be presented by equations 4.19 and 4.20 [187];

$$R = \sigma \frac{(1-F)}{1-\sigma F}$$ Equation 4. 19

Where R represents the observed rejection and F is a parameter that depends on the rejection coefficient, solute permeability, and solvent flux and is formulated by below equation:

$$F = \exp(-\frac{1-\sigma}{P_s} J_V)$$ Equation 4. 20

F is a dimensionless parameter which depends on the reflection coefficient, solvent flux, and solute permeability. The reflection coefficient represent the rejection capability of a membrane. No rejection happens when σ = 0 and 100% rejection occurs when σ = -1. In other words, σ can be considered as the maximum rejection at an infinite volume flux.

The SKK model taking into consideration the observed rejection and reflection coefficient, suggests a relationship between the logarithm of solute membrane parameters and the flux of solvent by the following equation [192]:

$$\ln[X] = -\frac{(1-\sigma)}{P_s} . J_w$$ Equation 4. 21

where X can be represented by below equation

$$X = \left(\frac{1}{(1-\sigma)} - \frac{1}{1-R_{obs}}\right) . \frac{(1-\sigma)}{\sigma}$$ Equation 4. 22

assuming $C_f = C_m$, the following expression can be obtained from equations 4.20 and 4.21;

$$P_s = \frac{J_s - J_w \times C_s \times (1-\sigma)}{C_f - C_p}$$ Equation 4. 23

Substituting the value of P_s given by equation 4.23 from equation 4.22 gives us:

$$ln\left[\left(\frac{1}{1-\sigma}-z\right).\frac{1-\sigma}{\sigma}\right]+\frac{1-\sigma}{a-b(1-\sigma)}J_w=0 \qquad \text{Equation 4. 24}$$

where $z=(\frac{1}{1-R_{obs}})$, $a=\frac{J_s}{C_f-C_p}$ and $b=\frac{J_w.C_s}{C_f-C_p}$

Using analytical methods, and experimental measurements for J_w, the equation 4.24 can be solved and the values of reflection coefficient (σ) that makes the equation equal to zero can be obtained. Then using equation 4.19, the solute permeability (P_s) can be obtained.

Modification of Steric hindrance pore model to analyze the separation behavior

In this section, Steric hindrance pore model along with experimental results was utilized to obtain the structural parameters of the SKK model. The Steric hindrance pore model has been used successfully to estimate the structural membranes parameters of both ultrafiltration and nanofiltration membranes for the separation of solutes from aqueous solutions [193, 194]. A SKK model combined with Steric hindrance pore model was developed in this work in order to analyze the rejection of the synthesize nanocomposite membranes. First, the structural parameters and equation parameters to utilize in the SKK model is calculated using a modified steric hindrance pore model and the rejection of the membranes at different flow rates. Then SKK model was employed to predict

rejection of the membranes. The experimental data also is used to validate the model. The modification of the steric hindrance model was carried out to adjust the model to nanocomposite membranes synthesized in this work.

The following assumption were made while using and modifying the steric hindrance model:

1. Only the dense top layer of the membrane is responsible for the heavy metal ions rejection.
2. The selective layer of the membranes consists of only cylindrical pores with the same diameter in the entire membrane structure.
3. The heavy metal ions are spherical.
4. The driving forces are pressure and concentration gradients.
5. Membrane fouling is not considered in the model.
6. Diffusivity of the copper ions in the feed concentration (100 ppm copper solution) is equal to diffusion of copper ions in pure water.
7. Nanoparticles have been distributed uniformly along the pore faces and membrane matrix.
8. The adsorption of heavy metal ions follows the Freundlich adsorption model and corresponds to three layers adsorption on adsorption sites.

According to Steric Hindrance model, frictional forces and steric effect are hindering the transport of spherical ions through cylindrical pores [195]. Following this model the solute permeability (Ps) and reflection coefficient (σ) are given as [193];

$$\sigma = 1 - S_F\{1 + (^{16}/_{9})q^2 \qquad \text{Equation 4. 25}$$

$$P_s = D \times S_D\ (^{\varepsilon}/_{\Delta x}) \qquad \text{Equation 4. 26}$$

where

$$S_D = (1-q)^2$$

$$S_F = 2(1-q)^2 - (1-q)^4$$

and

$$q = \frac{r_s}{r_{p,eff}}$$

S_D and S_F are the Steric hindrance factors for diffusion and convection respectively. D is diffusion coefficient of the solute, ε is the membrane porosity, Δx is membrane thickness, r_s is the Stokes radius of the solute, and $r_{p,eff}$ is the effective pore radius.

In order to modify the Steric hindrance model to use for the nanocomposite membranes in this work, adsorption of the ions on the surface of the pores was also taken into account. As discussed in previous sections, the adsorption isotherms of the synthesized membranes fits Freundlich better. The Freundlich model assumes multilayer adsorption of the solute on the adsorption sites. To estimate the effective pore size, first the pore size

of the top dense layer of the membranes was measured experimentally by Hagen-Poiseuille.

$$L_p = \frac{\varepsilon {r_p}^2}{8\mu\Delta x} \qquad \text{Equation 4. 27}$$

where μ is the solution (water) viscosity.

Then assuming 6 layers adsorption of solute on the pore surface (3 layers at each faces of the pore walls), an effective pore size for the membranes was calculated using below equation;

$$r_{p,eff} = r_p - (6 \times r_s) \qquad \text{Equation 4. 28}$$

Figure 4.23 shows the schematic of the approach for approximating the effective pore size of the membranes.

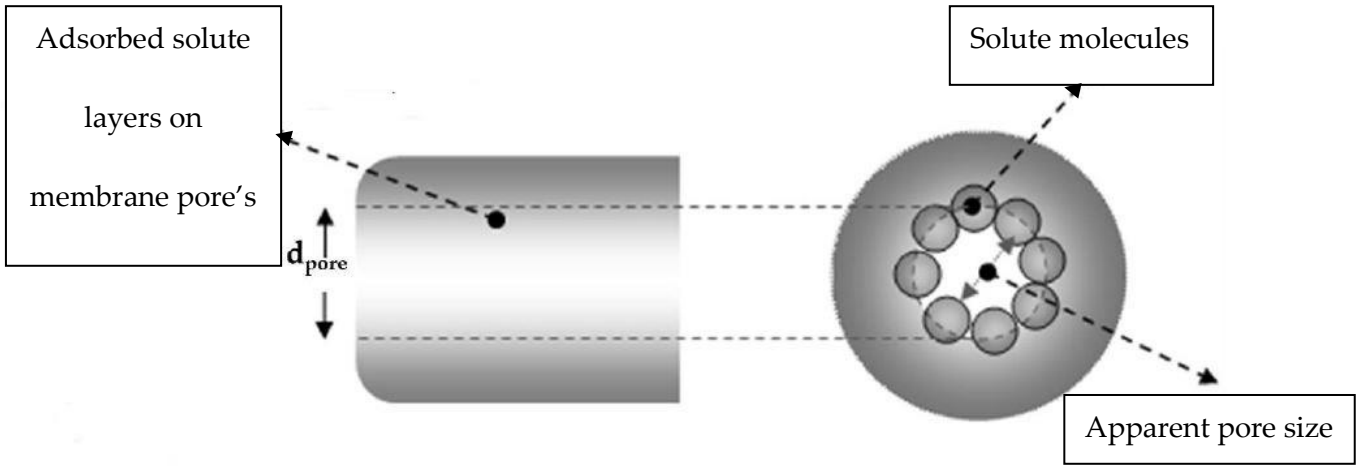

Figure 4.23. Schematic representation of the membranes pore

In order to calculate the predicted rejection of the membranes, first using the equations 4.25 and 4.26 solute permeability and reflection coefficient were calculated. It should be noted that the effective pore size was used to calculate the structural parameters by Steric hindrance model. Then using equations 4.19 and 4.20, F parameter and R (predicted rejection) were calculated. Table 4.11 shows the result of obtained σ, R, for the tested membranes. Comparison between experimental and calculated rejection values show that the proposed model could predict the rejection values satisfactorily. The predicted and experimental rejection of copper ions for M 3, M 4, and M5 membranes are 47%, 73%, 60% and 58%, 87%, and 69% respectively.

Table 4. 11 Structural parameters, and experiment and calculated rejections of the membranes

Membrane	r_s(nm)	$r_{p,eff}$	D(m^2/s)	Δx(nm)	F	L_p(L/m^2.hr.bar)	σ	R_{model} (%)	R_{exp} (%)
M 3	0.3	2.1	7.4×10^{-10}	470	0.64	9.26	0.71	47	58
M 4	0.3	1.9	7.4×10^{-10}	443	0.68	11.40	0.93	73	87
M 5	0.3	1.8	7.4×10^{-10}	413	0.71	10.21	0.82	60	69

The main reasons for the difference between the predicted and experimental rejection can be listed as below:

1. To establish the model, it was assumed that the membranes and ions have no electrical charge. The interaction of the charged membranes and the positively

charged heavy metal ions alters the membrane process, and can be a reason for the discrepancy between model prediction and experimental measurements.

2. To establish the model, it was assumed that there is no fouling in the membrane process. Fouling and accumulation of solute in the surface and pores of the membranes can change the separation process. Accumulation of solute (heavy metal ions) on the surface of the membrane makes a concentration gradient between the feed and surface layer. This acts as an auxiliary separation mechanism and improve the rejection of the membranes. It should be mentioned that in order to minimize the effect of surface film, the feed was constantly stirring in the dead end cell during the filtration experiments.
3. In this model, only the top dense layer was taken into account, and the effect of the other layers of the membrane (finger-like pore and macro-voids) of the separation process were neglected. It was also assumed that the selective layer of the membranes consists of only cylindrical pores with the same diameter in the entire membrane structure.

4.3.7. Conclusion

APTES modified alumina nanoparticles (γ-Al_2O_3) were incorporated in PES membranes to enhance the removal of Cu(II) ions from aqueous solutions. The morphology and performance of the nanocomposite membranes were analyzed extensively. It was revealed that by adding the modified nanoparticles to the PES membranes, the

hydrophilicity, total porosity, BET surface area, thermal stability and glass transition temperature, were all improved. The combination of higher porosity and lower hydrophobicity of the membranes surface led to a significantly higher water flux. Moreover, the copper ion removal increased from 11%, in the case of neat polymer membranes, to 87% for the nanocomposite membrane containing 4 wt% of modified alumina nanoparticles. Batch adsorption studies showed that the adsorption of copper ions on the membranes fits a Freundlich model, which corresponds to heterogeneous adsorption sites.

Spieger-Kedem-Katchalsky (SKK) model was successfully employed to model the rejection performance of the nanocomposite membranes. Steric Hindrance model was also modified and was used to determine membranes transport parameters. The hypothetical pre radii, solute permeability, and reflection coefficient was obtained using the modified Steric Hindrance model. The theoretical rejection values obtained by the SKK model showed good correlations with experimental values. The suggested model is a novel model top predict nanocomposite membranes rejection for heavy metal ions removal from water.

4.4. Conclusion

- PES asymmetric nanocomposite membranes synthesized with phase inversion immersion precipitation method. All of the membranes demonstrated a typical asymmetric structure and fully developed macro-pores due to the instantaneous de-mixing, irrespective of polymer concentration and temperature of the casting solution in the range of 16-20 wt. % and 30 to 50° C respectively.
- PES membranes prepared with higher amounts of polymer (PES) exhibited lower total porosity, smaller mean pore size, lower permeability, and less surface area.
- PES membranes prepared with a higher solution temperature, exhibited larger pore size, higher hydrophilicity, and higher water flux. In addition, increasing the casting temperature led to a decrease in the tensile strength of the membranes.
- Polymer concentration and casting temperature can be used as two main processing factors to custom tailor PES membranes.
- Incorporating alumina nanoparticles enhanced the PES membranes' hydrophilicity by decreasing the water contact angle from 68° to 57°; enhanced tensile strength of the membranes by 40% (2.8 to 3.9 MPa); enhanced the overall porosity and the BET surface area, and hence the permeability and water flux of the membranes. Also the lead ion removal increased from 10%, in the case of pure PES membranes, to 61% for nanocomposite membranes containing 1wt% of alumina nanoparticles.

- Incorporating higher mount of alumina nanoparticles (more than 1 wt.%) do not always lead to increasing the rejection of heavy metal ions. Agglomeration and not uniform dispersion of nanoparticles is the main reason of this finding.
- Modifying alumina nanoparticles (γ-Al_2O_3) with APTES enhanced the removal of Cu(II) ions from aqueous solutions up to 87% form feed concentration of 100 ppm.
- Modification of nanoparticles lead to formation Al-O-Si and Si-O-Si bonds of silane coupling agent at the surface of nanoparticles. APTES modified nanoparticles also display two additional bands at 1600 cm^{-1} and 2950 cm^{-1}. The peak at 1600 cm^{-1} can be attributed to the N-H vibrations, indicating the presence of R-NH_2 groups at the surface of modified nanoparticles.
- By adding the modified nanoparticles to the PES membranes, hydrophilicity, total porosity, BET surface area, thermal stability and glass transition temperature, were all improved. The combination of higher porosity and lower hydrophobicity of the membranes surface led to a significantly higher water flux.
- Copper ion removal increased from 11%, in the case of neat polymer membranes, to 87% for the nanocomposite membrane containing 4 wt. % of modified alumina nanoparticles.
- Static adsorption study showed that Freundlich model better represents the adsorption of lead ions on the membranes which corresponds to the heterogeneous adsorption sites (irrespective of modification of the nanoparticles).

- Classic composite theory is capable to model and predict the adsorption capacity of the nanocomposite membranes. The model employed in this work and the predictions were in good agreement with experiments.
- Spieger-Kedem-Katchalsky (SKK) model was successfully employed to model the rejection performance of the nanocomposite membranes. Steric Hindrance model was also modified and was used to determine membranes transport parameters. The hypothetical pre radii, solute permeability, and reflection coefficient was obtained using the modified Steric Hindrance model. The theoretical rejection values obtained by the SKK model showed good correlations with experimental values.

Recommendations for future work

- Develop a model to model the transport of charged ions through charged membranes
- Investigate the rejection of performance of nanocomposite membranes for multiple ions
- Compare the performance of different modification agents to optimize the modification process
- Utilizing the synthesized membranes as a base layer in TFC membranes to improve the rejection performance of TFC

- Investigating the anchoring of the nanoparticles to the polymer chain in the polymerization process

References:

1. Li, Y., et al., *Effects of novel silane modification of zeolite surface on polymer chain rigidification and partial pore blockage in polyethersulfone (PES)–zeolite A mixed matrix membranes.* Journal of Membrane Science, 2006. **275**(1-2): p. 17-28.
2. Rong, M., M. Zhang, and W. Ruan, *Surface modification of nanoscale fillers for improving properties of polymer nanocomposites: a review.* Materials science and technology, 2006. **22**(7): p. 787-796.
3. Mulder, J., *Basic principles of membrane technology*. 2012: Springer Science & Business Media.
4. Baker, R.W., *Membrane technology*. 2000: Wiley Online Library.
5. Nunes, S.P. and K.-V. Peinemann, *Membrane technology*. 2001: Wiley Online Library.
6. Ismail, A.F. and T. Matsuura, *Sustainable membrane technology for energy, water, and environment*. 2012: John Wiley & Sons.
7. Ng, L.Y., et al., *Polymeric membranes incorporated with metal/metal oxide nanoparticles: a comprehensive review.* Desalination, 2013. **308**: p. 15-33.
8. Yin, J. and B. Deng, *Polymer-matrix nanocomposite membranes for water treatment.* Journal of Membrane Science, 2015. **479**: p. 256-275.
9. Jhaveri, J.H. and Z. Murthy, *A comprehensive review on anti-fouling nanocomposite membranes for pressure driven membrane separation processes.* Desalination, 2016. **379**: p. 137-154.
10. Al Aani, S., et al., *Engineering nanocomposite membranes: Addressing current challenges and future opportunities.* Desalination, 2017. **401**: p. 1-15.
11. Zhao, H., et al., *Improving the antifouling property of polysulfone ultrafiltration membrane by incorporation of isocyanate-treated graphene oxide.* Physical Chemistry Chemical Physics, 2013. **15**(23): p. 9084-9092.
12. Hoek, E.M., et al., *Physical–chemical properties, separation performance, and fouling resistance of mixed-matrix ultrafiltration membranes.* Desalination, 2011. **283**: p. 89-99.
13. Razmjou, A., J. Mansouri, and V. Chen, *The effects of mechanical and chemical modification of TiO 2 nanoparticles on the surface chemistry, structure and fouling performance of PES ultrafiltration membranes.* Journal of Membrane Science, 2011. **378**(1): p. 73-84.
14. Rezvani-Boroujeni, A., et al., *Immoblization of thiol-functionalized nanosilica on the surface of poly (ether sulfone) membranes for the removal of heavy-metal ions from industrial wastewater samples.* Industrial & Engineering Chemistry Research, 2014. **54**(1): p. 502-513.
15. Prado, L.A., et al., *Surface modification of alumina nanoparticles with silane coupling agents.* Journal of the Brazilian Chemical Society, 2010. **21**(12): p. 2238-2245.

16. Xie, Y., et al., *Silane coupling agents used for natural fiber/polymer composites: A review.* Composites Part A: Applied Science and Manufacturing, 2010. **41**(7): p. 806-819.
17. Zularisam, A., A. Ismail, and R. Salim, *Behaviours of natural organic matter in membrane filtration for surface water treatment—a review.* Desalination, 2006. **194**(1-3): p. 211-231.
18. Alpatova, A., et al., *Fabrication of porous polymeric nanocomposite membranes with enhanced anti-fouling properties: effect of casting composition.* Journal of membrane science, 2013. **444**: p. 449-460.
19. Zhang, J., et al., *Preparation and characterization of novel polyethersulfone hybrid ultrafiltration membranes bending with modified halloysite nanotubes loaded with silver nanoparticles.* Industrial & Engineering Chemistry Research, 2012. **51**(7): p. 3081-3090.
20. Kim, E.-S., et al., *Development of nanosilver and multi-walled carbon nanotubes thin-film nanocomposite membrane for enhanced water treatment.* Journal of Membrane Science, 2012. **394**: p. 37-48.
21. Zodrow, K., et al., *Polysulfone ultrafiltration membranes impregnated with silver nanoparticles show improved biofouling resistance and virus removal.* Water research, 2009. **43**(3): p. 715-723.
22. Guillen, G.R., et al., *Preparation and characterization of membranes formed by nonsolvent induced phase separation: a review.* Industrial & Engineering Chemistry Research, 2011. **50**(7): p. 3798-3817.
23. Lofrano, G., et al., *Polymer functionalized nanocomposites for metals removal from water and wastewater: an overview.* Water Research, 2016.
24. Zhang, Y., et al., *Development of a sulfated Y-doped nonstoichiometric zirconia/polysulfone composite membrane for treatment of wastewater containing oil.* Separation and purification technology, 2009. **70**(2): p. 153-159.
25. Zinadini, S., et al., *Preparation of a novel antifouling mixed matrix PES membrane by embedding graphene oxide nanoplates.* Journal of Membrane Science, 2014. **453**: p. 292-301.
26. Luo, M.-L., et al., *Hydrophilic modification of poly (ether sulfone) ultrafiltration membrane surface by self-assembly of TiO 2 nanoparticles.* Applied Surface Science, 2005. **249**(1): p. 76-84.
27. Hołda, A.K., et al., *Study of polymer concentration and evaporation time as phase inversion parameters for polysulfone-based SRNF membranes.* Journal of Membrane Science, 2013. **442**: p. 196-205.
28. Kim, J. and B. Van der Bruggen, *The use of nanoparticles in polymeric and ceramic membrane structures: review of manufacturing procedures and performance improvement for water treatment.* Environmental Pollution, 2010. **158**(7): p. 2335-2349.
29. Susanto, H. and M. Ulbricht, *Characteristics, performance and stability of polyethersulfone ultrafiltration membranes prepared by phase separation method using*

different macromolecular additives. Journal of Membrane Science, 2009. **327**(1): p. 125-135.
30. Shen, L., et al., *Preparation and characterization of ZnO/polyethersulfone (PES) hybrid membranes.* Desalination, 2012. **293**: p. 21-29.
31. Van der Bruggen, B., *Chemical modification of polyethersulfone nanofiltration membranes: a review.* Journal of applied polymer science, 2009. **114**(1): p. 630-642.
32. Sadrzadeh, M. and S. Bhattacharjee, *Rational design of phase inversion membranes by tailoring thermodynamics and kinetics of casting solution using polymer additives.* Journal of Membrane Science, 2013. **441**: p. 31-44.
33. Amin, M., A. Alazba, and U. Manzoor, *A review of removal of pollutants from water/wastewater using different types of nanomaterials.* Advances in Materials Science and Engineering, 2014. **2014**.
34. Qu, X., P.J. Alvarez, and Q. Li, *Applications of nanotechnology in water and wastewater treatment.* Water research, 2013. **47**(12): p. 3931-3946.
35. Zhao, X., et al., *Polymer-supported nanocomposites for environmental application: a review.* Chemical engineering journal, 2011. **170**(2): p. 381-394.
36. Rohatgi, P.K., et al., *Synthesis and properties of metal matrix nanocomposites (MMNCS), syntactic foams, self lubricating and self-healing metals.* PRICM, 2013. **8**: p. 1515-1524.
37. Ghaemi, N., *A new approach to copper ion removal from water by polymeric nanocomposite membrane embedded with γ-alumina nanoparticles.* Applied Surface Science, 2016. **364**: p. 221-228.
38. Ghaemi, N., et al., *Polyethersulfone membrane enhanced with iron oxide nanoparticles for copper removal from water: Application of new functionalized Fe 3 O 4 nanoparticles.* Chemical Engineering Journal, 2015. **263**: p. 101-112.
39. Chan, K.H., et al., *Modification of PES membrane by PEG-coated cobalt doped iron oxide for improved Cu (II) removal.* Journal of Industrial and Engineering Chemistry, 2015. **27**: p. 283-290.
40. Tamime, A.Y., *Membrane processing: dairy and beverage applications*. 2012: John Wiley & Sons.
41. Smith, K., *Commercial membrane technology.* Membrane processing: dairy and beverage applications, 2013: p. 52-72.
42. Gilbert, B., et al., *The effects of nanoparticle aggregation processes on aggregate structure and metal uptake.* Journal of colloid and interface science, 2009. **339**(2): p. 285-295.
43. Teli, S.B., et al., *Fouling resistant polysulfone–PANI/TiO2 ultrafiltration nanocomposite membranes.* Industrial & Engineering Chemistry Research, 2013. **52**(27): p. 9470-9479.
44. Yin, J. and J. Zhou, *Novel polyethersulfone hybrid ultrafiltration membrane prepared with SiO 2-g-(PDMAEMA-co-PDMAPS) and its antifouling performances in oil-in-water emulsion application.* Desalination, 2015. **365**: p. 46-56.

45. Zhang, G., et al., *Novel polysulfone hybrid ultrafiltration membrane prepared with TiO 2-g-HEMA and its antifouling characteristics.* Journal of Membrane Science, 2013. **436**: p. 163-173.
46. Andrade, P.F., et al., *Improved antibacterial activity of nanofiltration polysulfone membranes modified with silver nanoparticles.* Water research, 2015. **81**: p. 333-342.
47. Zhang, M., et al., *Biogenic silver nanoparticles (bio-Ag 0) decrease biofouling of bio-Ag 0/PES nanocomposite membranes.* Water research, 2012. **46**(7): p. 2077-2087.
48. Mahmoudi, E., et al., *Novel nanohybrid polysulfone membrane embedded with silver nanoparticles on graphene oxide nanoplates.* Chemical Engineering Journal, 2015. **277**: p. 1-10.
49. Taurozzi, J.S., et al., *Effect of filler incorporation route on the properties of polysulfone–silver nanocomposite membranes of different porosities.* Journal of Membrane Science, 2008. **325**(1): p. 58-68.
50. Koseoglu-Imer, D.Y., et al., *The production of polysulfone (PS) membrane with silver nanoparticles (AgNP): physical properties, filtration performances, and biofouling resistances of membranes.* Journal of Membrane Science, 2013. **428**: p. 620-628.
51. Mollahosseini, A., et al., *The effect of silver nanoparticle size on performance and antibacteriality of polysulfone ultrafiltration membrane.* Desalination, 2012. **306**: p. 41-50.
52. Basri, H., et al., *Silver-filled polyethersulfone membranes for antibacterial applications—Effect of PVP and TAP addition on silver dispersion.* Desalination, 2010. **261**(3): p. 264-271.
53. Basri, H., A.F. Ismail, and M. Aziz, *Polyethersulfone (PES)–silver composite UF membrane: Effect of silver loading and PVP molecular weight on membrane morphology and antibacterial activity.* Desalination, 2011. **273**(1): p. 72-80.
54. Cao, X., et al., *Immobilization of silver nanoparticles onto sulfonated polyethersulfone membranes as antibacterial materials.* Colloids and Surfaces B: Biointerfaces, 2010. **81**(2): p. 555-562.
55. Organization, W.H., *Guildlines for Drinking Water Quality*. 2011: Geneva, Switzerland.
56. Huang, J., H. Wang, and K. Zhang, *Modification of PES membrane with Ag–SiO 2: reduction of biofouling and improvement of filtration performance.* Desalination, 2014. **336**: p. 8-17.
57. Sotto, A., et al., *Effect of nanoparticle aggregation at low concentrations of TiO 2 on the hydrophilicity, morphology, and fouling resistance of PES–TiO 2 membranes.* Journal of colloid and interface science, 2011. **363**(2): p. 540-550.
58. Li, J.-F., et al., *Effect of TiO 2 nanoparticles on the surface morphology and performance of microporous PES membrane.* Applied Surface Science, 2009. **255**(9): p. 4725-4732.

59. Esfahani, M.R., et al., *Effects of a dual nanofiller, nano-TiO 2 and MWCNT, for polysulfone-based nanocomposite membranes for water purification.* Desalination, 2015. **372**: p. 47-56.
60. Zhao, W., et al., *Fabrication of antifouling polyethersulfone ultrafiltration membranes using Pluronic F127 as both surface modifier and pore-forming agent.* Journal of Membrane Science, 2008. **318**(1): p. 405-412.
61. Vatanpour, V., et al., *Novel antibifouling nanofiltration polyethersulfone membrane fabricated from embedding TiO 2 coated multiwalled carbon nanotubes.* Separation and purification technology, 2012. **90**: p. 69-82.
62. Arsuaga, J.M., et al., *Influence of the type, size, and distribution of metal oxide particles on the properties of nanocomposite ultrafiltration membranes.* Journal of membrane science, 2013. **428**: p. 131-141.
63. Yang, Y., et al., *The influence of nano-sized TiO 2 fillers on the morphologies and properties of PSF UF membrane.* Journal of Membrane Science, 2007. **288**(1): p. 231-238.
64. Sotto, A., et al., *Doping of polyethersulfone nanofiltration membranes: antifouling effect observed at ultralow concentrations of TiO 2 nanoparticles.* Journal of Materials Chemistry, 2011. **21**(28): p. 10311-10320.
65. Rahimpour, A., et al., *TiO 2 entrapped nano-composite PVDF/SPES membranes: Preparation, characterization, antifouling and antibacterial properties.* Desalination, 2011. **278**(1): p. 343-353.
66. Bae, T.-H. and T.-M. Tak, *Effect of TiO 2 nanoparticles on fouling mitigation of ultrafiltration membranes for activated sludge filtration.* Journal of Membrane Science, 2005. **249**(1): p. 1-8.
67. Vatanpour, V., et al., *TiO 2 embedded mixed matrix PES nanocomposite membranes: influence of different sizes and types of nanoparticles on antifouling and performance.* Desalination, 2012. **292**: p. 19-29.
68. Rahimpour, A., et al., *Coupling TiO 2 nanoparticles with UV irradiation for modification of polyethersulfone ultrafiltration membranes.* Journal of Membrane Science, 2008. **313**(1): p. 158-169.
69. Wu, G., et al., *Preparation and characterization of PES/TiO 2 composite membranes.* Applied Surface Science, 2008. **254**(21): p. 7080-7086.
70. Hua, M., et al., *Heavy metal removal from water/wastewater by nanosized metal oxides: a review.* Journal of Hazardous Materials, 2012. **211**: p. 317-331.
71. Yang, Y., P. Wang, and Q. Zheng, *Preparation and properties of polysulfone/TiO2 composite ultrafiltration membranes.* Journal of Polymer Science Part B: Polymer Physics, 2006. **44**(5): p. 879-887.
72. Pereira, V.R., et al., *Preparation, characterization and the effect of PANI coated TiO 2 nanocomposites on the performance of polysulfone ultrafiltration membranes.* New Journal of Chemistry, 2015. **39**(1): p. 703-712.

73. Li, X.-q. and W.-x. Zhang, *Iron nanoparticles: the core-shell structure and unique properties for Ni (II) sequestration.* Langmuir, 2006. **22**(10): p. 4638-4642.
74. Daraei, P., et al., *Novel polyethersulfone nanocomposite membrane prepared by PANI/Fe 3 O 4 nanoparticles with enhanced performance for Cu (II) removal from water.* Journal of Membrane Science, 2012. **415**: p. 250-259.
75. Weerasekara, N.A., K.-H. Choo, and S.-J. Choi, *Metal oxide enhanced microfiltration for the selective removal of Co and Sr ions from nuclear laundry wastewater.* Journal of Membrane Science, 2013. **447**: p. 87-95.
76. Chan, K.H., et al., *Enhanced Cu (II) rejection and fouling reduction through fabrication of PEG-PES nanocomposite ultrafiltration membrane with PEG-coated cobalt doped iron oxide nanoparticle.* Journal of the Taiwan Institute of Chemical Engineers, 2015. **47**: p. 50-58.
77. Gohari, R.J., et al., *Fabrication and characterization of novel PES/Fe–Mn binary oxide UF mixed matrix membrane for adsorptive removal of As (III) from contaminated water solution.* Separation and Purification Technology, 2013. **118**: p. 64-72.
78. Daraei, P., et al., *Fouling resistant mixed matrix polyethersulfone membranes blended with magnetic nanoparticles: study of magnetic field induced casting.* Separation and Purification Technology, 2013. **109**: p. 111-121.
79. Wu, H., B. Tang, and P. Wu, *Development of novel SiO 2–GO nanohybrid/polysulfone membrane with enhanced performance.* Journal of Membrane Science, 2014. **451**: p. 94-102.
80. Ahmad, A., M. Majid, and B. Ooi, *Functionalized PSf/SiO 2 nanocomposite membrane for oil-in-water emulsion separation.* Desalination, 2011. **268**(1): p. 266-269.
81. Sun, M., et al., *Improved antifouling property of PES ultrafiltration membranes using additive of silica− PVP nanocomposite.* Industrial & Engineering Chemistry Research, 2009. **49**(2): p. 790-796.
82. Muhamad, M.S., M.R. Salim, and W.-J. Lau, *Preparation and characterization of PES/SiO2 composite ultrafiltration membrane for advanced water treatment.* Korean Journal of Chemical Engineering, 2015. **32**(11): p. 2319-2329.
83. Zhang, Y., et al., *Preparation and characterization of novel Ce-doped nonstoichiometric nanosilica/polysulfone composite membranes.* Separation and Purification Technology, 2008. **63**(1): p. 207-212.
84. Jin, L., et al., *Synthesis of a novel composite nanofiltration membrane incorporated SiO 2 nanoparticles for oily wastewater desalination.* Polymer, 2012. **53**(23): p. 5295-5303.
85. Aerts, P., et al., *Polysulfone–Aerosil composite membranes: Part 1. The influence of the addition of Aerosil on the formation process and membrane morphology.* Journal of Membrane Science, 2000. **176**(1): p. 63-73.
86. Aerts, P., et al., *Polysulfone–aerosil composite membranes: Part 2. The influence of the addition of aerosil on the skin characteristics and membrane properties.* Journal of Membrane Science, 2000. **178**(1): p. 1-11.

87. Shen, J.-n., et al., *Preparation and characterization of PES–SiO 2 organic–inorganic composite ultrafiltration membrane for raw water pretreatment.* Chemical engineering journal, 2011. **168**(3): p. 1272-1278.
88. Shariatmadar, F. and M. Mohsen-Nia, *PES/SiO2 nanocomposite by in situ polymerization: Synthesis, structure, properties, and new applications.* Polymer Composites, 2012. **33**(7): p. 1188-1196.
89. Vatanpour, V., et al., *Boehmite nanoparticles as a new nanofiller for preparation of antifouling mixed matrix membranes.* Journal of Membrane Science, 2012. **401**: p. 132-143.
90. Maximous, N., et al., *Optimization of Al 2 O 3/PES membranes for wastewater filtration.* Separation and Purification Technology, 2010. **73**(2): p. 294-301.
91. Rahmani, A., H.Z. Mousavi, and M. Fazli, *Effect of nanostructure alumina on adsorption of heavy metals.* Desalination, 2010. **253**(1): p. 94-100.
92. Fouladgar, M., M. Beheshti, and H. Sabzyan, *Single and binary adsorption of nickel and copper from aqueous solutions by γ-alumina nanoparticles: Equilibrium and kinetic modeling.* Journal of Molecular Liquids, 2015. **211**: p. 1060-1073.
93. Garcia-Ivars, J., et al., *Enhancement in hydrophilicity of different polymer phase-inversion ultrafiltration membranes by introducing PEG/Al 2 O 3 nanoparticles.* Separation and Purification Technology, 2014. **128**: p. 45-57.
94. Homayoonfal, M., et al., *Fabrication of alumina/polysulfone nanocomposite membranes with biofouling mitigation approach in membrane bioreactors.* Journal of Industrial and Engineering Chemistry, 2015. **22**: p. 357-367.
95. Mehrnia, M.R., Y.M. Mojtahedi, and M. Homayoonfal, *What is the concentration threshold of nanoparticles within the membrane structure? A case study of Al2O3/PSf nanocomposite membrane.* Desalination, 2015. **372**: p. 75-88.
96. Maximous, N., et al., *Preparation, characterization and performance of Al 2 O 3/PES membrane for wastewater filtration.* Journal of Membrane Science, 2009. **341**(1): p. 67-75.
97. Rinaldi, R. and U. Schuchardt, *On the paradox of transition metal-free alumina-catalyzed epoxidation with aqueous hydrogen peroxide.* Journal of Catalysis, 2005. **236**(2): p. 335-345.
98. Daraei, P., et al., *PAA grafting onto new acrylate-alumoxane/PES mixed matrix nano-enhanced membrane: Preparation, characterization and performance in dye removal.* Chemical engineering journal, 2013. **221**: p. 111-123.
99. Mojtahedi, Y.M., M.R. Mehrnia, and M. Homayoonfal, *Fabrication of Al2O3/PSf nanocomposite membranes: efficiency comparison of coating and blending methods in modification of filtration performance.* Desalination and Water Treatment, 2013. **51**(34-36): p. 6736-6742.
100. Genne, I., S. Kuypers, and R. Leysen, *Effect of the addition of ZrO 2 to polysulfone based UF membranes.* Journal of Membrane Science, 1996. **113**(2): p. 343-350.

101. Maximous, N., et al., *Performance of a novel ZrO 2/PES membrane for wastewater filtration.* Journal of Membrane Science, 2010. **352**(1): p. 222-230.
102. Maximous, N., et al., *Effect of the metal oxide particle distributions on modified PES membranes characteristics and performance.* Journal of Membrane Science, 2010. **361**(1): p. 213-222.
103. Zhang, Y., et al., *Synthesis of sulfated Y-doped zirconia particles and effect on properties of polysulfone membranes for treatment of wastewater containing oil.* Journal of hazardous materials, 2011. **192**(2): p. 559-567.
104. Huang, J., G. Arthanareeswaran, and K. Zhang, *Effect of silver loaded sodium zirconium phosphate (nanoAgZ) nanoparticles incorporation on PES membrane performance.* Desalination, 2012. **285**: p. 100-107.
105. Gohari, R.J., et al., *Novel polyethersulfone (PES)/hydrous manganese dioxide (HMO) mixed matrix membranes with improved anti-fouling properties for oily wastewater treatment process.* RSC Advances, 2014. **4**(34): p. 17587-17596.
106. Gohari, R.J., et al., *Improving performance and antifouling capability of PES UF membranes via blending with highly hydrophilic hydrous manganese dioxide nanoparticles.* Desalination, 2014. **335**(1): p. 87-95.
107. Gohari, R.J., et al., *Adsorptive removal of Pb (II) from aqueous solution by novel PES/HMO ultrafiltration mixed matrix membrane.* Separation and Purification Technology, 2013. **120**: p. 59-68.
108. Dong, C., et al., *Antifouling enhancement of poly (vinylidene fluoride) microfiltration membrane by adding Mg (OH) 2 nanoparticles.* Journal of Membrane Science, 2012. **387**: p. 40-47.
109. Su, Q., et al., *Fabrication of polymer-supported nanosized hydrous manganese dioxide (HMO) for enhanced lead removal from waters.* Science of the total environment, 2009. **407**(21): p. 5471-5477.
110. Su, Q., et al., *Use of hydrous manganese dioxide as a potential sorbent for selective removal of lead, cadmium, and zinc ions from water.* Journal of colloid and interface science, 2010. **349**(2): p. 607-612.
111. Qin, Q., et al., *An efficient approach for Pb (II) and Cd (II) removal using manganese dioxide formed in situ.* Chemical Engineering Journal, 2011. **172**(1): p. 68-74.
112. Balta, S., et al., *A new outlook on membrane enhancement with nanoparticles: the alternative of ZnO.* Journal of Membrane Science, 2012. **389**: p. 155-161.
113. Li, Q., et al., *Antimicrobial nanomaterials for water disinfection and microbial control: potential applications and implications.* Water research, 2008. **42**(18): p. 4591-4602.
114. Hossain, F., et al., *Antimicrobial nanomaterials as water disinfectant: applications, limitations and future perspectives.* Science of the total environment, 2014. **466**: p. 1047-1059.
115. Leo, C.-P., et al., *Polysulfone membranes blended with ZnO nanoparticles for reducing fouling by oleic acid.* Separation and purification technology, 2012. **89**: p. 51-56.

116. Wang, X., et al., *Mass production of micro/nanostructured porous ZnO plates and their strong structurally enhanced and selective adsorption performance for environmental remediation.* Journal of Materials Chemistry, 2010. **20**(39): p. 8582-8590.
117. Kikuchi, Y., et al., *Effect of ZnO loading to activated carbon on Pb (II) adsorption from aqueous solution.* Carbon, 2006. **44**(2): p. 195-202.
118. Nath, S., S.K. Ghosh, and S. Panigahi, *Synthesis of selenium nanoparticle and its photocatalytic application for decolorization of methylene blue under UV irradiation.* 2004.
119. Tran, P.L., et al., *An organo-selenium coating on cellulose inhibits Pseudomonas aeruginosa and Staphylococcus aureus biofilm formation.* Applied and Environmental Microbiology, 2009.
120. Low, D., et al., *Attachment of selenium to a reverse osmosis membrane to inhibit biofilm formation of S. aureus.* Journal of Membrane Science, 2011. **378**(1): p. 171-178.
121. Cioffi, N., et al., *Copper nanoparticle/polymer composites with antifungal and bacteriostatic properties.* Chemistry of Materials, 2005. **17**(21): p. 5255-5262.
122. Akar, N., et al., *Investigation of characterization and biofouling properties of PES membrane containing selenium and copper nanoparticles.* Journal of Membrane Science, 2013. **437**: p. 216-226.
123. Muhamad, M.S., M.R. Salim, and W.-J. Lau, *Preparation and characterization of PES/SiO 2 composite ultrafiltration membrane for advanced water treatment.* Korean Journal of Chemical Engineering, 2015. **32**(11): p. 2319-2329.
124. Ferlita, R.R., et al., *Cryo-snap: A simple modified freeze-fracture method for SEM imaging of membrane cross-sections.* Environmental Progress & Sustainable Energy, 2008. **27**(2): p. 204-209.
125. El-Hibri, M.J. and S.A. Weinberg, *Polysulfones.* Encyclopedia of polymer science and technology, 2002. **4**.
126. Marino, T., et al., *Polyethersulfone membranes prepared with Rhodiasolv® Polarclean as water soluble green solvent.* Journal of Membrane Science, 2018. **549**: p. 192-204.
127. Susanto, H., N. Stahra, and M. Ulbricht, *High performance polyethersulfone microfiltration membranes having high flux and stable hydrophilic property.* Journal of Membrane Science, 2009. **342**(1-2): p. 153-164.
128. Hołda, A.K. and I.F. Vankelecom, *Integrally skinned PSf-based SRNF-membranes prepared via phase inversion—Part A: Influence of high molecular weight additives.* Journal of Membrane Science, 2014. **450**: p. 512-521.
129. Kim, I.C. and K.H. Lee, *Effect of various additives on pore size of polysulfone membrane by phase-inversion process.* Journal of applied polymer science, 2003. **89**(9): p. 2562-2566.
130. Sivakumar, M., et al., *Studies on cellulose acetate–polysulfone ultrafiltration membranes: I. Effect of polymer composition.* Polymer international, 2005. **54**(6): p. 956-962.

131. Gohari, B. and N. Abu-Zahra, *Polyethersulfone Membranes Prepared with 3-Aminopropyltriethoxysilane Modified Alumina Nanoparticles for Cu (II) Removal from Water.* ACS Omega, 2018. **3**(8): p. 10154-10162.
132. Spruck, M., et al., *Influence of the coagulation medium on the performance of poly (ether sulfone) flat-sheet membranes.* Journal of Applied Polymer Science, 2015. **132**(11).
133. Rahimpour, A. and S.S. Madaeni, *Improvement of performance and surface properties of nano-porous polyethersulfone (PES) membrane using hydrophilic monomers as additives in the casting solution.* Journal of Membrane Science, 2010. **360**(1): p. 371-379.
134. Barth, C., et al., *Asymmetric polysulfone and polyethersulfone membranes: effects of thermodynamic conditions during formation on their performance.* Journal of Membrane Science, 2000. **169**(2): p. 287-299.
135. Li, Z. and C. Jiang, *Investigation into the rheological properties of PES/NMP/nonsolvent membrane-forming systems.* Journal of applied polymer science, 2001. **82**(2): p. 283-291.
136. Li, J.F., et al., *Hydrophilic microporous PES membranes prepared by PES/PEG/DMAc casting solutions.* Journal of applied polymer science, 2008. **107**(6): p. 4100-4108.
137. Said, N., et al., *Enhanced hydrophilic polysulfone hollow fiber membranes with addition of IONPs nano-fillers.* Polymer International, 2017.
138. Esmaeili, M., S.S. Madaeni, and J. Barzin, *The dependence of morphology of solid polymer electrolyte membranes on transient salt type: effect of cation type.* Polymer International, 2010. **59**(7): p. 1006-1013.
139. Ismail, A.F. and A.R. Hassan, *Effect of additive contents on the performances and structural properties of asymmetric polyethersulfone (PES) nanofiltration membranes.* Separation and Purification Technology, 2007. **55**(1): p. 98-109.
140. Tsai, H.A., et al., *Effect of temperature and span series surfactant on the structure of polysulfone membranes.* Journal of applied polymer science, 2002. **86**(1): p. 166-173.
141. Zheng, Q.-Z., et al., *The relationship between porosity and kinetics parameter of membrane formation in PSF ultrafiltration membrane.* Journal of membrane science, 2006. **286**(1): p. 7-11.
142. Zheng, Q.-Z., P. Wang, and Y.-N. Yang, *Rheological and thermodynamic variation in polysulfone solution by PEG introduction and its effect on kinetics of membrane formation via phase-inversion process.* Journal of membrane science, 2006. **279**(1): p. 230-237.
143. Saljoughi, E., M. Amirilargani, and T. Mohammadi, *Effect of PEG additive and coagulation bath temperature on the morphology, permeability and thermal/chemical stability of asymmetric CA membranes.* Desalination, 2010. **262**(1): p. 72-78.
144. Lee, K.-W., et al., *Trade-off between thermodynamic enhancement and kinetic hindrance during phase inversion in the preparation of polysulfone membranes.* Desalination, 2003. **159**(3): p. 289-296.

145. Saljoughi, E. and T. Mohammadi, *Cellulose acetate (CA)/polyvinylpyrrolidone (PVP) blend asymmetric membranes: Preparation, morphology and performance.* Desalination, 2009. **249**(2): p. 850-854.
146. Smolders, C., et al., *Microstructures in phase-inversion membranes. Part 1. Formation of macrovoids.* Journal of Membrane Science, 1992. **73**(2): p. 259-275.
147. Blanco, J.-F., et al., *Formation and morphology studies of different polysulfones-based membranes made by wet phase inversion process.* Journal of membrane science, 2006. **283**(1): p. 27-37.
148. Ma, Y., et al., *Effect of PEG additive on the morphology and performance of polysulfone ultrafiltration membranes.* Desalination, 2011. **272**(1): p. 51-58.
149. Hołda, A.K. and I.F. Vankelecom, *Understanding and guiding the phase inversion process for synthesis of solvent resistant nanofiltration membranes.* Journal of Applied Polymer Science, 2015. **132**(27).
150. Han, M.-J., *Effect of propionic acid in the casting solution on the characteristics of phase inversion polysulfone membranes.* Desalination, 1999. **121**(1): p. 31-39.
151. Yang, Z., et al., *Thiourea modified hyper-crosslinked polystyrene resin for heavy metal ions removal from aqueous solutions.* Journal of Applied Polymer Science, 2018. **135**(1).
152. Abbas, A., et al., *Heavy metal removal from aqueous solution by advanced carbon nanotubes: critical review of adsorption applications.* Separation and Purification Technology, 2016. **157**: p. 141-161.
153. Gholami, A., et al., *Preparation and characterization of polyvinyl chloride based nanocomposite nanofiltration-membrane modified by iron oxide nanoparticles for lead removal from water.* Journal of Industrial and Engineering Chemistry, 2014. **20**(4): p. 1517-1522.
154. Sweeney, E., et al., *Lead in drinking water: a response from the Atlantic PATH study.* Environmental Health Review, 2017. **60**(1): p. 9-13.
155. Shukla, N., et al., *Removal of Lead from Water Using Low Density Metal Oxide Nanoparticles.* Advanced Science, Engineering and Medicine, 2015. **7**(5): p. 398-405.
156. Kiran, M.G., K. Pakshirajan, and G. Das, *Heavy metal removal from multicomponent system by sulfate reducing bacteria: Mechanism and cell surface characterization.* Journal of hazardous materials, 2017. **324**: p. 62-70.
157. Gohari, R.J., et al., *Adsorptive removal of Pb (II) from aqueous solution by novel PES/HMO ultrafiltration mixed matrix membrane.* Separation and Purification Technology, 2013. **120**: p. 59-68.
158. Hebbar, R.S., et al., *Fabrication of polydopamine functionalized halloysite nanotube/polyetherimide membranes for heavy metal removal.* Journal of Materials Chemistry A, 2016. **4**(3): p. 764-774.
159. Simeonidis, K., et al., *Inorganic engineered nanoparticles in drinking water treatment: a critical review.* Environmental Science: Water Research & Technology, 2016. **2**(1): p. 43-70.

160. Ali, I. and V. Gupta, *Advances in water treatment by adsorption technology.* Nature protocols, 2006. **1**(6): p. 2661-2667.
161. Jyothi, M., et al., *Aminated polysulfone/TiO 2 composite membranes for an effective removal of Cr (VI).* Chemical Engineering Journal, 2016. **283**: p. 1494-1505.
162. Yurekli, Y., *Removal of heavy metals in wastewater by using zeolite nano-particles impregnated polysulfone membranes.* Journal of hazardous materials, 2016. **309**: p. 53-64.
163. Monticelli, O., et al., *Preparation and properties of polysulfone–clay composite membranes.* Journal of applied polymer science, 2007. **103**(6): p. 3637-3644.
164. Rahimi, M., et al., *Hydrophilic goethite nanoparticle as a novel antifouling agent in fabrication of nanocomposite polyethersulfone membrane.* Journal of Applied Polymer Science, 2016. **133**(26).
165. Unnikrishnan, L., et al., *Synthesis and characterization of polysulfone/clay nanocomposite membranes for fuel cell application.* Journal of Applied Polymer Science, 2012. **124**(S1).
166. Shao, L., et al., *Fabrication and characterization of solution cast MWNTs/PEI nanocomposites.* Journal of applied polymer science, 2009. **113**(3): p. 1879-1886.
167. Gohari, R.J., et al., *Fabrication and characterization of novel PES/Fe–Mn binary oxide UF mixed matrix membrane for adsorptive removal of As (III) from contaminated water solution.* Separation and Purification Technology, 2013. **118**: p. 64-72.
168. Afkhami, A., M. Saber-Tehrani, and H. Bagheri, *Simultaneous removal of heavy-metal ions in wastewater samples using nano-alumina modified with 2, 4-dinitrophenylhydrazine.* Journal of Hazardous Materials, 2010. **181**(1): p. 836-844.
169. Jin, H., et al., *Research on removal of fluoride in aqueous solution by alumina-modified expanded graphite composite.* Journal of Alloys and Compounds, 2015. **620**: p. 361-367.
170. Yang, D., et al., *Alumina nanofibers grafted with functional groups: a new design in efficient sorbents for removal of toxic contaminants from water.* Water research, 2010. **44**(3): p. 741-750.
171. Wang, X., et al., *Self-curled coral-like γ-Al 2 O 3 nanoplates for use as an adsorbent.* Journal of colloid and interface science, 2015. **453**: p. 244-251.
172. Pendergast, M.M. and E.M. Hoek, *A review of water treatment membrane nanotechnologies.* Energy & Environmental Science, 2011. **4**(6): p. 1946-1971.
173. Liu, Y., et al., *Hydrothermal synthesis of microscale boehmite and gamma nanoleaves alumina.* Materials Letters, 2008. **62**(8): p. 1297-1301.
174. Bhatnagar, A., E. Kumar, and M. Sillanpää, *Nitrate removal from water by nano-alumina: Characterization and sorption studies.* Chemical Engineering Journal, 2010. **163**(3): p. 317-323.

175. Khayet, M. and M. García-Payo, *X-Ray diffraction study of polyethersulfone polymer, flat-sheet and hollow fibers prepared from the same under different gas-gaps.* Desalination, 2009. **245**(1-3): p. 494-500.
176. Yi, X., et al., *Estimation of fouling stages in separation of oil/water emulsion using nano-particles Al 2 O 3/TiO 2 modified PVDF UF membranes.* Desalination, 2013. **319**: p. 38-46.
177. Yan, L., et al., *Application of the Al 2 O 3–PVDF nanocomposite tubular ultrafiltration (UF) membrane for oily wastewater treatment and its antifouling research.* Separation and Purification Technology, 2009. **66**(2): p. 347-352.
178. Fu, F. and Q. Wang, *Removal of heavy metal ions from wastewaters: a review.* Journal of environmental management, 2011. **92**(3): p. 407-418.
179. Mukherjee, R. and S. De, *Adsorptive removal of nitrate from aqueous solution by polyacrylonitrile–alumina nanoparticle mixed matrix hollow-fiber membrane.* Journal of Membrane Science, 2014. **466**: p. 281-292.
180. Mallakpour, S. and M. Madani, *A review of current coupling agents for modification of metal oxide nanoparticles.* Progress in Organic Coatings, 2015. **86**: p. 194-207.
181. Li, H., et al., *Seed-free synthesis of highly permeable zeolite NaA membranes through deposition of APTES-functionalized alumina particles on macroporous supports.* Journal of Membrane Science, 2014. **471**: p. 84-93.
182. Oh, S., et al., *Preparation of novel ceramic membranes modified by mesoporous silica with 3-aminopropyltriethoxysilane (APTES) and its application to Cu2+ separation in the aqueous phase.* Journal of Membrane Science, 2007. **301**(1-2): p. 118-125.
183. Demirel, E., et al., *Fe 2 O 3 nanocomposite PVC membrane with enhanced properties and separation performance.* Journal of Membrane Science, 2017. **529**: p. 170-184.
184. Jafarzadeh, Y., R. Yegani, and S. Tantekin-Ersolmaz, *Effect of TiO2 nanoparticles on structure and properties of high density polyethylene membranes prepared by thermally induced phase separation method.* Polymers for Advanced Technologies, 2015. **26**(4): p. 392-398.
185. Qdais, H.A. and H. Moussa, *Removal of heavy metals from wastewater by membrane processes: a comparative study.* Desalination, 2004. **164**(2): p. 105-110.
186. Wu, F., L. Feng, and L. Zhang, *Rejection prediction of isopropylantipyrine and antipyrine by nanofiltration membranes based on the Spiegler–Kedem–Katchalsky model.* Desalination, 2015. **362**: p. 11-17.
187. Nair, R., et al., *Implementation of Spiegler–Kedem and Steric Hindrance Pore Models for Analyzing Nanofiltration Membrane Performance for Smart Water Production.* Membranes, 2018. **8**(3): p. 78.
188. Darvishmanesh, S. and B. Van der Bruggen, *Mass Transport through Nanostructured Membranes: Towards a Predictive Tool.* Membranes, 2016. **6**(4): p. 49.
189. Jye, L.W. and A.F. Ismail, *Nanofiltration Membranes: Synthesis, Characterization, and Applications*. 2016: Crc Press.

190. Gilron, J., N. Gara, and O. Kedem, *Experimental analysis of negative salt rejection in nanofiltration membranes.* Journal of Membrane Science, 2001. **185**(2): p. 223-236.
191. Koter, S., *Determination of the parameters of the Spiegler–Kedem–Katchalsky model for nanofiltration of single electrolyte solutions.* Desalination, 2006. **198**(1-3): p. 335-345.
192. NAKAO, S.-I. and S. KIMURA, *Models of membrane transport phenomena and their applications for ultrafiltration data.* Journal of Chemical Engineering of Japan, 1982. **15**(3): p. 200-205.
193. Wang, X.-L., et al., *The electrostatic and steric-hindrance model for the transport of charged solutes through nanofiltration membranes.* Journal of Membrane Science, 1997. **135**(1): p. 19-32.
194. Wang, X.-L., et al., *Evaluation of pore structure and electrical properties of nanofiltration membranes.* Journal of chemical engineering of Japan, 1995. **28**(2): p. 186-192.
195. Mehta, A. and A.L. Zydney, *Permeability and selectivity analysis for ultrafiltration membranes.* Journal of Membrane Science, 2005. **249**(1-2): p. 245-249.

CURRICULUM VITAE

Behnam Gohari

Place of Birth: Mashhad, Iran

Education

B.Sc., Sharif University of Technology, September 2005

M.Sc., Iran University of Science and Technology, September 2008

Ph.D., University of Wisconsin-Milwaukee, December 2018